nature portfolio

https://doi.org/10.1038/s41591-022-01749-8

Supplementary information

Stratification of radiosensitive brain metastases based on an actionable S100A9/RAGE resistance mechanism

In the format provided by the authors and unedited

Supplementary Information

Title: Stratification of radiosensitive brain metastases based on an actionable S100A9/RAGE resistance mechanism.

Author list:

Cátia Monteiro[1**], Lauritz Miarka[1**], María Perea-García[1], Neibla Priego[1], Pedro García-Gómez[1], Laura Álvaro-Espinosa[1], Ana de Pablos-Aragoneses[1], Natalia Yebra[1], Diana Retana[1], Patricia Baena[1], Coral Fustero-Torre[2], Osvaldo Graña-Castro[2], Kevin Troulé[2], Eduardo Caleiras[3], Patricia Tezanos[4], Pablo Muela[4], Elisa Cintado[4], José Luis Trejo[4], Juan Manuel Sepúlveda[5], Pedro González-León[6], Luis Jiménez-Roldán[6,7], Luis Miguel Moreno[6], Olga Esteban[6], Ángel Pérez-Núñez[6,7], Aurelio Hernández-Lain[8], José Mazarico Gallego[9], Irene Ferrer[10,11], Rocío Suárez[10,11], Eva M. Garrido-Martín[10,11], Luis Paz-Ares[9,10,11,12], Celine Dalmasso[13], Elizabeth Cohen-Jonathan Moyal[13], Aurore Siegfried[14], Aisling Hegarty[15], Stephen Keelan[15], Damir Varešlija[15], Leonie S. Young[15], Malte Mohme[16], Yvonne Goy[17], Harriet Wikman[18], Jose Fernández-Alén[19], Guillermo Blasco[19], Lucía Alcázar[19], Clara Cabañuz[20], Sergei I. Grivennikov[21,†], Andrada Ianus[22], Noam Shemesh[22], Claudia C. Faria[23,24], Rebecca Lee[25,26], Paul Lorigan[25,26], Emilie Le Rhun[27], Michael Weller[27], Riccardo Soffietti[28], Luca Bertero[29], Umberto Ricardi[30], Joaquim Bosch-Barrera[31,32,33], Elia Sais[31,32], Eduard Teixidor[31,32], Alejandro Hernández-Martínez[31,32], Alfonso Calvo[11,34], Javier Aristu[35], Santiago M. Martin[36], Alvaro Gonzalez[37], Omer Adler[38], Neta Erez[38], RENACER[39], Manuel Valiente[1*].

Affiliations:

[1]Brain Metastasis Group, CNIO; Madrid, 28029, Spain.

[2]Bioinformatics Unit, CNIO; Madrid, 28029, Spain.

[3]Histopathology Core Unit, CNIO; Madrid, 28029, Spain.

[4]Department of Translational Neuroscience, Cajal Institute, CSIC; Madrid, 28002, Spain.

[5]Neuro-Oncology Unit, Hospital Universitario 12 de Octubre; Madrid, 28041, Spain.

[6]Neurosurgery Unit, Hospital Universitario 12 de Octubre; Madrid, 28041, Spain.

[7]Department of Surgery, Universidad Complutense de Madrid, Madrid, 28040; Spain.

[8]Neuropathology Unit, Hospital Universitario 12 de Octubre; Madrid, 28041, Spain.

[9]Medical Oncology, Hospital Universitario 12 de Octubre; Madrid, 28041, Spain.

[10]CNIO-H12O Clinical Cancer Research Unit, Fundación de Investigación Biomédica i+12 and CNIO, Madrid, 28029, Spain.

[11]CIBERONC

[12]Department of Medicine, Universidad Complutense de Madrid, Madrid, 28040, Spain.

[13]Radiation Oncology Department, Institut Claudius Regaud, IUCT-Oncopole; Toulouse, 31100, France.

[14]Anatomopathology Department, CHU Toulouse, IUCT-Oncopole; Toulouse, 31100, France.

[15]Endocrine Oncology Research Group, RCSI University of Medicine and Health Sciences; Dublin, D02 YN77, Ireland.

[16]Department of Neurosurgery, University Medical Center Hamburg-Eppendorf; Hamburg, 20246, Germany.

[17]Department of Radiation Oncology, University Medical Center Hamburg-Eppendorf; Hamburg, 20246, Germany.

[18]Department of Tumor Biology, University Medical Center Hamburg-Eppendorf; Hamburg, 20246, Germany.

[19]Department of Neurosurgery, Hospital Universitario de La Princesa; Madrid, 28006, Spain.

[20]Department of Pathology, Hospital Universitario La Paz; Madrid, 28046, Spain.

[21]Cancer Prevention and Control Program, Fox Chase Cancer Center, 333 Cottman Ave, Philadelphia, PA, 19111, United States of America.

[22]Champalimaud Research, Champalimaud Centre for the Unknown; Lisbon, 1400-038, Portugal.

[23]Instituto de Medicina Molecular João Lobo Antunes, Facultade de Medicina, Universidade de Lisboa; Lisboa, 1649-028, Portugal.

[24]Department of Neurosurgery, Hospital de Santa Maria, Centro Hospitalar Universitário Lisboa Norte (CHULN); Lisboa, 1649-028, Portugal.

[25]Faculty of Biology Medicine and Health, The University of Manchester; Manchester, M13 9PL, United Kingdom.

[26]The Christie NHS Foundation Trust; Manchester, M20 4BX, United Kingdom.

[27]Department of Neurology, University Hospital Zurich; Zurich, 8091, Switzerland.

[28]Division of Neuro-Oncology, Department of Neuroscience Rita Levi Montalcini, University of Turin; Turin, 10126, Italy.

[29]Department of Medical Sciences, University of Turin; Turin, 10126, Italy.

[30]Department of Oncology, University of Turin; Turin, 10126, Italy.

[31]Department of Medical Oncology, Catalan Institute of Oncology, Doctor Josep Trueta University Hospital; Girona, 17007, Spain.

[32]Girona Biomedical Research Institute (IDIBGi); Salt, 17190, Spain.

[33]Department of Medical Sciences, University of Girona; Girona, 17003, Spain.

[34]IDISNA, Program in Solid Tumors, Center for Applied Medical Research (CIMA), University of Navarra; Pamplona, 31008, Spain.

[35]Department of Oncology, University Clinic of Navarra; Madrid, 28027, Spain.

[36]Department of Oncology, University Clinic of Navarra; Pamplona, 31008, Spain.

[37]Department of Biochemistry, University Clinic of Navarra; Pamplona, 31008, Spain.

[38]Department of Pathology, Sackler Faculty of Medicine, Tel Aviv University; Tel Aviv, 69978, Israel.

[39]Biobank; CNIO; Madrid, 28029; Spain.

**These authors contributed equally to this work.

*Corresponding author. Email: mvaliente@cnio.es.

[†]Current address: Departments of Medicine and of Biomedical Sciences, Cedars-Sinai Cancer, Cedars-Sinai Medical Center; Los Angeles, CA, 90048, United States of America.

Supplementary Figures.

Supplementary Figure 1.

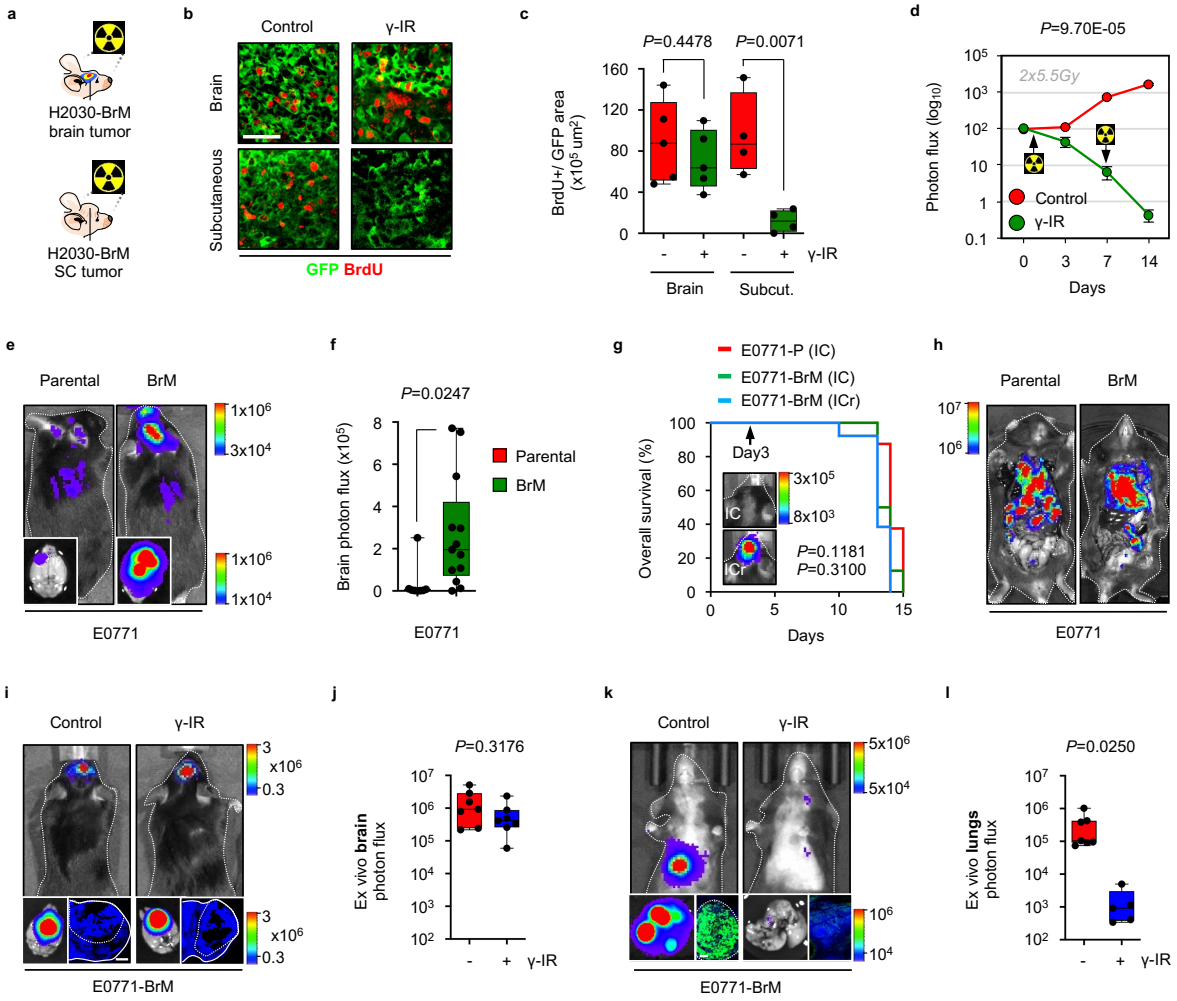

Acquired radioresistance in experimental brain metastasis. a, Schema of experimental design. **b**, Representative images of H2030-BrM tumors (GFP+) before and after 72 hours after irradiation with a single dose of 10Gy. Scale bar: 50 μm. **c**, Quantification of BrdU+ cancer cells from experiment in (**b**). Values are shown in box-and-whisker plots where every dot represents an independent brain metastasis or subcutaneous tumor and the line in the box corresponds to the median. The boxes go from the upper to the lower quartiles and the whiskers go from the minimum to the maximum value (n=4, non-irradiated brain metastases; n=4, irradiated brain metastases; n=4, non-irradiated subcutaneous tumors; n=4, irradiated subcutaneous tumors). *P* value is calculated using two-tailed t test. **d**, Quantification of H2030-BrM cells after long-term culture and

fractionated doses of irradiation. A total dose of 11Gy was delivered into two doses of 5.5Gy. Each dot indicates the mean bioluminescence value at each time point normalized for the initial value of the control ± sem (n=3 wells per condition). *P* value is calculated using two-tailed t test at the last time point. **e**, Representative images of C57BL/6 mice two weeks after being inoculated with E0771-P or E0771-BrM cells IC. Images in the lower left corner show the BLI of brains *ex vivo*. Dotted line indicates the mouse body. **f**, Quantification of BLI in the head of mice intracardially injected with E0771-P or E0771-BrM cells. Values are shown in box-and-whisker plots where every dot represents a different brain and the line in the box corresponds to the median. The boxes go from the upper to the lower quartiles and the whiskers go from the minimum to the maximum value (n=8 mice, E0771-P; n=13 mice, E0771-BrM). *P* value is calculated using two-tailed t test. **g**, Survival curve comparing E0771-P (n=8) with E0771-BrM (n=8) cell lines inoculated IC and the E0771-BrM inoculated intracranially (Icr) (n=13). *P* value is calculated using log rank (Mantel-Cox) test two-sided (E0771-P versus E0771-BrM from IC injection, P=0.1181; E0771-BrM from IC versus E0771-BrM from Icr injection, P=0.3100). Representative BLI images of mice inoculated with E0771-BrM IC versus Icr are also shown at 3 days post-inoculation. **h**, Representative images of mice inoculated with E0771-P or E0771-BrM IC showing the extensive burden of extracranial metastases with both cell lines. **i**, Representative images of C57BL/6 mice two weeks after being inoculated with E0771-BrM cells iCr and left untreated or treated with WBRT (10 x 3Gy). Dotted line indicated the body of mice. Additional images show the BLI of brains *ex vivo* as well as the histology where similar tumor masses are detected. Dotted line indicated the metastasis. Scale bar: 10 mm. **j**, Quantification of BLI in the brain *ex vivo*. Values are shown in box-and-whisker plots where every dot represents a different brain and the line in the box corresponds to the median. The boxes go from the upper to the lower quartiles and the whiskers go from the minimum to the maximum value (n=7 mice in each experimental condition). Y-axis is scaled logarithmic. *P* value is calculated using two-tailed t test. **k**, Representative images of C57BL/6 mice 3 weeks after being inoculated with E0771-BrM cells into the lateral tail-vein and left untreated or treated with irradiation to the lung only (10 x 3Gy). Dotted line indicated the body of mice. Additional images show the BLI of lungs *ex vivo* as well as the histology. Dotted line indicated the metastasis. Scale bar: 100 μm. **l**, Quantification of bioluminescence of the lungs *ex vivo*. Values are shown in box-and-whisker plots where every dot represents a different lung and the line in the box corresponds to the median. The boxes go from the upper to the lower quartiles

and the whiskers go from minimum to maximum value (n=7, non-irradiated mice; n=5, irradiated mice). Y-axis is scaled logarithmic. *P* value is calculated using Mann-Whitney test, two-sided.

Supplementary Figure 2.

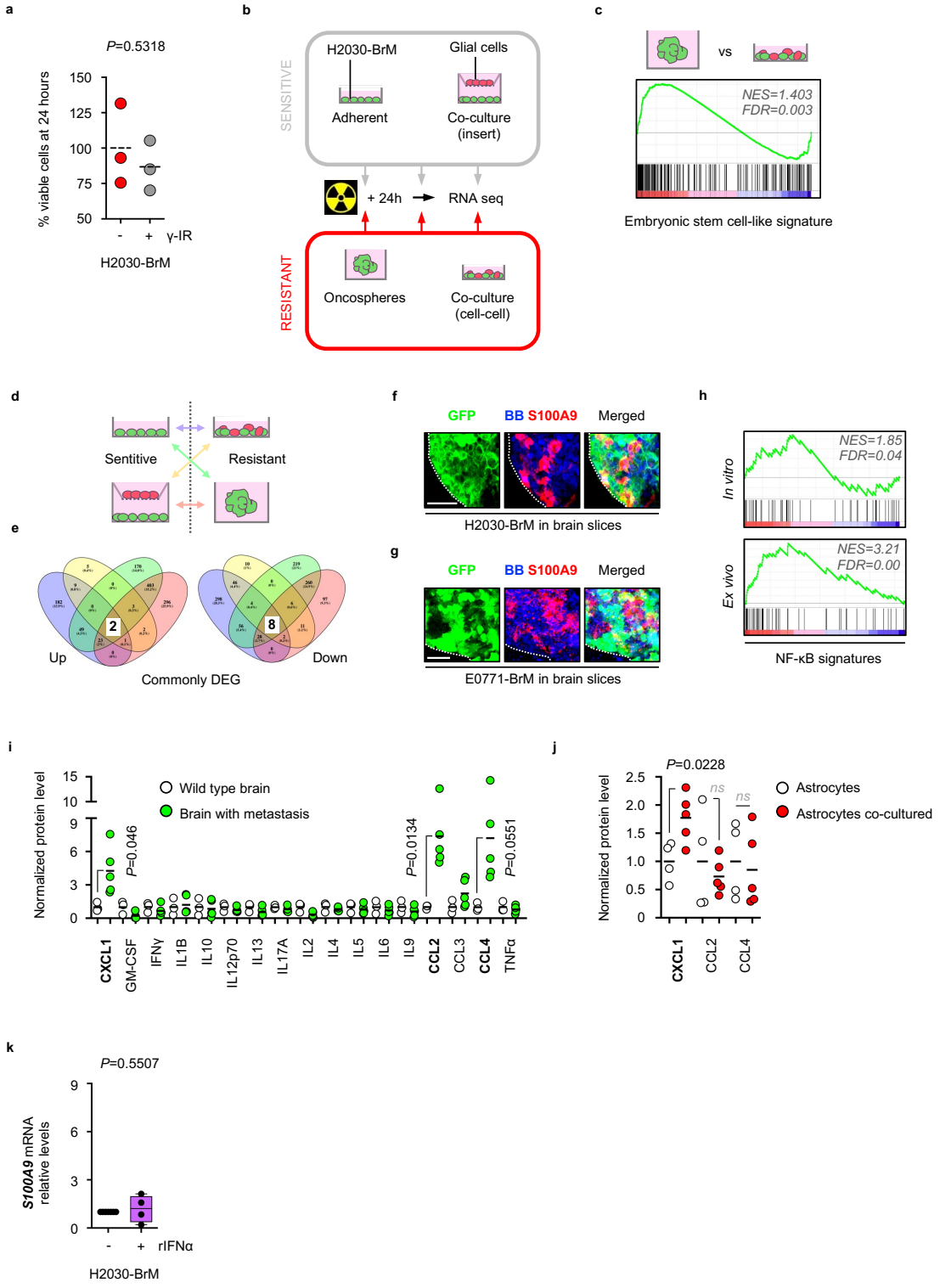

Contact-dependent astrocyte-released cytokines induce S100A9 secretion in cancer cells

triggering NF-κB activation. a, Quantification of *in vitro* viable cell fraction 24 hours after 10Gy irradiation as determined by manual cell counting of DAPI+ nuclei. Values are percentages of un-irradiated controls and shown in a dot plot where each dot represents an independent culture and the line in the box corresponds to the median (each n=3). *P* value was calculated using two-tailed t-test. **b**, Schema of experimental design. **c**, Gene Set Enrichment Analysis (GSEA) was performed on a pre-ranked list of differentially expressed genes between resistant culture preparations including oncospheres and co-cultures. The embryonic stem cell-like signature is significantly enriched in oncospheres (Supplementary Table 2). The green curve corresponds to the Enrichment Score, while the Normalized Enrichment Score (NES) and the False Discovery Rate (FDR) are shown in the graph. **d**, Schema of the different comparisons done with the transcriptomes from resistant and sensitive preparations to identify commonly deregulated genes. **e**, Venn diagram indicating commonly upregulated and downregulated genes in resistant *in vitro* surrogates under the condition shown in (**b**). Colors in the circles represent the comparison indicated with the arrows in (**d**) with the same color code. **f**, **g**, Representative immunofluorescent images of H2030-BrM and E0771-BrM cells plated on organotypic brain slices *ex vivo*. Scale bars: 50 μm. This experiment was repeated three times with similar results. **h**, Representative graphs of positively enriched gene sets depicting induction of NF-κB among a pre-ranked list of differentially expressed genes from resistant culture preparations *in vitro* and *ex vivo* (Supplementary Table 6). The green curve corresponds to the Enrichment Score, while the Normalized Enrichment Score (NES) and the False Discovery Rate (FDR) are shown in each graph. **i**, Quantification of 17 murine cytokines in wild type mice brains and mice brains with H2030-BrM brain metastasis by multiplex cytokine assay. Values indicate cytokine concentration and are shown in a dot plot where each dot represents a brain and the line corresponds to the median (n=3, normal brains; n=5, brain metastasis brains). *P* values are calculated using two-tailed t test. **j**, Quantification of 3 selected murine cytokines in conditioned media (CM) from astrocytes cultured alone and astrocyte-H2030-BrM co-cultures *in vitro* by multiplex cytokine assay. Values indicate relative cytokine concentration to the astrocyte culture alone and are shown in a dot plot where each dot represents an independent experiment and the line corresponds to the median (n=4, CM from astrocytes; n=5, CM from astrocyte-H2030-BrM co-cultures). *P* values are calculated using two-tailed t test. **k**, Quantification of *S100A9* expression levels in H2030-BrM 3d after a single dose (10Gy) of radiation and treatment with either control or rIFNα. Expression values were normalized to their

respective non-irradiated control for each culture condition. Values are shown as box-and-whisker plots where every dot represents an independent experiment and the line in the box corresponds to the median (n=4, each experimental condition). Whiskers go from minimum to maximum values. *P* value is calculated using two-tailed t test.

Supplementary Figure 3.

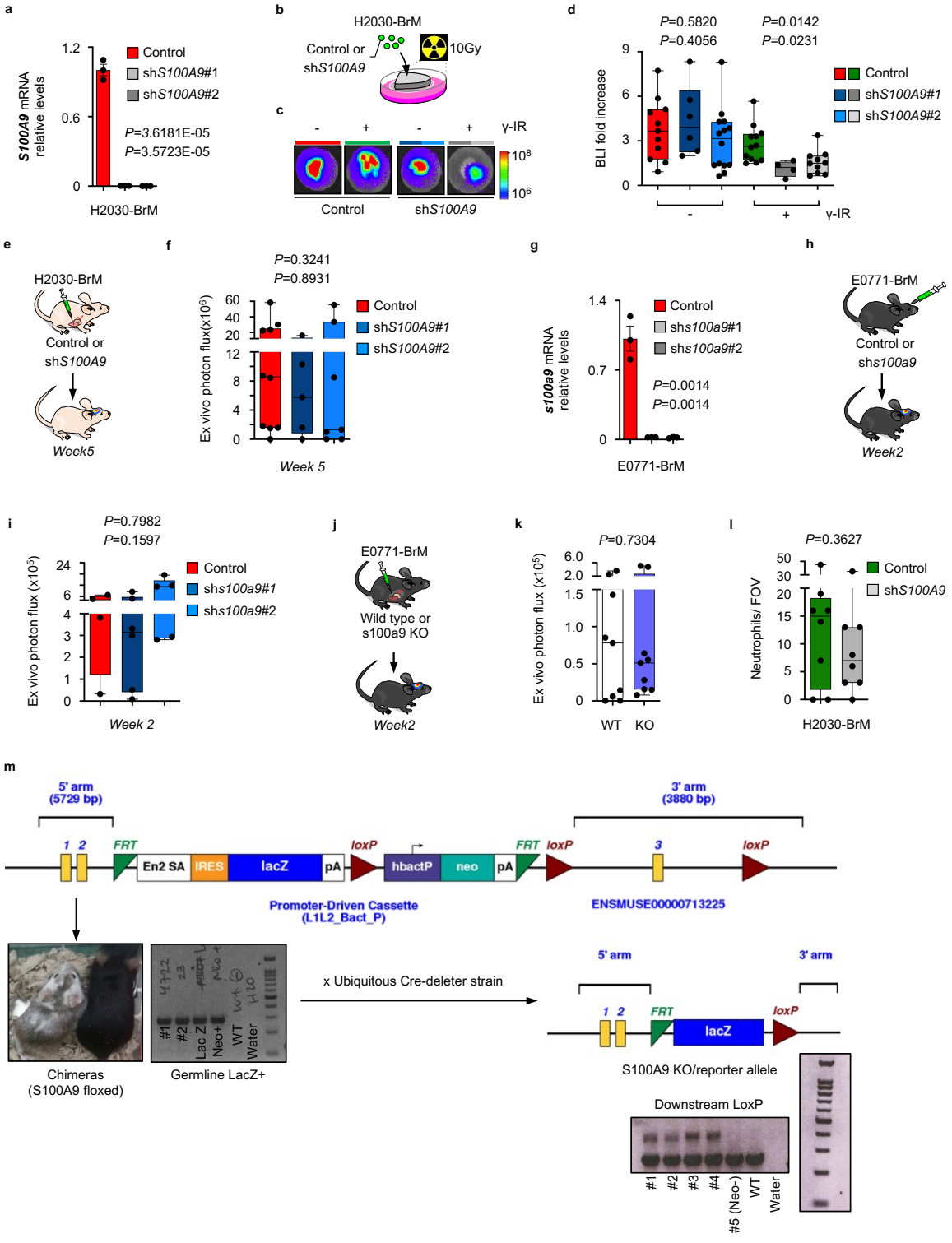

Targeting S100A9 in cancer cells radiosensitizes experimental lung and breast cancer brain

metastases in a NF-κB-JunB-dependent manner. a and **g**, Quantification of human *S100A9* (**a**) or mouse *S100a9* (**g**) gene expression by qRT-PCR in H2030-BrM and E0771-BrM cells transduced with a scrambled shRNA as control or two different shRNA against human *S100A9* (sh*S100A9*#1 and sh*S100A9*#2) or mouse *S100a9* (sh*S100a9*#1 and sh*S100a9*#2), respectively. Bars represents the mean ± s.e.m where every dot represents an independent culture (n = 3 cultures per experimental condition). P value was calculated using two-tailed t-test. **b**, Schema of experimental design. **c**, Representative bioluminescence images of brain organotypic cultures with metastatic cancer cells, transduced with a shRNA against *S100A9* or a scrambled shRNA as control, 72 hours after irradiation (10Gy, single dose) or no irradiation (0Gy). Color coded lines correlates with the corresponding bars in (**d**). **d**, Quantification of BLI from metastatic cells, transduced with either a scrambled shRNA as control (control), or one of two different shRNAs against *S100A9* (sh*S100A9*#1, sh*S100A9*#2), growing in organotypic brain cultures 72 hours after irradiation (10Gy, single dose) or no irradiation. Values were normalized to their respective non-irradiated controls and are shown in box-and-whisker plots where every dot represents an independent culture and the line in the box corresponds to the median. The boxes go from the upper to the lower quartiles and the whiskers go from the minimum to the maximum value (n=11, non-irradiated brain slices with H2030-BrM control; n=6, non-irradiated brain slices with H2030-BrM sh*S100A9#1*; n=14, non-irradiated brain slices with H2030-BrM sh*S100A9#2*; n=12, irradiated brain slices with H2030-BrM control; n=4, irradiated brain slices with H2030-BrM sh*S100A9#1*; n=10, irradiated brain slices with H2030-BrM sh*S100A9#2*). *P* value is calculated using two-tailed t test. **e** and **h**, Schema of experimental design. **f** and **i**, Quantification of the bioluminescence at the endpoint of the experiments depicted in (**e**, **h**) comparing brains from non-irradiated mice injected with H2030-BrM (**f**) or E0771-BrM (**i**) transduced with corresponding shRNA. Values are shown in box-and-whisker plots where every dot represents a different brain and the line in the box corresponds to the median. The boxes go from the upper to the lower quartiles and the whiskers go from the minimum to the maximum value (n=10, H2030-BrM control; n=5, H2030-BrM sh*S100A9*#1; n=7, H2030-BrM sh*S100A9*#2; n=4, E0771-BrM control; n=6, E0771-BrM sh*S100a9*#1; n=5, E0771-BrM sh*S100a9*#2). *P* value is calculated using two-tailed t test. **j**, Schema of experimental design. **k**, Quantification of the *ex vivo* photon flux at the endpoint of the experiment depicted in (**j**) comparing brains from $S100A9^{+/+}$ and $S100A9^{-/-}$ mice injected intracardially with E0771-BrM. Values are shown in box-and-whisker plots where every

dot represents a different brain and the line in the box corresponds to the median (n=9, S100A9$^{+/+}$ mice; n=9, S100A9$^{-/-}$ mice). The boxes go from the upper to the lower quartiles and the whiskers go from the minimum to the maximum value. *P* value was calculated using Mann-Whitney test, two-sided. **l**, Quantification of the numbers of neutrophils per FOV in brain metastasis from H2030-BrM control or sh*S100A9,* using the NIMP-R14 staining. For both conditions equal numbers of lesions of different sizes were chosen. Values are shown in box-and-whisker plots where every dot represents a metastatic lesion and the line in the box corresponds to the median. The boxes go from the upper to the lower quartiles and the whiskers go from minimum to maximum value (n=8 FOV from 2 brains, H2030-BrM control; n=8 FOV from three brains, H2030-BrM sh*S100A9*). *P* value was calculated using two-tailed t test.

Supplementary Figure 4.

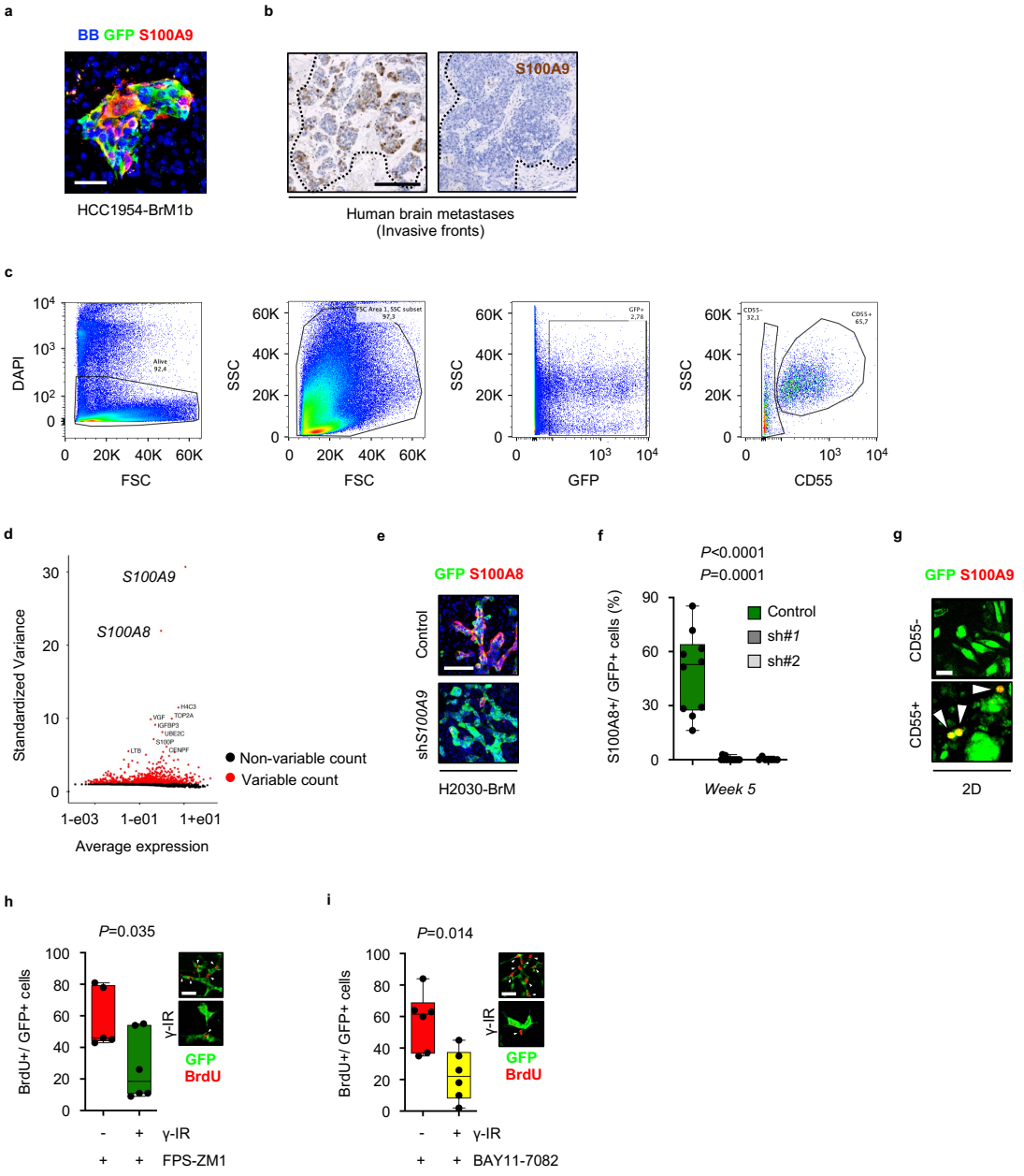

S100A9-mediated radioresistance is linked to cancer stem cell properties and sensitivity to RAGE and NF-κB inhibition. a, Representative image of a brain metastasis generated by HCC1954-BrMb. Scale bar: 50 µm. This experiment was repeated three times with similar results. **b**, Representative images of invasive fronts from human brain metastases (dotted lines). Scale bar: 200 µm. This experiment was performed once using the available samples with invasive fronts. **c**,

Gating strategy for fluorescence activated cell sorting (FACS) of CD55- and CD55+ cells from H2030-BrM brain metastases. **d**, Graph shows a subset of genes that exhibit high cell-to-cell variation in the dataset

obtained after modelling the mean-variance relationship inherent in single-cell data with Seurat[21]. **e**, Representative images of H2030-BrM Control and sh*S100A9* brain metastases. Scale bar: 100 μm. **f**, Quantification of the percentage of S100A8+ GFP+ positive cells in irradiated brain metastatic lesions *in vivo,* generated from intracardiac injection of H2030-BrM Control, H2030-BrM sh*S100A9#1* or H2030-BrM sh*S100A9#2* cells. Values are shown in box-and-whisker plots where every dot represents a metastatic lesion and the line in the box corresponds to the median. The boxes go from the upper to the lower quartiles and the whiskers go from the minimum to the maximum value (n=10 FOV, 2 brains, H2030-BrM Control + γ-IR; n=14 FOV, 3 brains, H2030-BrM sh*S100A9*#1 + γ-IR; n=7 FOV, 2 brains, H2030-BrM sh*S100A9*#2 + γ-IR). *P* value was calculated using two-tailed Mann-Whitney Test. **g**, Representative immunofluorescent images of sorted CD55- and CD55+ cells grown *in vitro.* Scale bar: 25 μm. This experiment was performed three times with similar results. **h**, Representative images and quantification of the mean percentage of BrdU+ cells per GFP+ cells in brain organotypic cultures with H2030-BrM after treatment with 10 μM of FPS-ZM1 and 10Gy irradiation or no irradiation. Values are shown in box-and-whisker plots where every dot represents an independent culture and the line in the box corresponds to the median. The boxes go from the upper to the lower quartiles and the whiskers go from the minimum to the maximum value (n=5, non-irradiated H2030-BrM; n=6 irradiated H2030-BrM, both treated with FPS-ZM1). *P* value is calculated using two-tailed t test. Scale bar: 50 μm. **i**, Representative images and quantification of the mean percentage of BrdU+ cells per GFP+ cells in brain organotypic cultures with H2030-BrM after treatment with 50 μM of BAY-117081 and 10Gy irradiation or no irradiation. Values are shown in box-and-whisker plots where every dot represents an independent culture and the line in the box corresponds to the median. The boxes go from the upper to the lower quartiles and the whiskers go from the minimum to the maximum value (n=6, non-irradiated H2030-BrM; n=6, irradiated H2030-BrM, both treated with BAY-117081). *P* value is calculated using two-tailed t test. Scale bar: 50 μm.

Supplementary Figure 5.

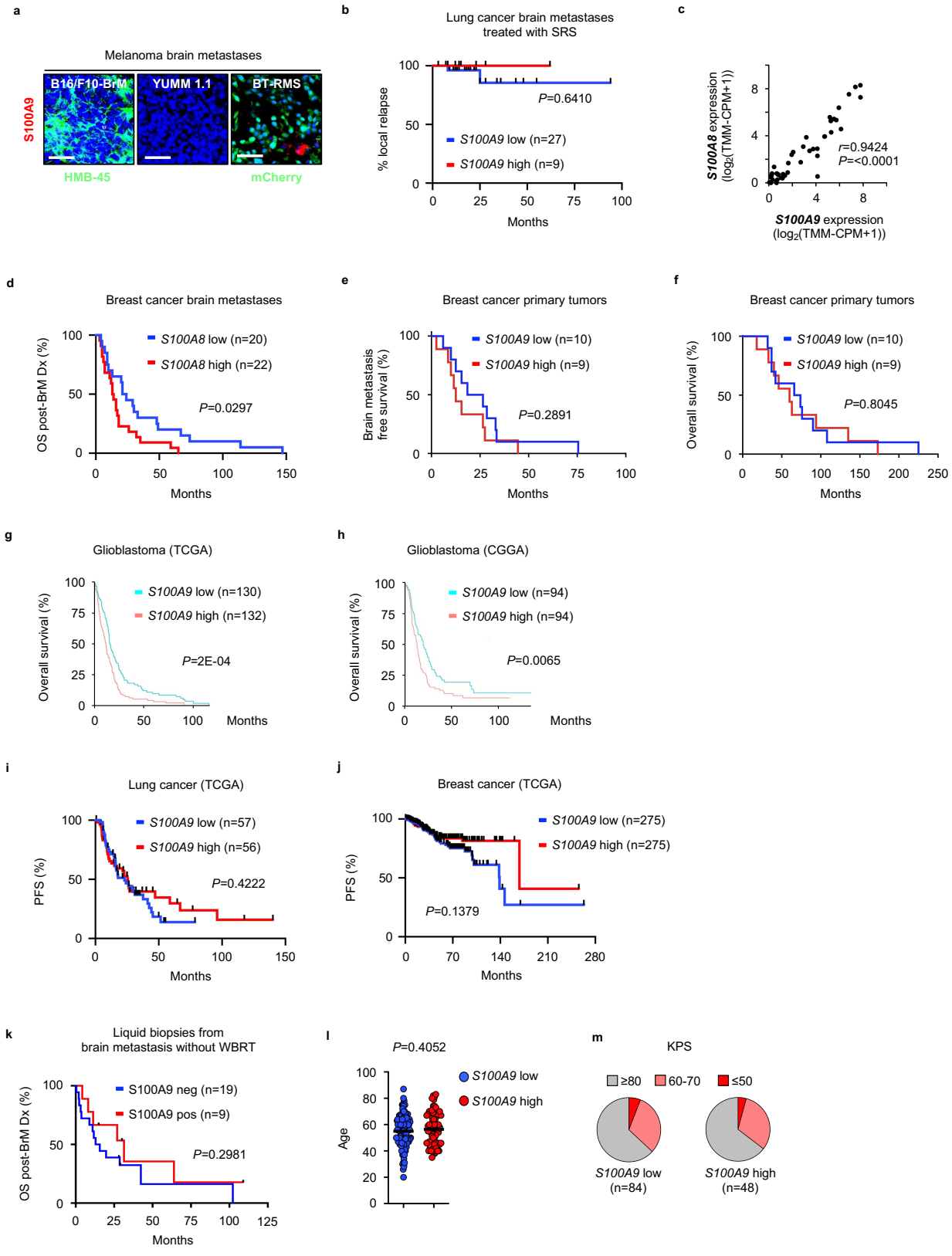

S100A9 is a brain metastasis biomarker of therapeutic response to WBRT. a, Representative images of immunofluorescent staining for S100A9 in brain metastases from three different murine brain metastatic melanoma models (B16/F10-BrM, YUMM1.1, BT-RMS). Scale bars: 50 μm. The experiment was performed three times for each model with similar results. **b**, Analysis of time to relapse in a cohort of 36 lung cancer brain metastasis patients treated with stereotactic radiosurgery (SRS). Data is shown as a Kaplan-Meier plot and two groups of patients (S100A9 low/high) were delineated by using 5% of S100A9 immunohistochemical staining positivity as a cut-off. *P* value was calculated using log rank (Mantel-Cox) test. **c**, Correlation of *S100A9* and *S100A8* gene expression in each respective patient from a cohort of 42 breast cancer brain metastases. Pearson R correlation coefficient and corresponding *P* value were calculated. **d**, Analysis of survival post-brain metastasis diagnosis in a cohort of 42 breast cancer brain metastasis patients. Only patients that received radiotherapy were included. Data is shown as a Kaplan-Meier plot and two groups of patients (S100A8 low/high) were delineated according to their *S100A8* mRNA expression levels in brain metastasis. *P* value was calculated using log rank (Mantel-Cox) test. **e**, Analysis of brain metastasis-free survival from primary tumor diagnosis in a previously published cohort of 19 breast cancer brain metastasis patients. Data is shown as a Kaplan-Meier plot and two groups of patients (S100A9 low/high) were delineated according to their *S100A9* mRNA expression levels in brain metastasis by using the median of *S100A9* expression as a cut-off. *P* value was calculated using log rank (Mantel-Cox) test. **f**, Analysis of overall survival post-primary tumor diagnosis in a previously published cohort of 19 breast cancer brain metastasis patients. Data is shown as a Kaplan-Meier plot and two groups of patients (S100A9 low/high) were delineated according to their *S100A9* mRNA expression levels in brain metastasis by using the median of *S100A9* expression as a cut-off. *P* value was calculated using log rank (Mantel-Cox) test. **g**, **h**, Analysis of overall survival post-primary tumor diagnosis in the glioblastoma TCGA (**g**) and CGGA (**h**) cohorts treated with the standard-of-care, which includes neurosurgery, radiotherapy and temozolomide [42]. Data is shown as a Kaplan-Meier plot and two groups of patients (S100A9 low/high) were delineated according to their *S100A9* mRNA expression levels in brain metastasis by using the 1st and 4th quartile of *S100A9* expression as a cut-off. *P* value was calculated using log rank (Mantel-Cox) test. **i**, **j**, Analysis of progression-free survival in the TCGA lung cancer (**i**) and breast cancer (**j**) cohort. Only patients that were treated with radiotherapy were included. Data is shown as Kaplan-Meier plots and two groups of patients (S100A9 low/high) were

delineated according to their S100A9 mRNA expression levels in primary lung and breast tumors using the respective median expression as cut-off. *P* value was calculated using log rank (Mantel-Cox) test. **k**, Analysis of survival post-brain metastasis diagnosis in a combined cohort of lung cancer brain metastasis patients (3 cases) and breast cancer brain metastasis patients (25 cases) that did not receive WBRT. Data is shown as a Kaplan-Meier plot and two groups of patients (S100A9 negative/positive) were delineated by their S100A9 positivity in serum samples. *P* value was calculated using log rank (Mantel-Cox) test. **l**, Analysis of patient age at neurosurgery/WBRT of 73 S100A9 high and 128 S100A9 low patients from all cohorts of brain metastasis patients used in this study where age was available (Supplementary Tables 13, 15, 16, 17 and 21). Values are shown in dot plots where each dot represents a patient and the line corresponds to the median. *P* value was calculated using two-tailed t-test. **m**, Analysis of KPS score at neurosurgery/WBRT of S100A9 48 high and 84 S100A9 low patients from all cohorts of brain metastasis patients used in this study where KPS was available (Supplementary Tables 13, 15, 17 and 21). Values are shown in pie charts representing percentages of each respective KPS score in either S100A9 high or low patients. For S100A9 high, 2 patients had a KPS score <50, 15 patients had a score 60-70 and 31 patients had a score >80. For S100A9 low patients, 5 patients had a KPS score <50, 26 patients had a score of 60-70 and 51 patients had a score >80.

Supplementary Figure 6.

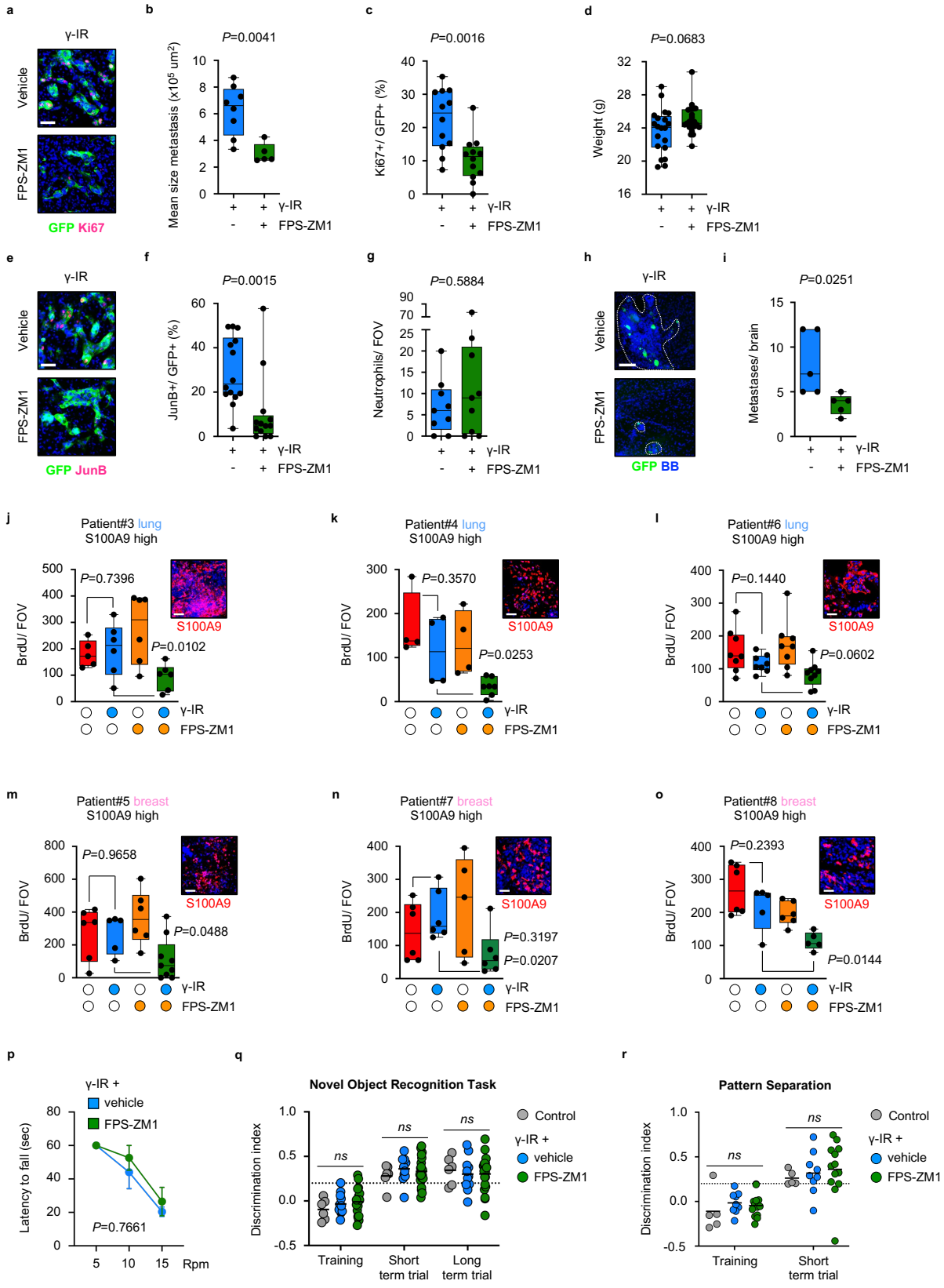

FPS-ZM1 radiosensitizes experimental and human brain metastases. a, Representative images of brain metastases at the experimental endpoint as described in (Fig. 6a). Scale bar: 50 μm. **b**, Quantification of H2030-BrM metastasis mean size in mice treated with WBRT and vehicle or FPS-ZM1 as indicated in (Fig.6a). Values are shown in box-and-whisker plots where every dot represents a brain and the line in the box corresponds to the median. The boxes go from the upper to the lower quartiles and the whiskers go from the minimum to the maximum value (n=8, Vehicle + γ-IR; n=5, FPS-ZM1 + γ-IR). *P* value was calculated using two-tailed t-test. **c**, Quantification of proliferation using Ki67 in H2030-BrM metastases from mice treated with WBRT and vehicle or FPS-ZM1 as indicated in (Fig. 6a). Values are shown in box-and-whisker plots where every dot represents a metastatic lesion obtained from 4 brains in each experimental condition and the line in the box corresponds to the median. The boxes go from the upper to the lower quartiles and the whiskers go from the minimum to the maximum value (n=12, Vehicle + γ-IR; n=12, FPS-ZM1 + γ-IR). *P* value was calculated using two-tailed t-test. **d**, Quantification of mouse weight at the end of the experiment as indicated in (Fig. 6a) comparing mice treated with WBRT and vehicle or FPS-ZM1. Values are shown in box-and-whisker plots where every dot represents a mouse and the line in the box corresponds to the median. The boxes go from the upper to the lower quartiles and the whiskers go from the minimum to the maximum value (n=20, Vehicle + γ-IR; n=21, FPS-ZM1 + γ-IR). *P* value was calculated using two-tailed t-test. **e**, Representative images of brain metastases at the experimental endpoint as described in (Fig. 6a) stained for JunB. Scale bar: 50 μm. **f**, Quantification of JunB+ GFP+ H2030-BrM cells in mice treated with WBRT and vehicle or FPS-ZM1 as indicated in (Fig. 6a). Values are shown in box-and-whisker plots where every dot represents a metastatic lesion obtained from 4 brains in each experimental condition and the line in the box corresponds to the median. The boxes go from the upper to the lower quartiles and the whiskers go from the minimum to the maximum value (n=14 metastases from 4 mice, Vehicle + γ-IR; n=13 metastases from 4 mice, FPS-ZM1 + γ-IR). *P* value was calculated using two-tailed Mann-Whitney Test. **g**, Quantification of neutrophils per FOV in H2030-BrM brain metastasis from mice treated with either WBRT and vehicle or FPS-ZM1, using the NIMP-R14 staining. For both conditions equal numbers of lesions of different sizes were chosen. Values are shown in box-and-whisker plots where every dot represents a metastatic lesion and the line in the box corresponds to the median. The boxes go from the upper to the lower quartiles and the whiskers go from minimum to maximum value (n=9 FOV, each experimental condition). *P* value was

calculated using two-tailed t test. **h**, Representative images of brain metastases at the experimental endpoint as described in (Extended Data Fig. 5a). Scale bar: 75 μm. **i**, Quantification of E0771-BrM metastases in mice treated with WBRT and vehicle or FPS-ZM1 as indicated in (Extended Data Fig. 5a). Values are shown in box-and-whisker plots where every dot represents a mouse and the line in the box corresponds to the median. The boxes go from the upper to the lower quartiles and the whiskers go from the minimum to the maximum value (n=5, Vehicle + γ-IR; n=5, FPS-ZM1 + γ-IR). *P* value was calculated using two-tailed t-test. **j**-**o**, Quantification of BrdU+ cancer cells in PDOC treated with FPS-ZM1 and/or γ-IR obtained from patient#3 (**j**), patient#4 (**k**), patient#5 (**m**), patient#6 (**l**), patient#7 (**n**) and patient#8 (**o**). Values are shown in box-and-whisker plots where every dot represents a FOV (4-9 FOV per experimental condition obtained from 4-6 organotypic cultures) and the line in the box corresponds to the median. The boxes go from the upper to the lower quartiles and the whiskers go from the minimum to the maximum value. *P* value was calculated using two-tailed t-test. A representative image in each PDOC show S100A9 levels. Scale bar: 50 μm. **p**, Quantification of latency to fall at three different constant speeds of mice treated with WBRT and either vehicle or FPS-ZM1. Values shown are mean ± SEM (n=5 mice, each experimental condition). *P* value was calculated using two-tailed t-test. **q**, Quantification of discrimination index comparing different groups when trained and when short term and long-term memories were evaluated. Values are shown in a scatter dot plot where every dot represents a mouse and the line corresponds to the mean (n=6, Control; n=13, Vehicle + γ-IR, n=20, FPS-ZM1 + γ-IR). Calculation of *P* values are detailed in Supplementary Table 24. **r**, Quantification of discrimination index comparing different groups when trained and when short term memory was evaluated. Values are shown in a scatter dot plot where every dot represents a mouse and the line corresponds to the mean (n=6, Control; n=13, Vehicle + γ-IR, n=20, FPS-ZM1 + γ-IR). Calculation of *P* values are detailed in Supplementary Table 24.

Supplementary Tables.

Supplementary Table 1.

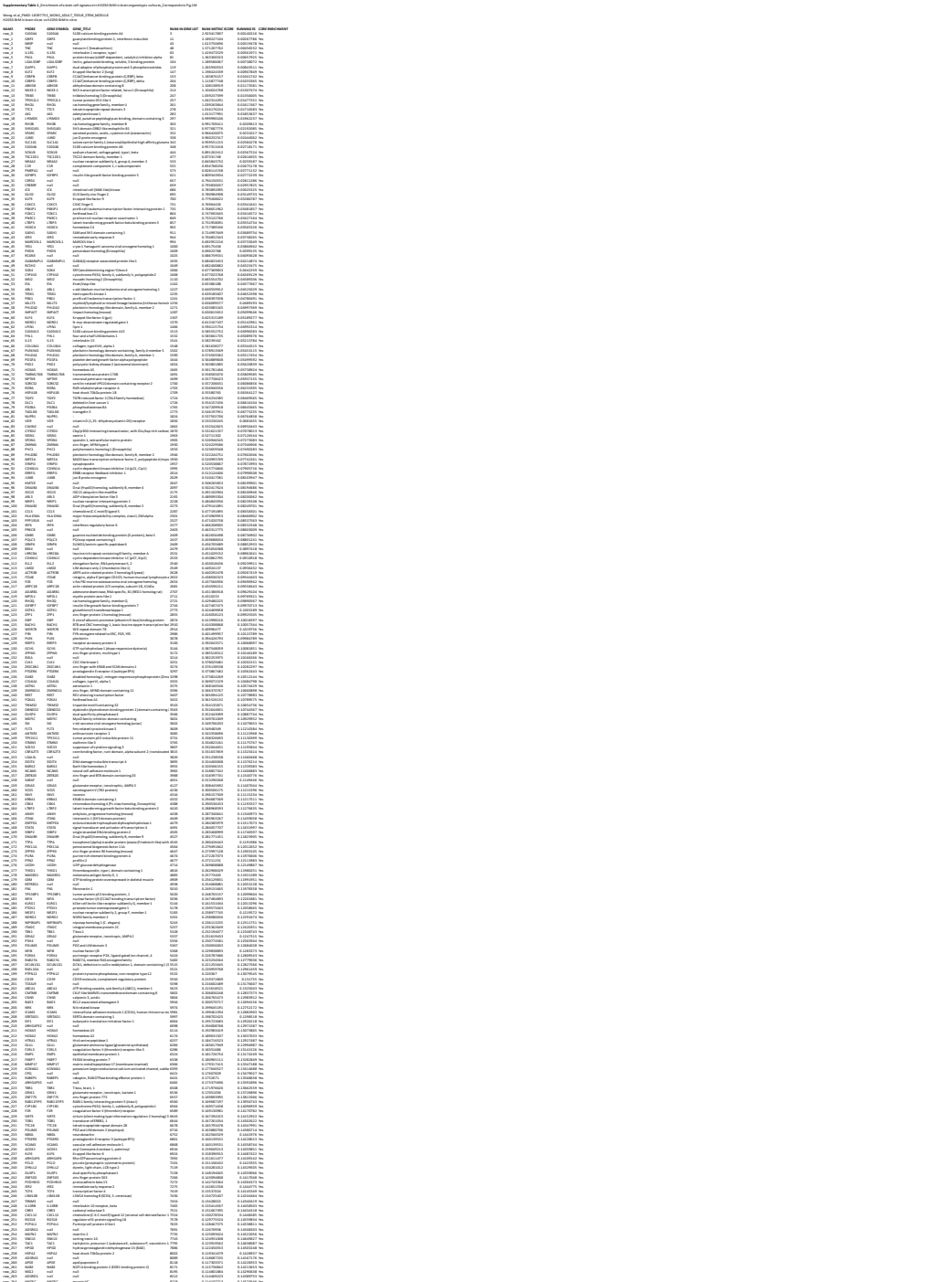

Supplementary Table 1. Enrichment of a stem cell signature in H2030-BrM in brain organotypic cultures_Correspondence Fig.1A

Wang, et al. | NASJ-18-00775J_WANG_ADULT_TRIUM_STEM_SIGNATURE

H2030-BrM in brain slices vs H2030-BrM in vitro

NAME	PROBE	GENE SYMBOL	GENE_TITLE	RANK IN GENE LIST	RANK METRIC SCORE	RUNNING ES	CORE ENRICHMENT
row_0	510044	510044	510 ribosomal biogenesis 44	3	2.93165 7807	0.00140514	Yes
row_1	10893	10893	guanylate binding protein 1, interferon-inducible	11	2.18167 7434	0.00267788	Yes
row_2	4859	nuc	nucleic	43	1.61376886	0.00346787	Yes
row_3	3576	IL2RA	interleukin 2 receptor, alpha	45	1.60 7 1 7 1	0.00 4 2 7 7	Yes
row_4	IL1R1	IL1R1	interleukin 1 receptor, type I	63	1.42437 3129	0.00 4 2 9 7 1	Yes
row_5	PIK3	PIK3	protein kinase (cAMP-dependent, catalytic) inhibitor alpha	81	1.30 3 3 0 3 2 3	0.00 5 7 9 2 5	Yes
row_6	5 2 4 3	5 2 4 3	5 2 4 3 ribosomal biogenesis homolog (S. cerevisiae)	1 2 4	1.2 3 3 3 3 3 3	0.00 5 7 9 2 5	Yes
row_7	DUSP1	DUSP1	dual specificity phosphatase 1	1 2 9	1.2 0 3 3 3 3 3	0.00 6 2 1 1 1	Yes
row_8	KLF2	KLF2	Kruppel-like factor 2 (lung)	1 4 7	1.1 9 6 2 4 3 3 9	0.00 6 7 8 4 1	Yes
row_9	CBFA2	CBFA2	CCAAT/enhancer-binding protein (C/EBP), beta	1 5 3	1.1 8 3 7 5 3 3 7	0.00 7 4 1 7 4 1	Yes
row_10	CEBPD	CEBPD	CCAAT/enhancer-binding protein (C/EBP), delta	2 0 4	1.1 7 3 8 7 7 0 8	0.00 8 3 3 5 6 1	Yes
row_11	CEBPB	CEBPB	CCAAT/enhancer-binding protein (C/EBP), beta	2 1 4	1.1 6 9 3 3 3 3 3	0.00 8 8 3 3 6 1	Yes
row_12	NR3C1	NR3C1	NR3 C1 nuclear receptor subfamily 3, group C, member 1	2 1 4	1.1 6 6 6 1 7 0 8	0.00 9 3 7 7 5 1	Yes
row_13	TR4S	TR4S	tr4 ddx hormone 4 [Drosophila]	2 4 7	1.0 9 5 2 7 5 9 9	0.01 0 0 6 2 0 5	No
row_14	CBFA2	CBFA2	core-binding factor, alpha 2	2 5 3	1.0 9 3 3 3 3 3 3	0.01 0 3 3 3 3 1	No
row_15	RHOA	RHOA	ras homolog gene family, member A	2 6 1	1.0 9 2 6 3 6 6 4	0.01 0 6 7 6 6 1	No
row_16	TIC3	TIC3	tetratricopeptide repeat domain 3	2 7 6	1.0 8 6 7 5 2 3 1	0.01 0 7 0 8 5 1	No
row_17	CD69	CD69	CD69 molecule	2 8 3	1.0 8 4 3 3 3 3 3	0.01 0 7 7 3 3 1	No
row_18	LYSA05	LYSA05	lysA2 arsenite peptidoglycan binding domain containing 5	2 9 7	1.0 8 0 9 9 5 2 6 6	0.01 0 8 2 3 7 1	No
row_19	RHOB	RHOB	ras homolog gene family, member B	3 0 5	1.0 8 1 7 8 5 6 1 1	0.01 0 9 6 2 1	No
row_20	SH3D1A6	SH3D1A6	SH3 domain (SRC3 like-receptor)in 61	3 2 1	1.0 7 9 8 7 7 7 6	0.01 1 0 3 0 8 6	No
row_21	SPARC	SPARC	secreted protein, acidic, cysteine-rich (osteonectin)	3 3 2	1.0 7 8 4 2 6 0 7 5	0.01 1 0 5 2 7	No
row_22	SLC1A3	SLC1A3	solute carrier family 1 (neuronal/epithelial high affinity glutamate	3 4 3	1.0 7 7 0 3 3 3 3 3	0.01 1 0 7 7 7 1	No
row_23	SLC1A1	SLC1A1	solute carrier family 1 (neuronal/epithelial high affinity glutamate	3 5 2	1.0 7 6 9 1 2 2 1 5	0.01 1 0 9 2 7 6	No
row_24	510048	510048	510 ribosomal biogenesis 48	3 6 8	1.0 7 5 7 3 1 6 1 8	0.01 1 0 7 2 7 1	No
row_25	TIC3	TIC3	tetratricopeptide repeat domain 3	3 7 4	1.0 7 5 2 3 3 3 3 3	0.01 1 0 7 7 7 1	No
row_26	TIC1S5	TIC1S5	TIC1S domain family, member 5	3 7 7	1.0 7 5 1 7 6 6	0.01 1 0 8 2 6 1	No
row_27	NR4A2	NR4A2	nuclear receptor subfamily 4, group A, member 2	3 9 5	1.0 6 9 8 5 7 5 2	0.01 1 0 9 2 6 1	No
row_28	C1R	C1R	complement component 1, r subcomponent	3 9 5	1.0 6 7 8 2 3 3 6	0.01 1 0 7 5 7 6	No
row_29	PIAP5A2	null	null	3 7 3	1.0 6 5 2 1 1 7 6 8	0.01 1 1 1 1 2	No
row_30	PIAP5A2	null	null	3 7 4	1.0 6 5 2 1 1 7 6 8	0.01 1 1 1 1 2	No
row_31	CBFA1	null	null	3 7 7	1.0 6 4 9 7 7 7 7	0.01 1 1 2 8 6	No
row_32	CREB1	null	null	3 8 7	1.0 6 4 1 1 2 8 5	0.01 1 1 3 8 6	No
row_33	CREBF	null	null	4 0 9	1.0 6 3 8 3 3 3 7	0.01 1 1 5 3 6	No
row_34	CD4	CD4	CD4 molecule, cell (1988-1be)/mouse	4 1 0	1.0 6 3 5 3 3 3 3	0.01 1 1 6 3 6	No
row_35	GLI2	GLI2	GLI2 family zinc finger 2	4 9 1	1.0 5 8 9 6 4 9 8	0.01 1 4 7 5 1	No
row_36	KLF9	KLF9	Kruppel-like factor 9	7 9 3	0.7 7 5 3 8 4 2 2	0.01 5 8 7 9 7	No
row_37	CD4 5	CD4 5	CD4(Drager 5	7 5 1	0.7 6 9 6 6 1 3 5	0.01 5 8 4 4 1	No
row_38	PIAP1	PIAP1	prolif cell 1 lactamase trigger factor 1 like interacting protein 1	7 5 5	0.7 6 8 0 1 9 6 2	0.01 5 8 5 1 7	No
row_39	PIAP1	PIAP1	prolif cell 1 lactamase trigger factor 1 like interacting protein 1	7 5 5	0.7 6 8 0 1 9 6 2	0.01 5 8 5 1 7	No
row_40	PIAP2	PIAP2	protein-rich nuclear receptor coactivator 1	8 0 9	0.7 5 5 2 2 7 8 6	0.01 6 2 7 1 6 1	No
row_41	LTBP1	LTBP1	latent transforming growth factor beta binding protein 3	8 1 7	0.7 5 1 9 6 8 8 1	0.01 6 3 7 3 1	No
row_42	null	null	null	8 1 8	0.7 5 1 8 3 3 3 3	0.01 6 3 7 3 1	No
row_43	SASH1	SASH1	SAM and SH3 domain containing 1	9 1 1	0.7 4 9 9 7 6 6 9	0.01 6 8 8 7 3 6 1	No
row_44	6931	6931	normalization early response 1	9 6 4	0.7 4 8 0 2 3 6 3	0.01 7 0 7 6 2 6 1	No
row_45	NR4A3	NR4A3	nuclear receptor subfamily 4, group A, member 3	9 9 1	0.7 4 6 8 3 3 3 3	0.01 7 2 2 3 1	No
row_46	NR3 1	NR3 1	NR3 1 nuclear receptor subfamily 3, group C, member 1	1 0 3 3	0.7 4 5 3 1 3 3 3	0.01 7 3 3 3 1	No
row_47	DUSP4	DUSP4	dual specificity phosphatase 4	1 0 3 8	0.7 4 3 7 7 7 7 3	0.01 7 3 4 3 1	No
row_48	GABARAPL1	GABARAPL1	(GABA(A) receptor-associated protein like 1	1 0 3 9	0.7 4 3 6 8 2 8 3	0.01 7 3 8 7 6	No
row_49	5 2 4 3	5 2 4 3	5 2 4 3 ribosomal biogenesis homolog (S. cerevisiae)	1 0 4 1	0.7 4 3 3 3 3 3 3	0.01 7 3 8 7 6	No
row_50	SOX4	SOX4	SRY (sex determining region Y)-box 4	1 0 8 8	0.7 3 9 8 8 5 3	0.01 7 5 3 3 1	No
row_51	CYP1A2	CYP1A2	cytochrome P450, family 1, subfamily I, polypeptide 2	1 0 8 8	0.7 3 2 1 7 5 8	0.01 8 1 2 9 1	No
row_52	TIC3	TIC3	tetratricopeptide repeat domain 3 [Drosophila]	1 1 0 2	0.7 3 1 3 3 3 3 3	0.01 8 1 3 8 1	No
row_53	FOS	FOS	FBJ murine osteosarcoma viral oncogene homolog	1 1 4 2	0.7 3 0 3 8 1 8 8	0.01 8 2 7 8 6 1	No
row_54	ABL1	ABL1	v-abl Abelson murine leukemia viral oncogene homolog 1	1 2 3 7	0.7 2 9 5 9 9 5 2	0.01 8 2 8 2 6	No
row_55	GLI2	GLI2	GLI2 family zinc finger 2	1 2 9 1	0.7 2 8 9 4 3 6 8	0.01 8 3 3 7 6 1	No
row_56	PIK3	PIK3	protein-rich nuclear receptor coactivator 1	1 2 4 1	0.7 2 8 7 3 5 0 8	0.01 8 3 7 6 1	No
row_57	PIAP2	PIAP2	protein-rich nuclear receptor coactivator 2 (trithorax homolog)	1 2 7 1	0.7 2 7 1 7 5 6 6	0.01 8 4 1 1 6 1	No
row_58	PIAP2A2	PIAP2A2	phe-lactin-homology-like domain, family A, member 2	1 2 7 5	0.7 2 6 8 3 2 4 5	0.01 8 4 2 6 1	No
row_59	IMPACT	IMPACT	impact homolog (mouse)	1 2 8 7	0.7 2 5 9 3 5 8 2	0.01 8 4 6 1	No
row_60	PIAP1	PIAP1	protein-rich nuclear receptor 1	1 3 0 3	0.7 2 5 3 3 3 3 3	0.01 8 4 8 1	No
row_61	NR4A1	NR4A1	N-myc downstream-regulated gene 1	1 3 7 5	0.7 2 3 4 7 3 3 7	0.01 8 5 6 1	No
row_62	LPIN1	LPIN1	lipin 1	1 4 4 6	0.7 2 1 1 7 5 1	0.01 8 5 7 1	No
row_63	PIAP1	PIAP1	protein-rich nuclear receptor coactivator 1	1 4 4 7	0.7 2 1 1 7 5 1	0.01 8 5 7 1	No
row_64	PIK3	PIK3	four-and-a-half LIM domains 1	1 5 1 2	0.7 1 9 8 1 7 5 5	0.01 8 6 3 1	No
row_65	IL15	IL15	interleukin 15	1 5 4 1	0.7 1 9 7 9 4 0	0.01 8 7 5 6	No
row_66	COL18A1	COL18A1	collagen, type XVIII, alpha 1	1 5 4 8	0.7 1 8 9 8 2 7 7	0.01 8 8 1 1	No
row_67	PLEKH2	PLEKH2	pleckstrin homology domain containing, family B member 5	1 5 4 2	0.7 1 8 9 1 3 5 8	0.01 8 8 1 1 1	No
row_68	PLEKH2	PLEKH2	pleckstrin homology-like domain, family B, member 2	1 5 4 3	0.7 1 8 9 1 3 5 8	0.01 8 8 1 1 1	No
row_69	PLEP2	PLEP2	platelet-derived growth factor alpha polypeptide	1 5 4 6	0.7 1 8 8 8 6 6 8	0.01 8 9 0 2	No
row_70	PIK3 2	PIK3 2	polycystic kidney disease 2 (autosomal dominant)	1 5 5 4	0.7 1 8 8 1 3 8 5	0.01 8 9 3 8 1	No
row_71	5 2 4 3	5 2 4 3	5 2 4 3 homolog	1 5 5 5	0.7 1 8 8 0 0 0 0	0.01 8 9 3 8 1	No
row_72	COL18A1	COL18A1	collagen, type XVIII, alpha 1	1 5 4 8	0.7 1 8 9 8 2 7 7	0.01 8 8 1 1 1	No
row_73	TNFRSF6	TNFRSF6	transmembrane protein 1 7 8 8	1 5 9 5	0.7 1 8 5 6 7 6 6	0.01 8 9 0 2	No
row_74	NFTD5	NFTD5	nuclear receptor subfamily 4, group A, member 2	1 5 9 9	0.7 1 7 7 5 6 2 3	0.01 8 9 3 8 1	No
row_75	SOX12	SOX12	sox9 (sry-related HMG-box)-activated string receptor 2	1 7 0 0	0.7 1 7 2 6 5 5 1	0.01 9 0 0 8 6	No
row_76	RORA	RORA	RAR-related orphan receptor A	1 7 0 2	0.7 1 6 9 0 3 5 5	0.01 9 0 3 3 9 6	No
row_77	TGIF2	TGIF2	TGFB-induced factor 2 (TALE family homeobox)	1 7 1 4	0.7 1 6 4 3 3 3 3	0.01 9 0 4 3 9 6	No
row_78	TGIF2	TGIF2	TGFB-induced factor 2 (TALE family homeobox)	1 7 3 4	0.7 1 5 4 3 3 3 3	0.01 9 0 5 8 9 6	No
row_79	DLC1	DLC1	deleted in liver cancer 1	1 7 3 6	0.7 1 5 3 7 0 8	0.01 9 0 5 8 9 6	No
row_80	TGIF2	TGIF2	TGFB-induced factor 2	1 7 3 6	0.7 1 5 3 7 0 8	0.01 9 0 5 8 9 6	No
row_81	TGIF2	TGIF2	TGFB-induced factor 2	1 7 3 6	0.7 1 5 3 7 0 8	0.01 9 0 5 8 9 6	No
row_82	TGIF2	TGIF2	TGFB-induced factor 2	1 7 3 6	0.7 1 5 3 7 0 8	0.01 9 0 5 8 9 6	No
row_83	TGIF2	TGIF2	TGFB-induced factor 2	1 7 3 6	0.7 1 5 3 7 0 8	0.01 9 0 5 8 9 6	No
row_84	TGIF2	TGIF2	TGFB-induced factor 2	1 7 3 6	0.7 1 5 3 7 0 8	0.01 9 0 5 8 9 6	No
row_85	TGIF2	TGIF2	TGFB-induced factor 2	1 7 3 6	0.7 1 5 3 7 0 8	0.01 9 0 5 8 9 6	No
row_86	TGIF2	TGIF2	TGFB-induced factor 2	1 7 3 6	0.7 1 5 3 7 0 8	0.01 9 0 5 8 9 6	No
row_87	TGIF2	TGIF2	TGFB-induced factor 2	1 7 3 6	0.7 1 5 3 7 0 8	0.01 9 0 5 8 9 6	No
row_88	TGIF2	TGIF2	TGFB-induced factor 2	1 7 3 6	0.7 1 5 3 7 0 8	0.01 9 0 5 8 9 6	No
row_89	TGIF2	TGIF2	TGFB-induced factor 2	1 7 3 6	0.7 1 5 3 7 0 8	0.01 9 0 5 8 9 6	No
row_90	TGIF2	TGIF2	TGFB-induced factor 2	1 7 3 6	0.7 1 5 3 7 0 8	0.01 9 0 5 8 9 6	No
row_91	TGIF2	TGIF2	TGFB-induced factor 2	1 7 3 6	0.7 1 5 3 7 0 8	0.01 9 0 5 8 9 6	No
row_92	TGIF2	TGIF2	TGFB-induced factor 2	1 7 3 6	0.7 1 5 3 7 0 8	0.01 9 0 5 8 9 6	No
row_93	TGIF2	TGIF2	TGFB-induced factor 2	1 7 3 6	0.7 1 5 3 7 0 8	0.01 9 0 5 8 9 6	No
row_94	TGIF2	TGIF2	TGFB-induced factor 2	1 7 3 6	0.7 1 5 3 7 0 8	0.01 9 0 5 8 9 6	No
row_95	TGIF2	TGIF2	TGFB-induced factor 2	1 7 3 6	0.7 1 5 3 7 0 8	0.01 9 0 5 8 9 6	No
row_96	TGIF2	TGIF2	TGFB-induced factor 2	1 7 3 6	0.7 1 5 3 7 0 8	0.01 9 0 5 8 9 6	No
row_97	TGIF2	TGIF2	TGFB-induced factor 2	1 7 3 6	0.7 1 5 3 7 0 8	0.01 9 0 5 8 9 6	No
row_98	TGIF2	TGIF2	TGFB-induced factor 2	1 7 3 6	0.7 1 5 3 7 0 8	0.01 9 0 5 8 9 6	No
row_99	TGIF2	TGIF2	TGFB-induced factor 2	1 7 3 6	0.7 1 5 3 7 0 8	0.01 9 0 5 8 9 6	No
row_100	TGIF2	TGIF2	TGFB-induced factor 2	1 7 3 6	0.7 1 5 3 7 0 8	0.01 9 0 5 8 9 6	No
row_101	TGIF2	TGIF2	TGFB-induced factor 2	1 7 3 6	0.7 1 5 3 7 0 8	0.01 9 0 5 8 9 6	No
row_102	TGIF2	TGIF2	TGFB-induced factor 2	1 7 3 6	0.7 1 5 3 7 0 8	0.01 9 0 5 8 9 6	No
row_103	TGIF2	TGIF2	TGFB-induced factor 2	1 7 3 6	0.7 1 5 3 7 0 8	0.01 9 0 5 8 9 6	No
row_104	TGIF2	TGIF2	TGFB-induced factor 2	1 7 3 6	0.7 1 5 3 7 0 8	0.01 9 0 5 8 9 6	No
row_105	TGIF2	TGIF2	TGFB-induced factor 2	1 7 3 6	0.7 1 5 3 7 0 8	0.01 9 0 5 8 9 6	No
row_106	TGIF2	TGIF2	TGFB-induced factor 2	1 7 3 6	0.7 1 5 3 7 0 8	0.01 9 0 5 8 9 6	No
row_107	TGIF2	TGIF2	TGFB-induced factor 2	1 7 3 6	0.7 1 5 3 7 0 8	0.01 9 0 5 8 9 6	No
row_108	TGIF2	TGIF2	TGFB-induced factor 2	1 7 3 6	0.7 1 5 3 7 0 8	0.01 9 0 5 8 9 6	No
row_109	TGIF2	TGIF2	TGFB-induced factor 2	1 7 3 6	0.7 1 5 3 7 0 8	0.01 9 0 5 8 9 6	No
row_110	TGIF2	TGIF2	TGFB-induced factor 2	1 7 3 6	0.7 1 5 3 7 0 8	0.01 9 0 5 8 9 6	No
row_111	TGIF2	TGIF2	TGFB-induced factor 2	1 7 3 6	0.7 1 5 3 7 0 8	0.01 9 0 5 8 9 6	No
row_112	TGIF2	TGIF2	TGFB-induced factor 2	1 7 3 6	0.7 1 5 3 7 0 8	0.01 9 0 5 8 9 6	No
row_113	TGIF2	TGIF2	TGFB-induced factor 2	1 7 3 6	0.7 1 5 3 7 0 8	0.01 9 0 5 8 9 6	No
row_114	TGIF2	TGIF2	TGFB-induced factor 2	1 7 3 6	0.7 1 5 3 7 0 8	0.01 9 0 5 8 9 6	No
row_115	TGIF2	TGIF2	TGFB-induced factor 2	1 7 3 6	0.7 1 5 3 7 0 8	0.01 9 0 5 8 9 6	No
row_116	TGIF2	TGIF2	TGFB-induced factor 2	1 7 3 6	0.7 1 5 3 7 0 8	0.01 9 0 5 8 9 6	No
row_117	TGIF2	TGIF2	TGFB-induced factor 2	1 7 3 6	0.7 1 5 3 7 0 8	0.01 9 0 5 8 9 6	No
row_118	TGIF2	TGIF2	TGFB-induced factor 2	1 7 3 6	0.7 1 5 3 7 0 8	0.01 9 0 5 8 9 6	No
row_119	TGIF2	TGIF2	TGFB-induced factor 2	1 7 3 6	0.7 1 5 3 7 0 8	0.01 9 0 5 8 9 6	No
row_120	TGIF2	TGIF2	TGFB-induced factor 2	1 7 3 6	0.7 1 5 3 7 0 8	0.01 9 0 5 8 9 6	No
row_121	TGIF2	TGIF2	TGFB-induced factor 2	1 7 3 6	0.7 1 5 3 7 0 8	0.01 9 0 5 8 9 6	No
row_122	TGIF2	TGIF2	TGFB-induced factor 2	1 7 3 6	0.7 1 5 3 7 0 8	0.01 9 0 5 8 9 6	No
row_123	TGIF2	TGIF2	TGFB-induced factor 2	1 7 3 6	0.7 1 5 3 7 0 8	0.01 9 0 5 8 9 6	No
row_124	TGIF2	TGIF2	TGFB-induced factor 2	1 7 3 6	0.7 1 5 3 7 0 8	0.01 9 0 5 8 9 6	No
row_125	TGIF2	TGIF2	TGFB-induced factor 2	1 7 3 6	0.7 1 5 3 7 0 8	0.01 9 0 5 8 9 6	No
row_126	TGIF2	TGIF2	TGFB-induced factor 2	1 7 3 6	0.7 1 5 3 7 0 8	0.01 9 0 5 8 9 6	No
row_127	TGIF2	TGIF2	TGFB-induced factor 2	1 7 3 6	0.7 1 5 3 7 0 8	0.01 9 0 5 8 9 6	No
row_128	TGIF2	TGIF2	TGFB-induced factor 2	1 7 3 6	0.7 1 5 3 7 0 8	0.01 9 0 5 8 9 6	No
row_129	TGIF2	TGIF2	TGFB-induced factor 2	1 7 3 6	0.7 1 5 3 7 0 8	0.01 9 0 5 8 9 6	No
row_130	TGIF2	TGIF2	TGFB-induced factor 2	1 7 3 6	0.7 1 5 3 7 0 8	0.01 9 0 5 8 9 6	No
row_131	TGIF2	TGIF2	TGFB-induced factor 2	1 7 3 6	0.7 1 5 3 7 0 8	0.01 9 0 5 8 9 6	No
row_132	TGIF2	TGIF2	TGFB-induced factor 2	1 7 3 6	0.7 1 5 3 7 0 8	0.01 9 0 5 8 9 6	No
row_133	TGIF2	TGIF2	TGFB-induced factor 2	1 7 3 6	0.7 1 5 3 7 0 8	0.01 9 0 5 8 9 6	No
row_134	TGIF2	TGIF2	TGFB-induced factor 2	1 7 3 6	0.7 1 5 3 7 0 8	0.01 9 0 5 8 9 6	No
row_135	TGIF2	TGIF2	TGFB-induced factor 2	1 7 3 6	0.7 1 5 3 7 0 8	0.01 9 0 5 8 9 6	No
row_136	TGIF2	TGIF2	TGFB-induced factor 2	1 7 3 6	0.7 1 5 3 7 0 8	0.01 9 0 5 8 9 6	No
row_137	TGIF2	TGIF2	TGFB-induced factor 2	1 7 3 6	0.7 1 5 3 7 0 8	0.01 9 0 5 8 9 6	No
row_138	TGIF2	TGIF2	TGFB-induced factor 2	1 7 3 6	0.7 1 5 3 7 0 8	0.01 9 0 5 8 9 6	No
row_139	TGIF2	TGIF2	TGFB-induced factor 2	1 7 3 6	0.7 1 5 3 7 0 8	0.01 9 0 5 8 9 6	No
row_140	TGIF2	TGIF2	TGFB-induced factor 2	1 7 3 6	0.7 1 5 3 7 0 8	0.01 9 0 5 8 9 6	No
row_141	TGIF2	TGIF2	TGFB-induced factor 2	1 7 3 6	0.7 1 5 3 7 0 8	0.01 9 0 5 8 9 6	No
row_142	TGIF2	TGIF2	TGFB-induced factor 2	1 7 3 6	0.7 1 5 3 7 0 8	0.01 9 0 5 8 9 6	No
row_143	TGIF2	TGIF2	TGFB-induced factor 2	1 7 3 6	0.7 1 5 3 7 0 8	0.01 9 0 5 8 9 6	No
row_144	TGIF2	TGIF2	TGFB-induced factor 2	1 7 3 6	0.7 1 5 3 7 0 8	0.01 9 0 5 8 9 6	No
row_145	TGIF2	TGIF2	TGFB-induced factor 2	1 7 3 6	0.7 1 5 3 7 0 8	0.01 9 0 5 8 9 6	No
row_146	TGIF2	TGIF2	TGFB-induced factor 2	1 7 3 6	0.7 1 5 3 7 0 8	0.01 9 0 5 8 9 6	No
row_147	TGIF2	TGIF2	TGFB-induced factor 2	1 7 3 6	0.7 1 5 3 7 0 8	0.01 9 0 5 8 9 6	No
row_148	TGIF2	TGIF2	TGFB-induced factor 2	1 7 3 6	0.7 1 5 3 7 0 8	0.01 9 0 5 8 9 6	No
row_149	TGIF2	TGIF2	TGFB-induced factor 2	1 7 3 6	0.7 1 5 3 7 0 8	0.01 9 0 5 8 9 6	No
row_150	TGIF2	TGIF2	TGFB-induced factor 2	1 7 3 6	0.7 1 5 3 7 0 8	0.01 9 0 5 8 9 6	No
row_151	TGIF2	TGIF2	TGFB-induced factor 2	1 7 3 6	0.7 1 5 3 7 0 8	0.01 9 0 5 8 9 6	No
row_152	TGIF2	TGIF2	TGFB-induced factor 2	1 7 3 6	0.7 1 5 3 7 0 8	0.01 9 0 5 8 9 6	No
row_153	TGIF2	TGIF2	TGFB-induced factor 2	1 7 3 6	0.7 1 5 3 7 0 8	0.01 9 0 5 8 9 6	No
row_154	TGIF2	TGIF2	TGFB-induced factor 2	1 7 3 6	0.7 1 5 3 7 0 8	0.01 9 0 5 8 9 6	No
row_155	TGIF2	TGIF2	TGFB-induced factor 2	1 7 3 6	0.7 1 5 3 7 0 8	0.01 9 0 5 8 9 6	No
row_156	TGIF2	TGIF2	TGFB-induced factor 2	1 7 3 6	0.7 1 5 3 7 0 8	0.01 9 0 5 8 9 6	No
row_157	TGIF2	TGIF2	TGFB-induced factor 2	1 7 3 6	0.7 1 5 3 7 0 8	0.01 9 0 5 8 9 6	No
row_158	TGIF2	TGIF2	TGFB-induced factor 2	1 7 3 6	0.7 1 5 3 7 0 8	0.01 9 0 5 8 9 6	No
row_159	TGIF2	TGIF2	TGFB-induced factor 2	1 7 3 6	0.7 1 5 3 7 0 8	0.01 9 0 5 8 9 6	No
row_160	TGIF2	TGIF2	TGFB-induced factor 2	1 7 3 6	0.7 1 5 3 7 0 8	0.01 9 0 5 8 9 6	No
row_161	TGIF2	TGIF2	TGFB-induced factor 2	1 7 3 6	0.7 1 5 3 7 0 8	0.01 9 0 5 8 9 6	No
row_162	TGIF2	TGIF2	TGFB-induced factor 2	1 7 3 6	0.7 1 5 3 7 0 8	0.01 9 0 5 8 9 6	No
row_163	TGIF2	TGIF2	TGFB-induced factor 2	1 7 3 6	0.7 1 5 3 7 0 8	0.01 9 0 5 8 9 6	No
row_164	TGIF2	TGIF2	TGFB-induced factor 2	1 7 3 6	0.7 1 5 3 7 0 8	0.01 9 0 5 8 9 6	No
row_165	TGIF2	TGIF2	TGFB-induced factor 2	1 7 3 6	0.7 1 5 3 7 0 8	0.01 9 0 5 8 9 6	No
row_166	TGIF2	TGIF2	TGFB-induced factor 2	1 7 3 6	0.7 1 5 3 7 0 8	0.01 9 0 5 8 9 6	No
row_167	TGIF2	TGIF2	TGFB-induced factor 2	1 7 3 6	0.7 1 5 3 7 0 8	0.01 9 0 5 8 9 6	No
row_168	TGIF2	TGIF2	TGFB-induced factor 2	1 7 3 6	0.7 1 5 3 7 0 8	0.01 9 0 5 8 9 6	No
row_169	TGIF2	TGIF2	TGFB-induced factor 2	1 7 3 6	0.7 1 5 3 7 0 8	0.01 9 0 5 8 9 6	No
row_170	TGIF2	TGIF2	TGFB-induced factor 2	1 7 3 6	0.7 1 5 3 7 0 8	0.01 9 0 5 8 9 6	No
row_171	TGIF2	TGIF2	TGFB-induced factor 2	1 7 3 6	0.7 1 5 3 7 0 8	0.01 9 0 5 8 9 6	No
row_172	TGIF2	TGIF2	TGFB-induced factor 2	1 7 3 6	0.7 1 5 3 7 0 8	0.01 9 0 5 8 9 6	No
row_173	TGIF2	TGIF2	TGFB-induced factor 2	1 7 3 6	0.7 1 5 3 7 0 8	0.01 9 0 5 8 9 6	No
row_174	TGIF2	TGIF2	TGFB-induced factor 2	1 7 3 6	0.7 1 5 3 7 0 8	0.01 9 0 5 8 9 6	No
row_175	TGIF2	TGIF2	TGFB-induced factor 2	1 7 3 6	0.7 1 5 3 7 0 8	0.01 9 0 5 8 9 6	No
row_176	TGIF2	TGIF2	TGFB-induced factor 2	1 7 3 6	0.7 1 5 3 7 0 8	0.01 9 0 5 8 9 6	No
row_177	TGIF2	TGIF2	TGFB-induced factor 2	1 7 3 6	0.7 1 5 3 7 0 8	0.01 9 0 5 8 9 6	No
row_178	TGIF2	TGIF2	TGFB-induced factor 2	1 7 3 6	0.7 1 5 3 7 0 8	0.01 9 0 5 8 9 6	No
row_179	TGIF2	TGIF2	TGFB-induced factor 2	1 7 3 6	0.7 1 5 3 7 0 8	0.01 9 0 5 8 9 6	No
row_180	TGIF2	TGIF2	TGFB-induced factor 2	1 7 3 6	0.7 1 5 3 7 0 8	0.01 9 0 5 8 9 6	No
row_181	TGIF2	TGIF2	TGFB-induced factor 2	1 7 3 6	0.7 1 5 3 7 0 8	0.01 9 0 5 8 9 6	No
row_182	TGIF2	TGIF2	TGFB-induced factor 2	1 7 3 6	0.7 1 5 3 7 0 8	0.01 9 0 5 8 9 6	No
row_183	TGIF2	TGIF2	TGFB-induced factor 2	1 7 3 6	0.7 1 5 3 7 0 8	0.01 9 0 5 8 9 6	No
row_184	TGIF2	TGIF2	TGFB-induced factor 2	1 7 3 6	0.7 1 5 3 7 0 8	0.01 9 0 5 8 9 6	No
row_185	TGIF2	TGIF2	TGFB-induced factor 2	1 7 3 6	0.7 1 5 3 7 0 8	0.01 9 0 5 8 9 6	No
row_186	TGIF2	TGIF2	TGFB-induced factor 2	1 7 3 6	0.7 1 5 3 7 0 8	0.01 9 0 5 8 9 6	No
row_187	TGIF2	TGIF2	TGFB-induced factor 2	1 7 3 6	0.7 1 5 3 7 0 8	0.01 9 0 5 8 9 6	No
row_188	TGIF2	TGIF2	TGFB-induced factor 2	1 7 3 6	0.7 1 5 3 7 0 8	0.01 9 0 5 8 9 6	No
row_189	TGIF2	TGIF2	TGFB-induced factor 2	1 7 3 6

upregulation of the gene set signature WONG_Adult_Tissue_Stem_Module. The table shows the upregulated genes belonging to the signature.

Supplementary Table 2.

Supplementary Table 2_Enrichment of a stem cell signature in H2030-BrM oncospheres_Corresponds to Fig.S2C

Ben Porath et al._PMID: 18443585_Geneset ESexp1 (SuppTable1)
Oncospheres vs co-culture with cell-cell contact

NAME	PROBE	GENE SYMBOL	GENE_TITLE	RANK IN GENE LIST	RANK METRIC SCORE	RUNNING ES	CORE ENRICHMENT
row_0	TEAD4	null	null	130	1.024573684	0.010472498	Yes
row_1	FGF2	null	null	132	1.021217823	0.026898688	Yes
row_2	SFRP1	null	null	153	0.930548549	0.040977463	Yes
row_3	SYNGR3	null	null	172	0.893029034	0.054544177	Yes
row_4	AP1M2	null	null	199	0.833103299	0.06677168	Yes
row_5	MCM3	null	null	253	0.750710666	0.07641269	Yes
row_6	CBS	null	null	291	0.70774138	0.08610575	Yes
row_7	SLC29A1	null	null	332	0.676245689	0.095151044	Yes
row_8	PRIM1	null	null	402	0.621987522	0.10197053	Yes
row_9	DIAPH2	null	null	403	0.621907115	0.11200221	Yes
row_10	MCM5	null	null	406	0.621322095	0.12193131	Yes
row_11	CDC6	null	null	443	0.602487028	0.12997313	Yes
row_12	MCM4	null	null	475	0.586127758	0.13798392	Yes
row_13	DHFR	null	null	494	0.577404022	0.14645945	Yes
row_14	CDT1	null	null	543	0.557014167	0.1532089	Yes
row_15	CDC25A	null	null	554	0.551998436	0.16164719	Yes
row_16	GAD1	null	null	600	0.534975529	0.16818087	Yes
row_17	MTHFD1	null	null	602	0.534266949	0.17675228	Yes
row_18	CDC20	null	null	613	0.530476332	0.18484342	Yes
row_19	RRAS2	null	null	626	0.524727225	0.19274867	Yes
row_20	RRM2	null	null	628	0.523922205	0.20115323	Yes
row_21	CHAF1A	null	null	635	0.522079408	0.2092952	Yes
row_22	DEK	null	null	660	0.512214065	0.21643974	Yes
row_23	MRE11A	null	null	661	0.512183785	0.22470152	Yes
row_24	NOLC1	null	null	666	0.509434938	0.23273268	Yes
row_25	PNN	null	null	710	0.496344447	0.23873636	Yes
row_26	MCM2	null	null	720	0.492111713	0.24625522	Yes
row_27	RFC4	null	null	732	0.486566156	0.25359148	Yes
row_28	UNG	null	null	737	0.483106762	0.26119795	Yes
row_29	BOP1	null	null	759	0.477881789	0.26792842	Yes
row_30	PUS1	null	null	797	0.467119783	0.2737401	Yes
row_31	RFC3	null	null	801	0.466049492	0.28111804	Yes
row_32	MCM6	null	null	814	0.461074591	0.28799653	Yes
row_33	NUDT1	null	null	877	0.444472969	0.29227862	Yes
row_34	FEN1	null	null	1022	0.41176331	0.29221416	Yes
row_35	ABCE1	null	null	1045	0.408603996	0.29778057	Yes
row_36	HSPD1	null	null	1076	0.403448015	0.30289122	Yes
row_37	ADD2	null	null	1077	0.403116792	0.3093937	Yes
row_38	RBBP8	null	null	1140	0.38980034	0.31279388	Yes
row_39	TFAM	null	null	1242	0.373224348	0.3141104	Yes
row_40	PFAS	null	null	1268	0.369595081	0.31890783	Yes
row_41	GART	null	null	1276	0.3679488	0.32451704	Yes
row_42	MSH6	null	null	1335	0.360455245	0.32763016	Yes
row_43	MCM7	null	null	1336	0.359999835	0.33343714	Yes
row_44	ILF3	null	null	1379	0.353750765	0.3371873	Yes
row_45	SMS	null	null	1380	0.353628218	0.34289148	Yes
row_46	DDX18	null	null	1469	0.341342807	0.34429917	Yes
row_47	NUP107	null	null	1549	0.3309187	0.34595785	Yes
row_48	CSE1L	null	null	1550	0.330876529	0.35129505	Yes
row_49	CCNA2	null	null	1562	0.329280615	0.3560942	Yes
row_50	DDX21	null	null	1569	0.329038084	0.36112234	Yes
row_51	ITPR3	null	null	1597	0.325574607	0.36511657	Yes
row_52	MICB	null	null	1630	0.321142226	0.36880645	Yes
row_53	MSH2	null	null	1637	0.319912225	0.37368736	Yes
row_54	HSPA8	null	null	1798	0.303086221	0.3711247	Yes
row_55	NTHL1	null	null	1917	0.287750632	0.37027076	Yes
row_56	PSIP1	null	null	1961	0.283292502	0.3728378	Yes
row_57	PODXL	null	null	1971	0.28224498	0.37697142	Yes
row_58	BUB1	null	null	2001	0.280100077	0.38013896	Yes
row_59	PRMT3	null	null	2089	0.271447152	0.38046578	Yes
row_60	MTHFD2	null	null	2149	0.266052991	0.38200957	Yes
row_61	PRPS1	null	null	2209	0.261414319	0.38347855	Yes
row_62	TMEFF1	null	null	2219	0.260237008	0.38725716	Yes
row_63	NFE2L3	null	null	2256	0.256974339	0.3897257	Yes
row_64	BIRC5	null	null	2305	0.251357108	0.39154473	Yes
row_65	KIF4A	null	null	2308	0.25125137	0.3955044	Yes
row_66	HESX1	null	null	2375	0.246089384	0.39640018	Yes
row_67	CRABP2	null	null	2378	0.24569416	0.4002702	Yes
row_68	GABRA5	null	null	2541	0.234240398	0.3965039	Yes
row_69	KCNS3	null	null	2660	0.225325122	0.39464298	Yes
row_70	SNRPA	null	null	2697	0.222264707	0.39655164	Yes
row_71	WDR12	null	null	2713	0.220593929	0.39941135	Yes
row_72	NPM3	null	null	2883	0.20950304	0.39492002	Yes
row_73	CHEK2	null	null	2912	0.207878739	0.39696917	Yes
row_74	BUB3	null	null	2985	0.203758284	0.3969027	Yes
row_75	MARS	null	null	3037	0.200757712	0.39776585	Yes
row_76	KIF5C	null	null	3123	0.195257187	0.3969568	Yes
row_77	PLCB3	null	null	3152	0.193671033	0.39877677	Yes
row_78	KPNA2	null	null	3157	0.193485945	0.40171152	Yes
row_79	NPM1	null	null	3185	0.191731483	0.40354678	Yes

Enrichment of a stem cell signature in H2030-BrM oncospheres. Transcriptomic changes experienced by H2030-BrM oncospheres that are not represented in H2030-BrM cells when grown

in co-culture conditions with cell-cell contacts with glial cells include the upregulation of the stem cell gene set signature described by Ben Porath et al[43]. The table shows the upregulated genes belonging to the signature.

Supplementary Table 3.

Supplementary Table 3_Commonly DEG in radioresistant conditions H2030-BrM in vitro_Corresponds to Fig.2A

	10Gy							
	Radio-sensitive conditions				Radio-resistant conditions			
	Adherent cells		Co-cultures (insert)		Oncospheres		Co-cultures (cell-cell contact)	
Gene ID	**Replica#1**	**Replica#2**	**Replica#1**	**Replica#2**	**Replica#1**	**Replica#2**	**Replica#1**	**Replica#2**
S100A9	7.59439	4.5155	28.5228	3.64529	1580.83	832.755	31.5604	42.0916
CITED4	7.12601	7.82344	8.75282	4.26437	15.209	13.2526	27.4243	26.4535
ADM2	1.06844	0.977898	2.24177	0.69009	0.318587	0.518863	0.610843	0.609238
SLC1A4	13.0187	13.2551	23.2088	10.885	6.15292	5.52887	7.13414	10.2621
B7H6	1.63611	1.20038	2.01825	1.4872	0.735604	0.462581	0.625675	0.963268
ASNS	111.828	123.523	206.443	85.6194	38.4651	63.7346	63.6966	74.4078
PPP1R15A	18.4296	20.1114	33.8886	12.1505	10.6333	11.6891	12.2159	11.0101
FAT4	5.42659	3.90715	7.35616	4.49208	1.1809	0.877306	1.41721	1.54036
SESN2	4.67358	5.33466	16.5771	3.37909	2.00617	3.8349	2.70772	3.44457
MAP1B	7.67632	8.15961	18.5048	9.30292	6.61733	2.98472	2.96531	3.51404

Abreviations

Adherent cells	Adh
Co-cultures (insert)	Insert
Oncospheres	Onco
Co-cultures (cell-cell contact)	Cocult

Commonly DEG in radioresistant conditions H2030-BrM *in vitro*. A signature showing the commonly upregulated (2) and downregulated (8) genes between radioresistant and radiosensitive conditions. FPKM values are shown for each gene, replica and experimental condition.

Supplementary Table 4.

Supplementary Table 4_Radioresistant signature in H2030-BrM in brain organotypic cultures_Corresponds to Fig.2B

	Radio-sensitive conditions		Radio-resistant conditions	
	Adherent cells		Brain slices	
Gene ID	**Replica#1**	**Replica#2**	**Replica#1**	**Replica#2**
S100A9	49.8806	30.1378	1887.2	2045.53
CITED4	24.4308	15.2641	43.5374	44.416
ADM2	1.2019	0.676868	0.598335	0.427862
SLC1A4	12.8192	13.0941	5.65409	5.50357
ASNS	192.069	140.292	55.8656	56.816
B7H6	0.992509	1.14978	0.367122	0.409746
FAT4	5.38556	6.71373	1.9204	1.79175
PPP1R15A	26.3816	30.8419	19.4836	19.2743
MAP1B	2.7817	3.75648	2.06515	2.12743

Radioresistant signature in H2030-BrM in brain organotypic cultures. The radio-resistance

signature is represented in H2030-BrM cells growing in organotypic cultures. FPKM values are shown for each gene, replica and experimental condition.

Supplementary Table 5.

Supplementary Table 5_Top 25 upregulated genes in H2030-BrM in brain organotypic cultures

FDR=0.05

Name	baseMean	log2FoldChange	lfcSE	stat	pvalue	padj
S100A9	17667.64142	4.345221815	0.2871146	15.13410111	9.64901E-52	3.86829E-49
S100A8	132.8617673	3.957446968	0.2811576	14.07554643	5.36883E-45	1.36658E-42
FAM83A	318.3020428	3.120515852	0.1859135	16.78477409	3.15427E-63	1.94546E-60
S100A4	716.0791138	2.927415658	0.1383012	21.16695316	1.9261E-99	4.41252E-96
SPNS2	137.6005157	2.91168495	0.2470245	11.78703023	4.55315E-32	4.32037E-30
PLP1	37.03272467	2.833083114	0.3424643	8.272638718	1.31026E-16	3.2226E-15
KIF5A	38.35076374	2.550084349	0.3421988	7.452055155	9.18973E-14	1.5966E-12
TMEM132B	59.56452267	2.490892934	0.3085066	8.074033979	6.80129E-16	1.56031E-14
CLDN4	125.2852834	2.440134849	0.2484883	9.819920129	9.24167E-23	4.32068E-21
ITGA10	215.6828891	2.435036971	0.2025878	12.01966465	2.80106E-33	2.87935E-31
NACAD	90.36572445	2.223636054	0.2682053	8.290797446	1.12492E-16	2.78382E-15
GBP2	93.26812085	2.221095795	0.2665493	8.332777828	7.89673E-17	1.98483E-15
MILR1	53.75359509	2.204661121	0.3114474	7.078759352	1.45451E-12	2.15967E-11
ALDH3A1	26.1311218	2.191499188	0.3478726	6.299717318	2.98189E-10	3.24187E-09
SHC2	147.2399142	2.189553474	0.2264569	9.668742929	4.09375E-22	1.79365E-20
DLL4	277.501276	2.177090104	0.1797622	12.11094752	9.24203E-34	9.88035E-32
ZNF295-AS1	53.91570455	2.094110378	0.3093444	6.769511546	1.29218E-11	1.69569E-10
TNFRSF19	259.3403404	2.063482861	0.1873033	11.01680075	3.17131E-28	2.29077E-26
ZNF467	918.9162207	2.01200798	0.1162718	17.3043549	4.36139E-67	4.3712E-64
AC068768.1	117.7816076	1.989998679	0.2436273	8.168209465	3.13E-16	7.41399E-15
SUSD2	806.1718396	1.982671353	0.2853347	6.948582267	3.68975E-12	5.21312E-11
LINC01801	74.59836121	1.902725079	0.2822235	6.741909134	1.56319E-11	2.03138E-10
FAM107B	5171.896475	1.90223444	0.0818393	23.24353298	1.6538E-119	6.6299E-116
LURAP1L	95.69413398	1.892097179	0.2586377	7.315628925	2.56179E-13	4.21774E-12
THRB	256.3074852	1.854725726	0.181294	10.23048867	1.44787E-24	7.68809E-23

Top 25 upregulated genes in H2030-BrM in brain organotypic cultures. Top 25 upregulated genes in H2030-BrM cells cultured on brain organotypic cultures compared to *in vitro* cultured conditions. DESeq2 was used to identify differentially expressed genes between two groups of samples based on a negative binomial distribution model. Values in the table represent normalized base mean expression level, Log2 fold change, shrinkage of effect size (lfcSE), Wald statistic, Wald test p-value and adjusted p-value below a given FDR cutoff, alpha = 0.05.

Supplementary Table 6.

Supplementary Table 6_Enrichment of NF-kB signatures in radioresistant conditions_Corresponds to Fig.S2H

NFKB signature_In vitro_REACTOME_MAP_KINASE_ACTIVATION_IN_TLR_CASCADE

Signature evaluated DEG H2030-BrM resistant (Onc-Cocult) vs sensitive (Adh-Insert) surrogates irradiated (10Gy)

NAME	GENE SYMBOL	RANK IN GENE LIST	RANK METRIC SCORE	RUNNING ES	CORE ENRICHMENT
row_0	DUSP6	57	1.055718184	0.017773056	Yes
row_1	FOS	236	0.597747922	0.029952288	Yes
row_2	MAP2K1	293	0.541081727	0.047771573	Yes
row_3	PPP2R1B	673	0.368947476	0.050658587	Yes
row_4	MAPK7	910	0.319571048	0.060156483	Yes
row_5	MAP2K3	1201	0.279324442	0.06715796	Yes
row_6	DUSP7	1239	0.273496807	0.08585562	Yes
row_7	TAB1	1545	0.240439445	0.092163645	Yes
row_8	CDK1	1622	0.234001532	0.10905833	Yes
row_9	PPP2R1A	1651	0.232045755	0.12817205	Yes
row_10	RPS6KA1	2289	0.187860012	0.119131744	Yes
row_11	MAPK3	2313	0.186190441	0.13847661	Yes
row_12	MAP2K6	2415	0.180324972	0.15421556	Yes
row_13	MAPKAPK3	3437	0.130279168	0.12742294	Yes
row_14	MAP2K4	3862	0.113285482	0.1282296	Yes
row_15	DUSP3	3978	0.108269811	0.14332132	Yes
row_16	PPP2CA	4288	0.096997254	0.14944443	Yes
row_17	ELK1	5069	0.072650999	0.13379323	Yes
row_18	RIPK2	5210	0.068864122	0.14772922	Yes
row_19	DUSP4	5308	0.066248477	0.16365308	Yes
row_20	MAPKAPK2	5846	0.051812474	0.15923575	Yes
row_21	MAP2K7	5911	0.050377205	0.1766852	Yes
row_22	PPP2R5D	5977	0.048563723	0.19408841	Yes
row_23	MAP3K7	6139	0.045003496	0.20705356	Yes
row_24	IRAK1	6338	0.040299404	0.21830818	Yes
row_25	CREB1	6693	0.032273497	0.22235096	Yes

NFKB signature_Ex vivo_REACTOME_MAP_KINASE_ACTIVATION_IN_TLR_CASCADE

Signature evaluated DEG H2030-BrM in brain slices vs H2030-BrM in vitro (Adh)

NAME	GENE SYMBOL	RANK IN GENE LIST	RANK METRIC SCORE	RUNNING ES	CORE ENRICHMENT
row_0	DUSP6	183	1.141023278	0.014733569	Yes
row_1	MAPK7	240	1.068263173	0.033405244	Yes
row_2	MAP2K6	304	0.987556219	0.051859856	Yes
row_3	ATF2	330	0.967172086	0.071492806	Yes
row_4	ELK1	429	0.898986399	0.08886211	Yes
row_5	DUSP3	576	0.826986849	0.104743004	Yes
row_6	TAB3	809	0.74672997	0.117957145	Yes
row_7	MAPK11	1177	0.651373148	0.1269851	Yes
row_8	IRAK2	1527	0.584053278	0.13657123	Yes
row_9	MAPKAPK2	1705	0.556251705	0.15149085	Yes
row_10	MEF2A	1950	0.520993769	0.16433288	Yes
row_11	CREB1	2277	0.478613585	0.1746322	Yes
row_12	MAP2K4	2421	0.461385131	0.19060613	Yes
row_13	TAB2	2573	0.446571827	0.20633197	Yes
row_14	FOS	2654	0.437566936	0.22425944	Yes
row_15	MAPK3	2657	0.437408179	0.24460559	Yes
row_16	MAP2K3	3009	0.399760306	0.25412968	Yes
row_17	RIPK2	3426	0.363707274	0.26163822	Yes
row_18	IRAK1	3437	0.362179995	0.2817363	Yes
row_19	DUSP4	3566	0.352443099	0.29817536	Yes
row_20	MAP3K7	3665	0.344691396	0.31554466	Yes
row_21	MEF2C	4414	0.288518876	0.3127583	Yes
row_22	MAP2K2	4825	0.262437075	0.3204529	Yes
row_23	RPS6KA2	5474	0.223521724	0.3207674	Yes
row_24	TRAF6	6166	0.190309897	0.31974855	Yes
row_25	PPP2R1A	6265	0.184291035	0.33711788	Yes
row_26	DUSP7	6687	0.16543071	0.34447137	Yes
row_27	TAB1	6893	0.159416139	0.35852274	Yes
row_28	MAPK1	8555	0.099293478	0.32742542	Yes
row_29	MAPK14	8560	0.099059172	0.34770957	Yes
row_30	MAPK8	8569	0.098485753	0.36786965	Yes
row_31	MAPK9	8630	0.096635945	0.3864173	Yes

Enrichment of NF-κB signatures in radioresistant conditions. Genes set enrichment analysis performed in radioresistant conditions both *in vitro* (upper table) and *ex vivo* (lower table) showed

gene signatures related to NF-κB. Components of the pathway represented in each experimental condition are shown.

Supplementary Table 7.

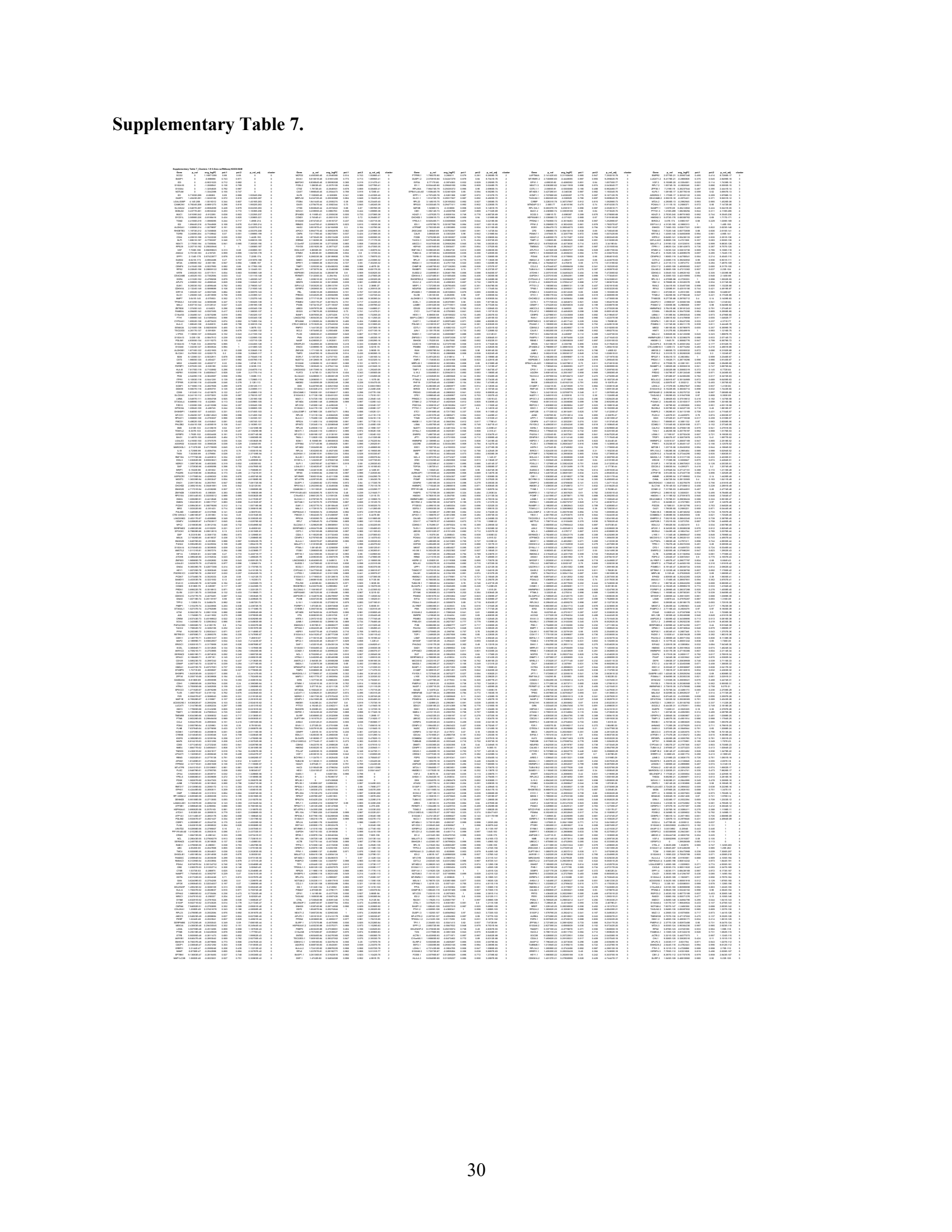

Gene	p_val	avg_logFC	pct.1	pct.2	p_val_adj	cluster
TPI1	1.79E-267	0.466437781	0.962	0.914	2.63E-263	0
TPI1.2	1.79E-267	0.466437781	0.962	0.914	2.63E-263	0
FTL	6.19E-66	0.459364307	0.999	0.999	2.26E-61	0
UPF1.2	4.89E-60	0.431223386	0.335	0.205	1.80E-56	0
TOP1	7.71E-59	0.496382396	0.968	0.943	2.81E-55	0
TOP1.2	7.71E-59	0.496382396	0.968	0.943	2.81E-55	0
LOC277.3	2.19E-56	0.511724109	0.901	0.499	7.91E-52	0
CTSD.2	8.00E-55	0.422721785	0.481	0.18	2.70E-50	0
PSMA7	1.26E-50	0.377705065	0.999	0.99	4.26E-46	0
FOS.2	9.48E-50	0.613978778	0.974	0.91	2.10712E-45	0
FOS	9.48E-50	0.613978778	0.974	0.91	2.10712E-45	0
ACTN4.2	8.9e-5.07	0.432852729	0.868	0.583	3.22259E-45	0
PCMP.2	3.75E-116	0.404937702	0.979	0.936	1.26307E-40	0
PCMP.1	3.75E-116	0.404937702	0.979	0.936	1.26307E-40	0
NTS1	1.02E-42	0.428170548	0.927	0.598	3.45707E-38	0
EIF1A1.3	5.6E-104E-96	0.433265618	1	1	1.91322E-88	0
EEL4NCP.4	2.03e-143	0.453749985	0.165	0.039	6.83897E-88	0
RAP1.2	1.7213E-81	0.4612202	0.391	0.099	8.62900E-87	0
RAP1.1	1.7213E-81	0.4612202	0.391	0.099	8.62900E-87	0
NCA	3.56E-81	0.43152	0.452	0.162	1.1.74152E-82	0
HLA.C.2	1.72e-80	0.47342631	0.509	0.756	5.80315E-86	0
EIF1.2	8.6E-81	0.4124677	0.975	0.998	2.9222E-82	0
MRPL32.3	9.26E-80	0.442245451	0.972	0.836	3.13997E-81	0
ACTB.2	1.2E-79	0.4124677	0.975	0.998	4.0.6E-81	0
LYN	1.36E-81	0.398.2E-80	0.158	0.012	4.2426E-81	0
TNFRSF12A	2.98E-128	0.41339501	0.488	0.198	7.68903E-83	0
EIF4A3.3	1.47E-80	0.729811.75	0.39	0.089	5.0025E-82	0
SYCE1L.3	5.46E-78E-86	0.7582473	0.974	0.775	1.1734E-81	0
SYCE1L.2	5.46E-78E-86	0.7582473	0.974	0.775	1.1734E-81	0
DYNC1H1	8.32E-69E-86	0.422552123	0.979	0.852	2.1082E-82	0
SPTAN1	1.85e7.6E-84	0.5408035	0.808	0.631	6.7539E-85	0
SPTAN1.2	1.85e7.6E-84	0.5408035	0.808	0.631	6.7539E-85	0
HLA.B.2	9.91e5E-85	0.45171451	0.275	0.035	2.4630.1E-78	0
HLA.B.1	9.91e5E-85	0.45171451	0.275	0.035	2.4630.1E-78	0
ANXA5.2	1.85e7.6E-84	0.5408035	0.808	0.631	6.7539E-85	0
ANXA5.1	1.85e7.6E-84	0.5408035	0.808	0.631	6.7539E-85	0
ACCA2.1	1.85e7.6E-84	0.41099653	0.752	0.428	6.2230E-78	0
ARPC2	3.02E+82	0.45622108	0.968	0.798	1.0208E-77	0
EF4A1	8.9696E-81	0.29648432	0.345	0.101	2.0178E-75	0
EF4A1.2	8.9696E-81	0.29648432	0.345	0.101	2.0178E-75	0
CST3.4	3.01E-82E-79	0.41153228	0.973	0.873	1.1.4153E-74	0
CSTL1.3	9.56E-79	0.42139298	0.752	0.417	3.2.4268E-73	0
TMP1.4	1.2868E-78	0.42207387	1	0.997	4.2903E-83	0
TPSG1.3	4.9736E-78	0.41439569	0.428	0.68	1.6930E-73	0
TPSG1.2	4.9736E-78	0.41439569	0.428	0.68	1.6930E-73	0
METTL9.1	8.9012E-77	0.44822064	0.468	0.279	2.2.1983E-72	0
BMS1E.1	7.8333E-77	0.44822064	0.825	0.89	2.2.6543E-72	0
TMP1.3	1.2868E-78	0.42207387	1	0.999	4.9220E-73	0
CCT5.1	1.2868E-78	0.42207387	1	0.999	4.9220E-73	0
PPIA.2	2.7717E-75	0.79802038	0.825	0.624	1.4918E-71	0
CCT5	4.61.5E05.75	0.32611135	0.964	0.948	1.6691E-70	0
EIF2.1	1.99e6E-74	0.4031421	0.968	0.91	6.7605E-70	0
EPC1.2	3.1091E-73	0.39555348	0.997	0.922	1.0226E-68	0
EPC1.1	3.1091E-73	0.39555348	0.997	0.922	1.0226E-68	0
ATG1	1.01E-72E-71	0.43553021	0.997	0.922	3.4.6219E-67	0
DAD1.1	1.6e6E-71	0.39672316	0.962	0.836	5.6730E-67	0
CS2	3.0e2E-70	0.39.5E-69	0.962	0.836	1.0.5E-65	0
CCP1B1.1	3.2746E-69	0.39570598	0.968	0.868	1.1.1163E-64	0
CCP1B1.2	3.2746E-69	0.39570598	0.968	0.868	1.1.1163E-64	0
GNB2L1	4.8671E-67	0.33724365	0.968	0.217	1.6.6762E-62	0
CHMP.1	6.6E-0E-67	0.44507202	0.899	0.84	1.6975E-62	0
CKS2	8.1999E-67	0.29564736	0.938	0.598	2.2.1705E-62	0
MEL4.3	8.8214E-66	0.3647724	0.947	0.758	2.2.4514E-61	0
MEL4.2	8.8214E-66	0.3647724	0.947	0.758	2.2.4514E-61	0
MEL4.1	8.8214E-66	0.3647724	0.947	0.758	2.2.4514E-61	0
MDJP.C	6.1526E-65	0.3.5727.73	0.903	0.676	1.5.6.1E-60	0
MDJP.1	6.1526E-65	0.3.5727.73	0.903	0.676	1.5.6.1E-60	0
ATP5A1.2	1.0.2E-64	0.3.5727.73	0.903	0.676	2.6.6.1E-60	0
ATP5A1.1	1.0.2E-64	0.3.5727.73	0.903	0.676	2.6.6.1E-60	0
TOP2	7.7e7E-62	0.32215.2	0.286	0.061	2.0.6E-57	0
PSG.C2	2.4016E-60	0.42809108	0.438	0.916	6.1.21.E-55	0
PSG.C1	2.4016E-60	0.42809108	0.438	0.916	6.1.21.E-55	0
PSG.2	3.4896E-60	0.43271372	0.766	0.836	8.8.8.E-55	0
PSG.1	3.4896E-60	0.43271372	0.766	0.836	8.8.8.E-55	0
ATP5D.2	8.2975E-60	0.43.5E-60	0.829	0.624	2.1.1.E-55	0
ATP5D.1	8.2975E-60	0.43.5E-60	0.829	0.624	2.1.1.E-55	0
ATP5D	8.2975E-60	0.43.5E-60	0.829	0.624	2.1.1.E-55	0
ATP5D.3	8.2975E-60	0.43.5E-60	0.829	0.624	2.1.1.E-55	0
ATP5D.4	8.2975E-60	0.43.5E-60	0.829	0.624	2.1.1.E-55	0
ATP5D.5	8.2975E-60	0.43.5E-60	0.829	0.624	2.1.1.E-55	0
ATP5D.6	8.2975E-60	0.43.5E-60	0.829	0.624	2.1.1.E-55	0
ATP5D.7	8.2975E-60	0.43.5E-60	0.829	0.624	2.1.1.E-55	0
ATP5D.8	8.2975E-60	0.43.5E-60	0.829	0.624	2.1.1.E-55	0
ATP5D.9	8.2975E-60	0.43.5E-60	0.829	0.624	2.1.1.E-55	0
ATP5D.10	8.2975E-60	0.43.5E-60	0.829	0.624	2.1.1.E-55	0
ATP5D.11	8.2975E-60	0.43.5E-60	0.829	0.624	2.1.1.E-55	0
ATP5D.12	8.2975E-60	0.43.5E-60	0.829	0.624	2.1.1.E-55	0
ATP5D.13	8.2975E-60	0.43.5E-60	0.829	0.624	2.1.1.E-55	0
ATP5D.14	8.2975E-60	0.43.5E-60	0.829	0.624	2.1.1.E-55	0
ATP5D.15	8.2975E-60	0.43.5E-60	0.829	0.624	2.1.1.E-55	0
ATP5D.16	8.2975E-60	0.43.5E-60	0.829	0.624	2.1.1.E-55	0
ATP5D.17	8.2975E-60	0.43.5E-60	0.829	0.624	2.1.1.E-55	0
ATP5D.18	8.2975E-60	0.43.5E-60	0.829	0.624	2.1.1.E-55	0
ATP5D.19	8.2975E-60	0.43.5E-60	0.829	0.624	2.1.1.E-55	0
ATP5D.20	8.2975E-60	0.43.5E-60	0.829	0.624	2.1.1.E-55	0
ATP5D.21	8.2975E-60	0.43.5E-60	0.829	0.624	2.1.1.E-55	0
ATP5D.22	8.2975E-60	0.43.5E-60	0.829	0.624	2.1.1.E-55	0
ATP5D.23	8.2975E-60	0.43.5E-60	0.829	0.624	2.1.1.E-55	0
ATP5D.24	8.2975E-60	0.43.5E-60	0.829	0.624	2.1.1.E-55	0
ATP5D.25	8.2975E-60	0.43.5E-60	0.829	0.624	2.1.1.E-55	0
ATP5D.26	8.2975E-60	0.43.5E-60	0.829	0.624	2.1.1.E-55	0
ATP5D.27	8.2975E-60	0.43.5E-60	0.829	0.624	2.1.1.E-55	0
ATP5D.28	8.2975E-60	0.43.5E-60	0.829	0.624	2.1.1.E-55	0
ATP5D.29	8.2975E-60	0.43.5E-60	0.829	0.624	2.1.1.E-55	0
ATP5D.30	8.2975E-60	0.43.5E-60	0.829	0.624	2.1.1.E-55	0
ATP5D.31	8.2975E-60	0.43.5E-60	0.829	0.624	2.1.1.E-55	0
ATP5D.32	8.2975E-60	0.43.5E-60	0.829	0.624	2.1.1.E-55	0
ATP5D.33	8.2975E-60	0.43.5E-60	0.829	0.624	2.1.1.E-55	0
ATP5D.34	8.2975E-60	0.43.5E-60	0.829	0.624	2.1.1.E-55	0
ATP5D.35	8.2975E-60	0.43.5E-60	0.829	0.624	2.1.1.E-55	0
ATP5D.36	8.2975E-60	0.43.5E-60	0.829	0.624	2.1.1.E-55	0
ATP5D.37	8.2975E-60	0.43.5E-60	0.829	0.624	2.1.1.E-55	0
ATP5D.38	8.2975E-60	0.43.5E-60	0.829	0.624	2.1.1.E-55	0
ATP5D.39	8.2975E-60	0.43.5E-60	0.829	0.624	2.1.1.E-55	0
ATP5D.40	8.2975E-60	0.43.5E-60	0.829	0.624	2.1.1.E-55	0
ATP5D.41	8.2975E-60	0.43.5E-60	0.829	0.624	2.1.1.E-55	0
ATP5D.42	8.2975E-60	0.43.5E-60	0.829	0.624	2.1.1.E-55	0
ATP5D.43	8.2975E-60	0.43.5E-60	0.829	0.624	2.1.1.E-55	0
ATP5D.44	8.2975E-60	0.43.5E-60	0.829	0.624	2.1.1.E-55	0
ATP5D.45	8.2975E-60	0.43.5E-60	0.829	0.624	2.1.1.E-55	0
ATP5D.46	8.2975E-60	0.43.5E-60	0.829	0.624	2.1.1.E-55	0
ATP5D.47	8.2975E-60	0.43.5E-60	0.829	0.624	2.1.1.E-55	0
ATP5D.48	8.2975E-60	0.43.5E-60	0.829	0.624	2.1.1.E-55	0
ATP5D.49	8.2975E-60	0.43.5E-60	0.829	0.624	2.1.1.E-55	0
ATP5D.50	8.2975E-60	0.43.5E-60	0.829	0.624	2.1.1.E-55	0
ATP5D.51	8.2975E-60	0.43.5E-60	0.829	0.624	2.1.1.E-55	0
ATP5D.52	8.2975E-60	0.43.5E-60	0.829	0.624	2.1.1.E-55	0
ATP5D.53	8.2975E-60	0.43.5E-60	0.829	0.624	2.1.1.E-55	0
ATP5D.54	8.2975E-60	0.43.5E-60	0.829	0.624	2.1.1.E-55	0
ATP5D.55	8.2975E-60	0.43.5E-60	0.829	0.624	2.1.1.E-55	0
ATP5D.56	8.2975E-60	0.43.5E-60	0.829	0.624	2.1.1.E-55	0
ATP5D.57	8.2975E-60	0.43.5E-60	0.829	0.624	2.1.1.E-55	0
ATP5D.58	8.2975E-60	0.43.5E-60	0.829	0.624	2.1.1.E-55	0
ATP5D.59	8.2975E-60	0.43.5E-60	0.829	0.624	2.1.1.E-55	0
ATP5D.60	8.2975E-60	0.43.5E-60	0.829	0.624	2.1.1.E-55	0
ATP5D.61	8.2975E-60	0.43.5E-60	0.829	0.624	2.1.1.E-55	0
ATP5D.62	8.2975E-60	0.43.5E-60	0.829	0.624	2.1.1.E-55	0
ATP5D.63	8.2975E-60	0.43.5E-60	0.829	0.624	2.1.1.E-55	0
ATP5D.64	8.2975E-60	0.43.5E-60	0.829	0.624	2.1.1.E-55	0
ATP5D.65	8.2975E-60	0.43.5E-60	0.829	0.624	2.1.1.E-55	0
ATP5D.66	8.2975E-60	0.43.5E-60	0.829	0.624	2.1.1.E-55	0
ATP5D.67	8.2975E-60	0.43.5E-60	0.829	0.624	2.1.1.E-55	0
ATP5D.68	8.2975E-60	0.43.5E-60	0.829	0.624	2.1.1.E-55	0
ATP5D.69	8.2975E-60	0.43.5E-60	0.829	0.624	2.1.1.E-55	0
ATP5D.70	8.2975E-60	0.43.5E-60	0.829	0.624	2.1.1.E-55	0
ATP5D.71	8.2975E-60	0.43.5E-60	0.829	0.624	2.1.1.E-55	0
ATP5D.72	8.2975E-60	0.43.5E-60	0.829	0.624	2.1.1.E-55	0
ATP5D.73	8.2975E-60	0.43.5E-60	0.829	0.624	2.1.1.E-55	0
ATP5D.74	8.2975E-60	0.43.5E-60	0.829	0.624	2.1.1.E-55	0
ATP5D.75	8.2975E-60	0.43.5E-60	0.829	0.624	2.1.1.E-55	0
ATP5D.76	8.2975E-60	0.43.5E-60	0.829	0.624	2.1.1.E-55	0
ATP5D.77	8.2975E-60	0.43.5E-60	0.829	0.624	2.1.1.E-55	0
ATP5D.78	8.2975E-60	0.43.5E-60	0.829	0.624	2.1.1.E-55	0
ATP5D.79	8.2975E-60	0.43.5E-60	0.829	0.624	2.1.1.E-55	0
ATP5D.80	8.2975E-60	0.43.5E-60	0.829	0.624	2.1.1.E-55	0
ATP5D.81	8.2975E-60	0.43.5E-60	0.829	0.624	2.1.1.E-55	0
ATP5D.82	8.2975E-60	0.43.5E-60	0.829	0.624	2.1.1.E-55	0
ATP5D.83	8.2975E-60	0.43.5E-60	0.829	0.624	2.1.1.E-55	0
ATP5D.84	8.2975E-60	0.43.5E-60	0.829	0.624	2.1.1.E-55	0
ATP5D.85	8.2975E-60	0.43.5E-60	0.829	0.624	2.1.1.E-55	0
ATP5D.86	8.2975E-60	0.43.5E-60	0.829	0.624	2.1.1.E-55	0
ATP5D.87	8.2975E-60	0.43.5E-60	0.829	0.624	2.1.1.E-55	0
ATP5D.88	8.2975E-60	0.43.5E-60	0.829	0.624	2.1.1.E-55	0
ATP5D.89	8.2975E-60	0.43.5E-60	0.829	0.624	2.1.1.E-55	0
ATP5D.90	8.2975E-60	0.43.5E-60	0.829	0.624	2.1.1.E-55	0
ATP5D.91	8.2975E-60	0.43.5E-60	0.829	0.624	2.1.1.E-55	0
ATP5D.92	8.2975E-60	0.43.5E-60	0.829	0.624	2.1.1.E-55	0
ATP5D.93	8.2975E-60	0.43.5E-60	0.829	0.624	2.1.1.E-55	0
ATP5D.94	8.2975E-60	0.43.5E-60	0.829	0.624	2.1.1.E-55	0
ATP5D.95	8.2975E-60	0.43.5E-60	0.829	0.624	2.1.1.E-55	0
ATP5D.96	8.2975E-60	0.43.5E-60	0.829	0.624	2.1.1.E-55	0
ATP5D.97	8.2975E-60	0.43.5E-60	0.829	0.624	2.1.1.E-55	0
ATP5D.98	8.2975E-60	0.43.5E-60	0.829	0.624	2.1.1.E-55	0
ATP5D.99	8.2975E-60	0.43.5E-60	0.829	0.624	2.1.1.E-55	0
ATP5D.100	8.2975E-60	0.43.5E-60	0.829	0.624	2.1.1.E-55	0
ATP5D.101	8.2975E-60	0.43.5E-60	0.829	0.624	2.1.1.E-55	0
ATP5D.102	8.2975E-60	0.43.5E-60	0.829	0.624	2.1.1.E-55	0
ATP5D.103	8.2975E-60	0.43.5E-60	0.829	0.624	2.1.1.E-55	0
ATP5D.104	8.2975E-60	0.43.5E-60	0.829	0.624	2.1.1.E-55	0
ATP5D.105	8.2975E-60	0.43.5E-60	0.829	0.624	2.1.1.E-55	0
ATP5D.106	8.2975E-60	0.43.5E-60	0.829	0.624	2.1.1.E-55	0
ATP5D.107	8.2975E-60	0.43.5E-60	0.829	0.624	2.1.1.E-55	0
ATP5D.108	8.2975E-60	0.43.5E-60	0.829	0.624	2.1.1.E-55	0
ATP5D.109	8.2975E-60	0.43.5E-60	0.829	0.624	2.1.1.E-55	0
ATP5D.110	8.2975E-60	0.43.5E-60	0.829	0.624	2.1.1.E-55	0
ATP5D.111	8.2975E-60	0.43.5E-60	0.829	0.624	2.1.1.E-55	0
ATP5D.112	8.2975E-60	0.43.5E-60	0.829	0.624	2.1.1.E-55	0
ATP5D.113	8.2975E-60	0.43.5E-60	0.829	0.624	2.1.1.E-55	0
ATP5D.114	8.2975E-60	0.43.5E-60	0.829	0.624	2.1.1.E-55	0
ATP5D.115	8.2975E-60	0.43.5E-60	0.829	0.624	2.1.1.E-55	0
ATP5D.116	8.2975E-60	0.43.5E-60	0.829	0.624	2.1.1.E-55	0
ATP5D.117	8.2975E-60	0.43.5E-60	0.829	0.624	2.1.1.E-55	0
ATP5D.118	8.2975E-60	0.43.5E-60	0.829	0.624	2.1.1.E-55	0
ATP5D.119	8.2975E-60	0.43.5E-60	0.829	0.624	2.1.1.E-55	0
ATP5D.120	8.2975E-60	0.43.5E-60	0.829	0.624	2.1.1.E-55	0
ATP5D.121	8.2975E-60	0.43.5E-60	0.829	0.624	2.1.1.E-55	0
ATP5D.122	8.2975E-60	0.43.5E-60	0.829	0.624	2.1.1.E-55	0
ATP5D.123	8.2975E-60	0.43.5E-60	0.829	0.624	2.1.1.E-55	0
ATP5D.124	8.2975E-60	0.43.5E-60	0.829	0.624	2.1.1.E-55	0
ATP5D.125	8.2975E-60	0.43.5E-60	0.829	0.624	2.1.1.E-55	0
ATP5D.126	8.2975E-60	0.43.5E-60	0.829	0.624	2.1.1.E-55	0
ATP5D.127	8.2975E-60	0.43.5E-60	0.829	0.624	2.1.1.E-55	0
ATP5D.128	8.2975E-60	0.43.5E-60	0.829	0.624	2.1.1.E-55	0
ATP5D.129	8.2975E-60	0.43.5E-60	0.829	0.624	2.1.1.E-55	0
ATP5D.130	8.2975E-60	0.43.5E-60	0.829	0.624	2.1.1.E-55	0
ATP5D.131	8.2975E-60	0.43.5E-60	0.829	0.624	2.1.1.E-55	0
ATP5D.132	8.2975E-60	0.43.5E-60	0.829	0.624	2.1.1.E-55	0
ATP5D.133	8.2975E-60	0.43.5E-60	0.829	0.624	2.1.1.E-55	0
ATP5D.134	8.2975E-60	0.43.5E-60	0.829	0.624	2.1.1.E-55	0
ATP5D.135	8.2975E-60	0.43.5E-60	0.829	0.624	2.1.1.E-55	0
ATP5D.136	8.2975E-60	0.43.5E-60	0.829	0.624	2.1.1.E-55	0
ATP5D.137	8.2975E-60	0.43.5E-60	0.829	0.624	2.1.1.E-55	0
ATP5D.138	8.2975E-60	0.43.5E-60	0.829	0.624	2.1.1.E-55	0
ATP5D.139	8.2975E-60	0.43.5E-60	0.829	0.624	2.1.1.E-55	0
ATP5D.140	8.2975E-60	0.43.5E-60	0.829	0.624	2.1.1.E-55	0
ATP5D.141	8.2975E-60	0.43.5E-60	0.829	0.624	2.1.1.E-55	0
ATP5D.142	8.2975E-60	0.43.5E-60	0.829	0.624	2.1.1.E-55	0
ATP5D.143	8.2975E-60	0.43.5E-60	0.829	0.624	2.1.1.E-55	0
ATP5D.144	8.2975E-60	0.43.5E-60	0.829	0.624	2.1.1.E-55	0
ATP5D.145	8.2975E-60	0.43.5E-60	0.829	0.624	2.1.1.E-55	0
ATP5D.146	8.2975E-60	0.43.5E-60	0.829	0.624	2.1.1.E-55	0
ATP5D.147	8.2975E-60	0.43.5E-60	0.829	0.624	2.1.1.E-55	0
ATP5D.148	8.2975E-60	0.43.5E-60	0.829	0.624	2.1.1.E-55	0
ATP5D.149	8.2975E-60	0.43.5E-60	0.829	0.624	2.1.1.E-55	0
ATP5D.150	8.2975E-60	0.43.5E-60	0.829	0.624	2.1.1.E-55	0
ATP5D.151	8.2975E-60	0.43.5E-60	0.829	0.624	2.1.1.E-55	0
ATP5D.152	8.2975E-60	0.43.5E-60	0.829	0.624	2.1.1.E-55	0
ATP5D.153	8.2975E-60	0.43.5E-60	0.829	0.624	2.1.1.E-55	0
ATP5D.154	8.2975E-60	0.43.5E-60	0.829	0.624	2.1.1.E-55	0
ATP5D.155	8.2975E-60	0.43.5E-60	0.829	0.624	2.1.1.E-55	0
ATP5D.156	8.2975E-60	0.43.5E-60	0.829	0.624	2.1.1.E-55	0
ATP5D.157	8.2975E-60	0.43.5E-60	0.829	0.624	2.1.1.E-55	0
ATP5D.158	8.2975E-60	0.43.5E-60	0.829	0.624	2.1.1.E-55	0
ATP5D.159	8.2975E-60	0.43.5E-60	0.829	0.624	2.1.1.E-55	0
ATP5D.160	8.2975E-60	0.43.5E-60	0.829	0.624	2.1.1.E-55	0
ATP5D.161	8.2975E-60	0.43.5E-60	0.829	0.624	2.1.1.E-55	0
ATP5D.162	8.2975E-60	0.43.5E-60	0.829	0.624	2.1.1.E-55	0
ATP5D.163	8.2975E-60	0.43.5E-60	0.829	0.624	2.1.1.E-55	0
ATP5D.164	8.2975E-60	0.43.5E-60	0.829	0.624	2.1.1.E-55	0
ATP5D.165	8.2975E-60	0.43.5E-60	0.829	0.624	2.1.1.E-55	0
ATP5D.166	8.2975E-60	0.43.5E-60	0.829	0.624	2.1.1.E-55	0
ATP5D.167	8.2975E-60	0.43.5E-60	0.829	0.624	2.1.1.E-55	0
ATP5D.168	8.2975E-60	0.43.5E-60	0.829	0.624	2.1.1.E-55	0
ATP5D.169	8.2975E-60	0.43.5E-60	0.829	0.624	2.1.1.E-55	0
ATP5D.170	8.2975E-60	0.43.5E-60	0.829	0.624	2.1.1.E-55	0
ATP5D.171	8.2975E-60	0.43.5E-60	0.829	0.624	2.1.1.E-55	0
ATP5D.172	8.2975E-60	0.43.5E-60	0.829	0.624	2.1.1.E-55	0
ATP5D.173	8.2975E-60	0.43.5E-60	0.829	0.624	2.1.1.E-55	0
ATP5D.174	8.2975E-60	0.43.5E-60	0.829	0.624	2.1.1.E-55	0
ATP5D.175	8.2975E-60	0.43.5E-60	0.829	0.624	2.1.1.E-55	0
ATP5D.176	8.2975E-60	0.43.5E-60	0.829	0.624	2.1.1.E-55	0
ATP5D.177	8.2975E-60	0.43.5E-60	0.829	0.624	2.1.1.E-55	0
ATP5D.178	8.2975E-60	0.43.5E-60	0.829	0.624	2.1.1.E-55	0
ATP5D.179	8.2975E-60	0.43.5E-60	0.829	0.624	2.1.1.E-55	0
ATP5D.180	8.2975E-60	0.43.5E-60	0.829	0.624	2.1.1.E-55	0
ATP5D.181	8.2975E-60	0.43.5E-60	0.829	0.624	2.1.1.E-55	0
ATP5D.182	8.2975E-60	0.43.5E-60	0.829	0.624	2.1.1.E-55	0
ATP5D.183	8.2975E-60	0.43.5E-60	0.829	0.624	2.1.1.E-55	0
ATP5D.184	8.2975E-60	0.43.5E-60	0.829	0.624	2.1.1.E-55	0
ATP5D.185	8.2975E-60	0.43.5E-60	0.829	0.624	2.1.1.E-55	0
ATP5D.186	8.2975E-60	0.43.5E-60	0.829	0.624	2.1.1.E-55	0
ATP5D.187	8.2975E-60	0.43.5E-60	0.829	0.624	2.1.1.E-55	0
ATP5D.188	8.2975E-60	0.43.5E-60	0.829	0.624	2.1.1.E-55	0
ATP5D.189	8.2975E-60	0.43.5E-60	0.829	0.624	2.1.1.E-55	0
ATP5D.190	8.2975E-60	0.43.5E-60	0.829	0.624	2.1.1.E-55	0
ATP5D.191	8.2975E-60	0.43.5E-60	0.829	0.624	2.1.1.E-55	0
ATP5D.192	8.2975E-60	0.43.5E-60	0.829	0.624	2.1.1.E-55	0
ATP5D.193	8.2975E-60	0.43.5E-60	0.829	0.624	2.1.1.E-55	0
ATP5D.194	8.2975E-60	0.43.5E-60	0.829	0.624	2.1.1.E-55	0
ATP5D.195	8.2975E-60	0.43.5E-60	0.829	0.624	2.1.1.E-55	0
ATP5D.196	8.2975E-60	0.43.5E-60	0.829	0.624	2.1.1.E-55	0
ATP5D.197	8.2975E-60	0.43.5E-60	0.829	0.624	2.1.1.E-55

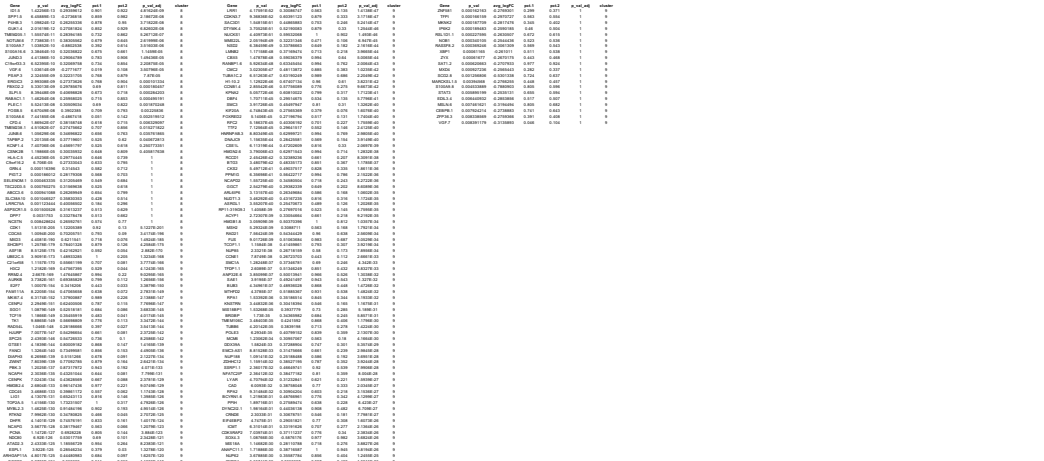

Gene	p_val	avg_logFC	pct.1	pct.2	p_val_adj	cluster
ID1-5	1.42226E-13	0.25339612	0.901	0.822	4.97452E-09	6
SPP1-5	4.45888E-13	-0.2738519	0.809	0.662	2.19872E-08	6
FHAD1-5	1.09620E-12	0.29243536	0.879	0.76	3.71562E-08	6
ID1-6	1.09620E-12	0.29243536	0.879	0.76	3.71562E-08	6
TMEM200A-5	1.10437E-11	0.32634156	0.732	0.602	3.29712E-07	6
NOTUM-5	7.73483E-11	0.39035992	0.879	0.643	2.67999E-06	6
S100A9-7	1.03582E-10	0.48823256	0.382	0.614	3.61903E-06	6
S100A10-6	5.38466E-10	0.32036822	0.675	0.661	1.14995-05	6
JUND-3	4.47198E-10	0.29560758	0.793	0.899	1.26439E-05	6
C1orf43-3	8.62306E-10	0.33249758	0.736	0.854	2.25979E-05	6
ID1-4	1.03582E-09	0.25339612	0.901	0.822	2.70116E-05	6
FOLH1-3	2.32420E-09	0.33221755	0.768	0.879	7.97E-05	6
ERO1L-3	2.99508E-09	0.27373826	0.768	0.954	0.000101334	6
FBXO2-3	6.33972E-09	0.29787875	0.69	0.811	0.000183037	6
SLPI-3	8.39448E-09	0.45998628	0.673	0.738	0.000242203	6
ID1-3	1.03582E-08	0.25339612	0.901	0.822	0.000297512	6
PLAC1-3	6.52413E-08	0.30509053	0.618	0.833	0.001875308	6
FOSB-5	6.67508E-08	0.3862588	0.709	0.793	0.00122658	6
S100A8-8	1.01916E-07	0.49871178	0.661	0.742	0.002919512	6
CD2-3	1.88638E-07	0.38158748	0.618	0.718	0.005226697	6
TMEM238-3	4.91582E-07	0.27479662	0.707	0.899	0.013577622	6
JUNB-4	1.09429E-06	0.31699522	0.956	0.763	0.030781965	6
ANXA1-5	1.09429E-06	0.31699522	0.956	0.763	0.030781965	6
KCNF1-4	7.40159E-06	0.45881797	0.629	0.818	0.205072301	6
CENKOB	1.78666E-05	0.35035932	0.648	0.809	0.495817838	6
HLA-C-5	4.69235E-05	0.29771445	0.648	0.756	1	6
C9orf16-2	8.7588E-05	0.27333543	0.633	0.795	1	6
ID1-2	0.000134812	0.25339612	0.901	0.822	1	6
FOS-2	0.000134812	0.39179358	0.868	0.703	1	6
EIF4ENIP-1	0.000443335	0.31126569	0.648	0.864	1	6
TSC22D3-5	0.000576279	0.31596839	0.526	0.816	1	6
ABCC3-5	0.000661096	0.26269969	0.854	0.799	1	6
SLC39A10-3	0.001556837	0.35853353	0.69	0.811	1	6
LRRC75A-3	0.001723924	0.45595932	0.166	0.296	1	6
ZFP36L1-5	0.002102553	0.3107284	0.923	0.777	1	6
DPP7-1	0.00221753	0.33274478	0.613	0.662	1	6
NCS7N	0.00842286242	0.29592781	0.574	0.77	1	6
CD9-1	1.91313E-206	1.12202088	0.962	0.13	0.132795-201	5
CDC42	1.05048E-200	0.75200761	0.793	0.09	3.47158E-196	5
ANXA2-1	1.26758E-179	0.78471228	0.978	0.139	4.18868E-175	5
RNDSP1	1.26758E-179	0.78471228	0.978	0.139	4.18868E-175	5
ASF1B	8.61268E-175	0.42129251	0.682	0.054	2.8452E-170	5
UBE2C-5	3.99061E-173	0.44853285	0.7	0.068	1.32334E-168	5
C21orf58	1.11787E-170	0.69681199	0.707	0.081	3.77718E-166	5
HIC2	1.37428E-169	0.67987395	0.529	0.042	4.53438E-165	5
RRM2-2	2.9937E-169	1.47343807	0.966	0.22	9.02266E-165	5
TOP2A-2	1.1438E-139	1.72210907	0.966	0.317	3.77926E-135	5
KIF7	1.15937E-132	0.65523113	0.819	0.158	3.8419E-128	5
FAM111A	8.22058E-104	0.67656838	0.638	0.072	2.72631E-100	5
MKI67-2	9.31718E-102	1.37903987	0.969	0.238	2.15988E-147	5
CENPU	2.29408E-101	0.62400906	0.797	0.133	7.79968E-147	5
ID3	1.09798E-149	0.6291301	0.966	0.095	3.66539E-145	5
TCF19	1.78668E-149	0.35400919	0.683	0.043	5.9712E-145	5
TPX2	1.78668E-149	0.35400919	0.683	0.043	5.9712E-145	5
RAD54L	1.5468E-148	0.39189868	0.397	0.027	5.16473E-144	5
HJURP	7.00779E-147	0.64228664	0.861	0.081	2.37258E-142	5
CPVL	2.43908E-146	0.64258533	0.708	0.1	8.25868E-142	5
STEF1	1.16106E-144	0.60059182	0.868	0.147	3.9166E-139	5
CDCA3	1.16106E-144	0.60059182	0.868	0.147	3.9166E-139	5
DAPK9	4.39966E-139	0.4151264	0.674	0.091	1.13297E-134	5
ZWINT	7.80308E-139	0.77592765	0.879	0.164	2.64218E-134	5
PBK-3	2.30202E-137	0.87317972	0.843	0.162	7.7971E-133	5
NCAPH	2.30308E-135	0.63251564	0.644	0.081	7.7996E-131	5
CENPK	7.02438E-135	0.62826569	0.667	0.089	2.37874E-130	5
HMGB2-2	2.9904E-133	0.96147436	0.977	0.231	9.07459E-129	5
CDC20	1.13207E-132	0.68532773	0.966	0.209	3.83337E-128	5
LIG1	4.15097E-132	0.65523113	0.819	0.168	1.2596E-128	5
TOP2A-5	1.41438E-130	1.72210907	1	0.317	4.79268E-126	5
MPHL-2-3	1.48208E-130	0.91484788	0.902	0.193	4.9614E-126	5
RTKN2	7.99628E-130	0.54376926	0.466	0.049	2.70723E-125	5
ASPM	1.08102E-129	0.68532773	0.966	0.216	3.66061E-125	5
NCAPG	3.56217E-128	0.56179167	0.803	0.099	1.20679E-123	5
PCNA	1.14728E-127	0.65828228	0.809	0.144	3.8854E-123	5
NEIL3	6.92E-126	0.63977756	0.69	0.101	2.34298E-121	5
ATAD2-3	2.42328E-126	1.16658728	0.954	0.264	8.2063E-121	5
E2F1	3.5632E-126	0.85566353	0.576	0.01	1.5276E-120	5
ANKMY2-5	4.90178E-126	0.64439903	0.664	0.097	1.6247E-120	5
CDC6	1.08102E-125	0.68532773	0.966	0.209	3.66061E-121	5
PRIM2	6.3923E-122	0.66258923	0.707	0.113	2.16356E-118	5
CEP152	9.24092E-124	0.48287866	0.655	0.094	3.13158E-119	5
TPX2-2	2.9979E-123	1.02630655	0.768	0.161	1.0153E-118	5
TYMS-5	6.41768E-123	1.00978253	0.954	0.243	2.29075E-118	5
CDC25A	1.1438E-122	0.68532773	0.966	0.216	3.87316E-118	5
PARP1-5	2.1658E-121	0.59997724	0.514	0.021	7.33468E-117	5
CCNA2	4.66931E-121	0.65027097	0.718	0.114	1.5422E-116	5
PRAP1	5.97628E-121	0.53164855	0.489	0.052	1.9271E-116	5
SKA3	6.24815E-121	0.39035332	0.329	0.061	2.1147E-116	5
CLSPN	7.09478E-121	0.77350951	0.819	0.156	2.4033E-116	5
CKAP2L	8.91568E-120	0.39035932	0.488	0.063	2.23998E-115	5
ZWILCH	1.03582E-119	0.68532773	0.966	0.209	3.66061E-115	5
RASD1	8.51163E-117	0.61956353	0.801	0.166	2.88268E-112	5
PCLAF-7	5.72468E-116	1.17997431	0.977	0.316	1.9381E-111	5
CDC6	8.73787E-116	0.64718858	0.966	0.263	2.29148E-111	5
CIT	1.2403E-114	0.65973894	0.793	0.156	4.1996E-110	5
KIF20A	1.2403E-114	0.65973894	0.793	0.156	4.1996E-110	5
CDT1	1.4566E-113	0.59843127	0.807	0.159	3.0277E-108	5
CDCA8	3.19488E-112	0.59934479	0.867	0.193	1.0726E-107	5
CENPM	1.87186E-110	0.69423766	0.672	0.139	6.3384E-106	5
ASL1	1.31368E-109	0.60212997	0.678	0.111	4.4851E-105	5
TACC3	1.85522E-109	0.70563269	0.903	0.205	6.2809E-105	5
SMIM1	7.49028E-109	0.45123932	0.769	0.162	2.5297E-104	5
CDC45	1.1438E-108	0.68532773	0.966	0.209	3.87316E-104	5
GINS2	1.08102E-107	0.67029928	0.739	0.152	3.66061E-103	5
RAB30	1.2031E-107	0.69695508	0.68	0.099	4.0732E-103	5
ORC6	2.3248E-107	0.69156353	0.801	0.166	7.8674E-103	5
HELLS	8.00178E-107	0.77242643	0.851	0.188	2.7092E-102	5
CDCA5	1.08102E-106	0.68532773	0.966	0.209	3.66061E-102	5
CDC25C	4.16368E-106	0.3917728	0.437	0.047	1.4097E-101	5
BIRC5	6.15991E-106	0.65696563	0.931	0.248	2.0756E-101	5
CEP55	7.19868E-106	0.61773307	0.77	0.147	2.4372E-101	5
RAD51	1.02068E-104	0.56454229	0.648	0.078	3.4716E-100	5
BIRC5-3	2.68898E-104	0.61928649	0.966	0.263	9.1019E-100	5
NUSAP1	7.72479E-102	0.27987724	0.402	0.042	2.6163E-97	5
KIAA0101	1.03582E-101	0.68532773	0.966	0.209	3.50702E-97	5
CENPE	4.36208E-102	0.65881207	0.649	0.11	1.4513E-97	5
EGR1	2.9412E-101	0.42195262	0.511	0.069	9.9578E-97	5
ASPM	8.95408E-101	0.64768723	0.589	0.088	2.3048E-96	5
PWRN3	3.124E-100	0.61772377	0.421	0.102	1.0581E-95	5
TK1	1.03582E-99	0.68532773	0.966	0.209	3.50702E-95	5
PKIG	2.01707E-99	0.65695507	0.759	0.161	6.8318E-95	5
BNC2	6.6264E-99	0.7582113	0.874	0.22	1.9656E-94	5
BARD1	2.29021E-98	0.59827423	0.603	0.099	7.6833E-94	5
CCNB2	6.03397E-98	0.29658653	0.356	0.034	1.8397E-93	5
CDC20-3	1.93734E-97	0.65695753	0.569	0.081	6.2636E-93	5
CENPF-3	1.5407E-97	0.71993742	0.963	0.227	5.2103E-93	5
ZWILCH-3	2.68898E-97	0.61928649	0.966	0.263	9.1019E-93	5
HMMR-1	1.2012E-96	0.69179229	0.813	0.203	4.0657E-92	5
RACGAP1	1.2671E-95	0.41503764	0.621	0.153	4.2900E-91	5
RRM1	3.7439E-95	0.57454278	0.813	0.203	1.2674E-90	5
DEPDC1B	4.07378E-95	0.57958659	0.53	0.08	1.3792E-90	5
CHAF1A	6.96228E-95	0.67439932	0.724	0.151	2.3213E-90	5
KIAA112	1.13269E-94	0.61673533	0.489	0.099	3.8343E-90	5
TOP2A	1.24268E-94	0.68532773	0.966	0.209	4.2072E-90	5
KIF2C	1.97515E-94	0.63425529	0.716	0.143	6.6859E-90	5
KIF14	1.91478E-94	0.54249798	0.606	0.97	6.4826E-90	5
PANDA	2.41568E-94	0.69021366	0.678	0.137	8.1765E-90	5
STIL	3.40128E-94	0.39035938	0.471	0.061	1.1515E-89	5
ANLN	4.08228E-94	0.68532773	0.966	0.209	1.3818E-89	5
DNA2	4.71788E-94	0.29653453	0.431	0.08	1.5968E-89	5
DTL	2.15919E-93	0.35695857	0.408	0.068	7.3104E-89	5
CDCA7	2.15919E-93	0.35695857	0.408	0.068	7.3104E-89	5
RRM2B-4	4.7455E-93	0.59883853	0.963	0.268	1.6062E-88	5
BUB1	8.0942E-93	0.29588844	0.431	0.083	2.7400E-88	5
BRCA2	9.15978E-93	0.58122584	0.431	0.084	3.1008E-88	5
CDKN3	1.07127E-92	0.59934479	0.867	0.193	3.6262E-88	5
CDC25B	1.07127E-92	0.59934479	0.867	0.193	3.6262E-88	5
LBR-1	3.37614E-92	0.6915233	0.802	0.227	1.1427E-87	5
NCAPG2	9.02456E-89	0.61707977	0.833	0.214	3.7910E-84	5
HAUS-3	4.86212E-88	0.59934479	0.867	0.193	1.6458E-83	5
MCM7	1.86327E-87	0.71437348	0.839	0.23	6.2926E-83	5
TYMS-DS-1	8.27268E-87	0.49119153	0.73	0.197	2.8299E-82	5
PRIM1	1.22243E-86	0.29425997	0.374	0.043	4.1396E-82	5
ZWINT-3	1.22243E-86	0.29425997	0.374	0.043	4.1396E-82	5
KIFAA	7.32297E-86	0.59883853	0.577	0.088	2.4796E-81	5
LMNB1	3.91901E-85	0.65482272	0.73	0.198	1.3903E-80	5
CENPH	8.04895E-85	0.63235367	0.797	0.185	2.7259E-80	5
UBE2T	9.61903E-85	0.73491869	0.879	0.265	3.3230E-80	5
MCM4	1.03582E-84	0.68532773	0.966	0.209	3.5070E-80	5
KIFAA	7.32297E-86	0.59883853	0.577	0.088	2.4796E-81	5
LMNB1	3.91901E-85	0.65482272	0.73	0.198	1.3903E-80	5
CENPH	8.04895E-85	0.63235367	0.797	0.185	2.7259E-80	5
UBE2T	9.61903E-85	0.73491869	0.879	0.265	3.3230E-80	5
MCM4	1.03582E-84	0.68532773	0.966	0.209	3.5070E-80	5
FEN1	4.19898E-83	0.62233856	0.53	0.098	1.4224E-78	5
NEIL3	7.35998E-83	0.57366997	0.443	0.062	2.4749E-78	5
KIF23	1.09889E-82	0.69429972	0.797	0.196	3.7576E-78	5
DSN1	2.75026E-82	0.39697273	0.64	0.154	9.3106E-78	5
TUBA1B-8	6.67299E-81	1.23163985	1	0.743	2.2507E-76	5
KIAA1C	4.32435E-81	0.39035927	0.408	0.064	1.4647E-76	5
ORC1	1.03582E-80	0.68532773	0.966	0.209	3.4966E-76	5
BRCA1	5.3968E-81	0.31157928	0.437	0.062	1.7173E-76	5
KIAA1-7	1.13419E-80	1.14995205	1	0.797	3.8269E-76	5
MCM2	8.09237E-80	0.59361952	0.992	0.11	2.7298E-75	5
MCM10	1.07088E-79	0.35402087	0.42	0.058	3.6245E-75
CENPA	1.07088E-79	0.35402087	0.42	0.058	3.6245E-75
GINS-3	9.40703E-79	0.39617733	0.564	0.124	3.1733E-74
DNA2	8.71788E-79	0.29653453	0.431	0.08	1.9396E-73
RRM2	2.39403E-78	0.33412982	0.64	0.162	8.0772E-74
ANLN	2.93343E-77	0.37648973	0.644	0.129	9.8955E-73
KIAA1245	9.17268E-77	0.64818688	0.707	0.176	3.1004E-72
DEMP2	3.29167E-76	0.33981261	0.963	0.164	1.1102E-71
CDC7	3.29167E-76	0.33981261	0.963	0.164	1.1102E-71
DEPDC1	7.66561E-76	0.67807871	0.64	0.098	2.5856E-71
CDKN2D	1.00728E-74	0.19638364	0.489	0.081	3.3976E-70
TUBA1B-2	1.15218E-73	0.99024161	0.994	0.697	3.8858E-69
ID3-2	1.15218E-73	0.99024161	0.994	0.697	3.8858E-69
FAM64A	2.42540E-73	0.56391997	0.61	0.171	8.1803E-69
HJURP-2	1.42178E-72	0.55336991	0.391	0.059	4.7958E-68
CDCA3-3	1.59402E-72	0.56391997	0.563	0.172	5.3764E-68
PHF19-3	2.91967E-71	0.67599891	0.831	0.321	9.8753E-67
DNMT1-4	8.92438E-71	0.7714229	0.95	0.416	3.0098E-66
INCENP	1.75727E-70	0.31172454	0.429	0.099	5.7903E-66
CDCA7L	2.42540E-70	0.56391997	0.563	0.172	8.1803E-66
MAD2	2.82437E-68	0.55336991	0.412	0.067	9.5257E-64
POLE	3.78624E-68	0.31522765	0.529	0.153	1.2726E-63
UHRF1	8.33268E-68	0.57366997	0.429	0.144	2.7999E-63
CHAF1	1.01739E-66	0.63035312	0.839	0.264	3.4433E-61
SOD2	1.39068E-65	0.39367362	0.626	0.111	4.6852E-61
TUBD1	4.29918E-65	0.71326511	0.991	0.263	1.4393E-60
TUBB	1.03582E-64	0.68532773	0.966	0.209	3.4966E-60
CKAP2	1.01739E-63	0.63035312	0.839	0.264	3.4433E-61
SPAG5	2.15701E-64	0.35896369	0.517	0.1	7.3027E-60
TMPO-2	1.78024E-63	0.7599855	0.966	0.236	6.0983E-59
PCNA-3	2.04789E-63	0.39839398	0.632	0.148	6.9332E-59
TUBA1B-3	2.04789E-63	0.39839398	0.632	0.148	6.9332E-59
MKI67	1.87151E-62	0.63275703	0.889	0.1	6.3355E-58
PLOD2	2.62702E-62	0.56317554	0.523	0.157	8.8967E-58
CKS1B-3	2.32196E-61	0.71851564	0.977	0.343	7.8601E-57
MYO1B	3.62218E-61	0.49833622	0.759	0.228	1.2263E-56
MSRB2	1.19237E-60	0.63035312	0.736	0.203	4.0370E-56
CENPW-2	1.39131E-60	0.49123977	0.606	0.241	4.8754E-60
CDCA7L-2	1.39131E-60	0.49123977	0.606	0.241	4.8754E-60
CCNB1-2	1.74857E-60	0.55035233	0.621	0.168	5.9192E-56
CCDC34	1.76937E-59	0.39632328	0.666	0.177	5.9427E-55
CDCA5-3	7.13346E-59	0.77473962	0.704	0.212	2.4151E-54
SPC24	1.97268E-58	0.29161508	0.45	0.097	6.6763E-54
CDC25A	2.07268E-58	0.29161508	0.45	0.097	7.0151E-54
RNASE4	3.96668E-58	0.49171423	0.766	0.23	1.3427E-53
CENPN	4.86322E-58	0.29612233	0.606	0.155	1.6459E-53
MCM5-1	6.71166E-58	0.47238252	0.472	0.083	2.2715E-53
NUF2	1.18036E-57	0.29755407	0.423	0.081	3.9951E-53
RAD51C	1.63358E-57	0.39675838	0.605	0.173	5.5287E-53
CALM2-3	2.29039E-57	0.63732294	1	0.606	7.8177E-53
CDC20-2	2.29039E-57	0.63732294	1	0.606	7.8177E-53
PLK1	3.73232E-53	0.65858205	0.648	0.132	1.2629E-48
HMGB3	4.07923E-53	0.33370504	0.569	0.139	1.3803E-48
RFC4	6.75926E-53	0.61243708	0.629	0.148	2.2873E-48
UBE2L3	3.39678E-52	0.74315724	1	0.802	1.1495E-47
STMN1-7	1.47438E-53	0.72491412	1	0.802	4.9903E-49
PLK1	3.73232E-53	0.65858205	0.648	0.132	1.2629E-48
HMGB3	4.07923E-53	0.33370504	0.569	0.139	1.3803E-48
RFC4	6.75926E-53	0.61243708	0.629	0.148	2.2873E-48
UBE2L3	3.39678E-52	0.74315724	1	0.802	1.1495E-47
CENPC	4.38437E-52	0.29701247	0.454	0.111	1.4838E-47

Gene	p_val	avg_logFC	pct.1	pct.2	p_val_adj	cluster
LMO1	4.17997E-52	0.35066747	0.843	0.135	1.4139E-47	9
CDH23-7	8.36838E-52	0.60391723	0.879	0.333	3.1719E-47	9
SYCP2-7	1.93815E-51	0.64869883	0.753	0.249	6.2411E-47	9
ANKRD36B	1.93815E-51	0.64869883	0.753	0.249	6.2411E-47	9
NACAD-5	4.43973E-51	0.59523066	1	0.462	1.4958E-46	9
MMRN2	2.20194E-49	0.32231344	0.471	0.106	6.7417E-45	9
NAIP5-2	2.20194E-49	0.32231344	0.471	0.106	6.7417E-45	9
LMNB2	1.17156E-48	0.37165473	0.713	0.218	3.5865E-44	9
CBS	1.47678E-48	0.56036379	0.954	0.61	0.000000	9
RAMP1-5	6.92653E-48	0.63343454	0.964	0.763	2.0904E-43	9
HMGN2-6	1.79505E-43	0.62971643	0.964	0.714	1.2832E-38	9
RCC2-7	2.45428E-43	0.32398238	0.989	0.297	8.5091E-38	9
BTD3	5.49078E-42	0.46533173	0.601	0.367	1.7769E-37	9
PPIA-6	6.30496E-42	0.44422717	0.964	0.788	2.0398E-37	9
PPIA-5	6.30496E-42	0.44422717	0.964	0.788	2.0398E-37	9
NCAPD3	1.69729E-40	0.34969004	0.718	0.243	5.4923E-36	9
CCNG1	1.69729E-40	0.34969004	0.718	0.243	5.4923E-36	9
DCK	2.62278E-40	0.29382339	0.989	0.297	8.4858E-36	9
ARL6IP6	5.13157E-40	0.28343866	0.686	0.168	1.6602E-35	9
SQSTM1	5.13157E-40	0.28343866	0.686	0.168	1.6602E-35	9
ADNDL1	5.95207E-40	0.25470673	0.489	0.126	1.9259E-35	9
RPL37A-5	1.03257E-39	0.25470673	0.489	0.126	3.3409E-35	9
ACYP1	2.72357E-39	0.33664664	0.661	0.218	8.2162E-35	9
HMGB1-8	3.09909E-39	0.59370398	1	0.812	1.0397E-34
MDH2	6.29324E-39	0.33887711	0.989	0.788	1.7921E-34
RAD21	7.56424E-39	0.54343229	0.96	0.638	2.5699E-34
ACTG1	1.10683E-38	0.41438863	0.989	0.807	3.5801E-34
ECGF1	1.10683E-38	0.41438863	0.989	0.807	3.5801E-34
RAPH1	2.33215E-38	0.28734159	0.648	0.173	7.8998E-34
CDH8-1	7.87369E-38	0.28720703	0.443	0.112	2.6681E-33
SMC4A	1.26434E-37	0.37343781	0.49	0.249	4.3438-33
TYQP-1-2	2.60899E-37	0.51342205	0.821	0.422	8.8237E-33
ANP32B-6	2.80099E-37	0.30013941	0.969	0.524	1.5038E-32
ANP32B	2.80099E-37	0.30013941	0.969	0.524	1.5038E-32
SSBP1-1	2.96017E-32	0.49484741	0.99	0.839	7.9968E-28
NFATC2IP	2.36412E-32	0.38437182	0.81	0.399	8.3438-28
LYAR	6.75756E-32	0.31202821	0.823	0.409	1.8257E-33
CA2	8.00935-32	0.39783648	0.77	0.333	2.0343E-27
ANP32E	1.03039E-31	0.30013941	0.969	0.524	2.7855E-27
BCRP3-4	2.21983E-31	0.48768961	0.742	0.408	6.0015E-27
RUBX	4.30987E-31	0.45553828	0.648	0.177	1.1653E-26
MTHFD2	4.3766E-31	0.51883367	0.931	0.539	1.6833E-32
RPA1	1.02393E-30	0.39196613	0.944	0.568	2.7683E-26
KIAA1598	3.33183E-31	0.33478745	0.648	0.185	1.1673E-31
DNM2	2.3033E-31	0.33678761	0.648	0.181	7.7961E-27
SEC24B	2.3033E-31	0.33678761	0.648	0.181	7.7961E-27
IGF	8.31614E-31	0.32163636	0.727	0.258	2.7246E-26
CSNK2B-2	2.21983E-31	0.48768961	0.742	0.408	6.0015E-27
CSNK2B-3	2.21983E-31	0.48768961	0.742	0.408	6.0015E-27
ANP32A-5	2.80099E-37	0.30013941	0.969	0.524	1.5038E-32
ANP32A	2.80099E-37	0.30013941	0.969	0.524	1.5038E-32
ACYP1-2	2.72357E-39	0.33664664	0.661	0.218	8.2162E-35
HMGB1-8	3.09909E-39	0.59370398	1	0.812	1.0397E-34
MDH2	6.29324E-39	0.33887711	0.989	0.788	1.7921E-34
RAD21	7.56424E-39	0.54343229	0.96	0.638	2.5699E-34
ACTG1	1.10683E-38	0.41438863	0.989	0.807	3.5801E-34
ECGF1	1.10683E-38	0.41438863	0.989	0.807	3.5801E-34
RAPH1	2.33215E-38	0.28734159	0.648	0.173	7.8998E-34
CDH8-1	7.87369E-38	0.28720703	0.443	0.112	2.6681E-33
SMC4A	1.26434E-37	0.37343781	0.49	0.249	4.3438-33
TYQP-1-2	2.60899E-37	0.51342205	0.821	0.422	8.8237E-33
ANP32B-6	2.80099E-37	0.30013941	0.969	0.524	1.5038E-32
ANP32B	2.80099E-37	0.30013941	0.969	0.524	1.5038E-32
SSBP1-1	2.96017E-32	0.49484741	0.99	0.839	7.9968E-28
NFATC2IP	2.36412E-32	0.38437182	0.81	0.399	8.3438-28
LYAR	6.75756E-32	0.31202821	0.823	0.409	1.8257E-33
CA2	8.00935-32	0.39783648	0.77	0.333	2.0343E-27
ANP32E	1.03039E-31	0.30013941	0.969	0.524	2.7855E-27
BCRP3-4	2.21983E-31	0.48768961	0.742	0.408	6.0015E-27
RUBX	4.30987E-31	0.45553828	0.648	0.177	1.1653E-26
MTHFD2	4.3766E-31	0.51883367	0.931	0.539	1.6833E-32
RPA1	1.02393E-30	0.39196613	0.944	0.568	2.7683E-26
KIAA1598	3.33183E-31	0.33478745	0.648	0.185	1.1673E-31
DNM2	2.3033E-31	0.33678761	0.648	0.181	7.7961E-27
SEC24B	2.3033E-31	0.33678761	0.648	0.181	7.7961E-27
IGF	8.31614E-31	0.32163636	0.727	0.258	2.7246E-26

cluster. Differentially expressed genes between the two groups of cells were identified using a non-parametric Wilcoxon Rank Sum test (Seurat default). Pct.1 corresponds to the fraction of cells in column "cluster" in the table, and pct.2 corresponds to the rest of cells in the other clusters/identities. The 'avg_logFC' column is giving the difference found in that gene in that cluster/identity compared to the rest. If the number is positive, it means that is upregulated, and if it is negative, it is downregulated. P_val_adj, adjusted p-value, based on Bonferroni correction using all features in the dataset.

Supplementary Table 8.

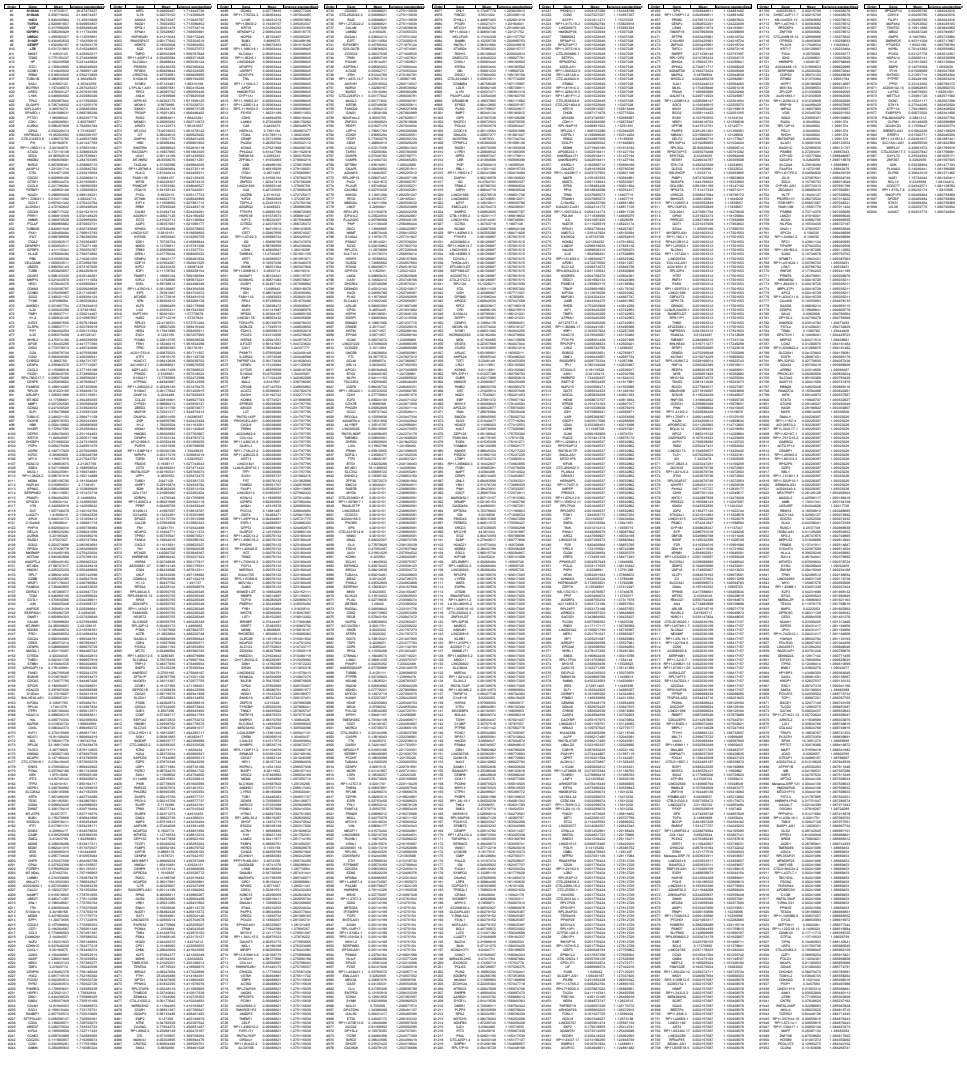

Top 2000 genes with high variable cell-to-cell expression in H2030-BrM brain metastasis.

Subset of genes that exhibit high cell-to-cell variation in the dataset (i.e., genes with high expression in some cells and low expression in others), obtained after modeling the mean-variance relationship inherent in single-cell data with Seurat. Top 10 genes are in bold.

Supplementary Table 9.

Supplementary Table 9_DEG in cluster 5 vs rest scRNAseq H2030-BrM

Gene	p_val	avg_logFC	pct.1	pct.2	p_val_adj
S100A9	1.1998E-222	2.75925766	0.905	0.571	4.0561E-218
S100A8	1.6171E-147	1.95845924	0.433	0.107	5.4746E-143
CTSL	3.3821E-268	1.30287996	0.985	0.747	1.1451E-263
IGFBP3	0	1.29926068	0.683	0.113	0
MT2A	8.6346E-124	0.95364259	0.997	0.985	2.9233E-119
STC1	8.33601E-98	0.93962756	0.769	0.454	2.8222E-93
S100A11	3.6935E-267	0.81428092	1	0.985	1.2505E-262
FAM83A	1.1357E-120	0.81322162	0.926	0.731	1.0616E-115
C15orf48	3.6152E-160	0.80969976	0.992	0.863	1.224E-155
HSPB8AA1	5.4478E-196	0.80614242	1	0.973	1.8444E-191
AREG	4.3171E-75	0.78830027	0.835	0.624	1.4616E-70
LUCAT1	2.1606E-101	0.71312452	0.801	0.495	7.3156E-97
SPP1	1.8232E-171	0.68438167	0.997	0.972	6.1727E-167
FERMT1	1.7419E-75	0.67249322	0.717	0.44	5.8973E-71
RSPO3	2.4532E-152	0.66772169	0.837	0.453	8.3056E-148
TAGLN2	3.9477E-135	0.65387522	0.985	0.869	1.3365E-130
ANGPTL4	1.8342E-82	0.63631562	0.666	0.351	6.2100E-78
TFPI2	3.3304E-161	0.63586598	0.999	0.978	1.1275E-156
IGFBP4	7.7946E-112	0.63316799	0.819	0.496	2.639E-107
TIMP1	1.2985E-78	0.62467369	1	0.987	4.3953E-74
PMEPA1	2.3769E-128	0.60972487E	0.95	0.731	8.0474E-124
AC003092.1	5.5417E-165	0.56661918S	0.512	0.129	1.8762E-160
IER3	9.9700326-61	0.56633145S	0.909	0.718	3.3754S5E-56
CXCL8	6.9327E-174	0.5651922	0.447	0.093	2.3471E-169
RASD1	1.508E-150	0.55571375T	0.477	0.12	5.1053E-146
BCYRN1	1.0859S5E-59	0.54088492G	0.604	0.326	3.6765S6E-55
PFDN2	6.9839E-159	0.53240151S	0.996	0.96	2.3645E-154
CDTL1	9.382E-79	0.521952979	0.732	0.417	3.2440BE-74
ACTN1	8.9410T6-97	0.520932787	0.856	0.581	3.0270BE-92
CIB1	8.3972E-112	0.51757579S	0.979	0.858	2.843E-107
TMSB10	1.1964S0-60	0.50454998T	0.757	0.509	4.0506S8-56
TGM2	6.5597N0-30	0.50344073	0.78	0.623	2.2323BE-25
DKK1	5.4664C-130	0.49935170T	0.604	0.214	1.8507E-125
TOP1	7.7313E-103	0.49845285T	0.968	0.841	2.6175ZE-98
ODC1	3.5229A5-73	0.48493288E	0.933	0.777	1.1926ZE-68
TPI1	1.7839E-107	0.48465782B	0.992	0.914	6.0395E-103
AKAP12	1.3357I1-64	0.48034906E	0.687	0.421	4.5221IE-60
FTH1	8.1215E-115	0.472885620	0.999	0.998	2.7496E-110
TMEM158	2.7565E-130	0.471370107	0.475	0.137	9.3324E-126
SLIRP	1.5447E-109	0.46918962Z	0.985	0.92	5.2296E-105
ASPH	3.0331S5E-82	0.4564233M	0.906	0.706	1.0269E-77
METTL9	6.5532167-77	0.4453280AZ	0.836	0.579	2.2186S5E-72
MRPL52	9.2656Z6-69	0.442449412	0.972	0.839	3.1369T6-64
ACTB	3.321E-120	0.44077972T	1	0.997	1.1244E-115
IGSF8	2.6276986-64	0.43928655S	0.728	0.448	8.8962B6-60
BTG1	1.0167B6-71	0.43690558	0.887	0.607	3.4424167-67
CEBPB	5.9312E6-54	0.43677747	0.839	0.626	2.0080961-49
ACOX2	1.8372E-82	0.43599297	0.752	0.428	6.2200387-78
MCL1	1.489E-68	0.43590529	0.808	0.585	5.0411T5-64
SERPINE2	1.2380I1-38	0.43484201	0.673	0.447	4.1914Z6-34
TNFRSF12A	2.0881Z6-67	0.43390598	0.488	0.188	7.0695I3E-63
UPP1	4.8945E-104	0.43123286	0.55	0.205	1.657I1E-99
NT5E	1.0242A4-94	0.42615847E	0.527	0.206	3.4676T6-90
TOP2A	1.7427B6-33	0.425922882	0.527	0.313	5.9935I6-29
MT1X	3.5407E-26	0.42466415	0.665	0.486	1.1987I4E-21
CITED4	8.6015E-101	0.42274156T	0.481	0.16	2.7066L96
DYNC1H1	6.2269S5-65	0.420504227	0.978	0.905	2.1082E-60
ISG20	2.3278S6-49	0.42031518	0.892	0.724	7.8911T5-45
LRP10	1.2657Z6-44	0.41869123R	0.837	0.7	4.2852T6-40
CALD1	3.383E-169	0.41294788B	0.406	0.085	1.1487E-164
NCL	5.8621665-63	0.41223476A	0.973	0.902	1.9846962-60
FXYD5	1.5388E-40	0.41105746S	0.78	0.565	5.2097T5-36
MCK	3.3891S5-91	0.407480003	0.64	0.292	1.1474X-86
PCNP	3.7797Y6-95	0.404637516	0.978	0.866	1.2830T6-90
IFITM3	1.3942T4-63	0.397113363	0.972	0.906	4.7204E4E-61
SAA1	3.6487E6-51	0.39807266	0.99	0.951	1.2484W6-47
DAD1	1.6466E6-71	0.385725158	0.942	0.805	5.5749Z6-67
CCL2	3.6442E-70	0.38435576	0.549	0.247	1.0981T6-65
PTGR1	6.4043Z6-60	0.380589808	0.764	0.506	2.1683Z6-55
HSPD1	7.6265S6-57	0.37941709	0.931	0.791	2.5845E-52
HSPA1	1.5019S6-58	0.378987434	0.919	0.745	5.0853I6-54
PGM7	1.2897E6-68	0.377705496	0.999	0.98	4.3631R6-64
AHSA1	3.0074W2-60	0.376741388	0.842	0.604	1.0162Z6-55
PLP2	1.1102T5-62	0.376074322	0.849	0.702	3.7546Z6-58
PRKDC	5.7199T6-62	0.36822198	0.951	0.823	1.9350S6-57
CPS1	3.2299E6-59	0.365154496	0.968	0.885	1.1102E6-54
GFPT1	3.1939E-73	0.365534459	0.987	0.922	1.0539A6-68
SPP1	1.6078E-63	0.364603416	0.581	0.356	5.4351E-59
ARNT2	6.3275E-107	0.360940214	0.916	0.676	2.1422E-97
CHCHD10	1.7332E-62	0.360648838	0.937	0.807	5.8619Z6-62
GSEA	7.1663S6-40	0.35868697	0.722	0.469	2.4235E-35
CKS1B	7.0318T6-20	0.356764478	0.761	0.675	2.3607I6-15
TCIM	2.1578E-261	0.354139677	0.238	0.009	7.3058E-257
SNRPF	4.3769T6-57	0.351463379	0.912	0.75	1.4818T6-52
ATP5MC3	2.4462B6-61	0.350555567	0.975	0.901	8.2823E-57
SLC20A1	2.8569I3-35	0.349863094	0.722	0.509	9.6724E-31
ATP5MJ	5.2070S5-63	0.349364722	0.965	0.887	3.1717AE-48
SMOC1	4.8475E-148	0.348647956	0.295	0.044	1.6412E-143
PSMD14	1.4261E-53	0.347338321	0.893	0.73	4.8268E-49
BCLA3	3.4270T6-51	0.345932651	0.879	0.693	1.1602T6-46
CDKN3	1.0860B6-36	0.343643367	0.55	0.324	3.6566E6-32
DUSP23	2.6151T6-38	0.343301677	0.881	0.73	8.8539Z6-34
GCLM	1.3307Z6-50	0.342373126	0.652	0.397	4.5052T6-46
CALM1	1.8010S6-48	0.341763589	0.996	0.974	6.0976S6-44
PAPOLA	2.3744S6-54	0.339476509	0.847	0.641	8.0137S6-50
GNG4	4.8671E6-67	0.337436826	0.501	0.217	1.6473C6-62
CALM2	1.4192S6-46	0.337219081	0.324	0.131	4.8050T6-42
CHL1	9.3058E-120	0.33628316	0.424	0.11	3.1505E-115
ATP5AI	1.5778E6-54	0.335757907	0.98	0.92	3.1171AE-49
PSMA3	4.1502I1E-50	0.335593798	0.896	0.75	1.4051E-45
TOP2	7.7637B6-57	0.333742344	0.534	0.268	2.6280I1E-52
NDUFC1	6.1026B6-65	0.332747739	0.968	0.874	2.0661E6-60
TESC	1.5778E6-54	0.332112646	0.356	0.159	5.3420I1E-50
CYTOR	6.2425T6-36	0.33159978	0.799	0.616	2.1134E-31
DLGAP5	1.0429S6-23	0.329830468	0.348	0.192	3.5310E-19
CCT6A	2.6873967-47	0.32681836	0.79	0.598	9.9307I3E-43
CCT3	4.6319Z6-75	0.326011353	0.894	0.949	1.5681I6E-70
SUPT16H	1.5951I6-38	0.324464396	0.93	0.672	5.4006E6-34
PHF19	1.5123B6-42	0.324378714	0.569	0.312	5.1233I6E-38
NMB	3.8290I3E-45	0.324295709	0.783	0.556	1.2963I6E-40
CNIH1	1.9285B6-40	0.323863536	0.627	0.624	6.5264I3-36
MAP3K20	1.1804S6-42	0.323137109	0.707	0.493	3.9965I3E-38
MGST1	1.2099I1E-47	0.321311574	0.961	0.861	4.6923Z6-43
SOF3L1	9.6505I1E-36	0.318986507	0.767	0.561	3.2672B6-31
APOC1	3.3812E-63	0.318951199	0.694	0.436	1.1477E-58
RHEB	3.1716T6-39	0.315950563	0.659	0.43	1.0736T6-34
CDCA4	2.8859S6-39	0.315868961	0.467	0.265	9.7029B6-35
PA2G4	3.1264W6-45	0.315400464	0.926	0.81	1.0585E-40
PHLDA2	4.4904B6-36	0.315082998	0.672	0.452	1.5203E-31
HMGB3	1.9528B6-40	0.313268236	0.554	0.324	6.6115B6-36
EIF3B	1.1026B6-46	0.31145478	0.924	0.762	3.7366B6-42
SNAPC1	2.2229A6-46	0.311380534	0.722	0.471	7.5259B6-42
SDHC	2.2864S6-47	0.308512341	0.962	0.865	7.6796S6-43
TPMI	6.1439E6-60	0.3069481	0.905	0.78	2.0801E-35
PXBP1	1.0590T6-39	0.306245679	0.826	0.659	3.5850B6-35
TUBA1B	1.3266A6-19	0.305492027	0.839	0.739	4.4914E-15
DTYMK	2.8924S6-33	0.304568228	0.527	0.324	9.4875T6-29
GLRX	3.8280B6-23	0.303747159	0.504	0.343	1.2964I4E-18
KYNU	1.7120T6-43	0.303611554	0.595	0.348	3.7663M-39
GRAMD1B	6.8124W6-33	0.301130784	0.884	0.737	2.3664I6-28
SAT1	1.9041E-32	0.300945237	0.986	0.92	6.4465Z6-28
RRM2	7.0835S6-24	0.299812711	0.386	0.222	2.3982I6-19
DDX24	9.5338Z6-41	0.299445299	0.919	0.812	3.2277T6-36
ZC3H15	1.3627I3E-40	0.298638639	0.78	0.575	4.6136I4E-36
TRIB3	7.1664I4E-48	0.29385792	0.374	0.163	2.4560I2E-43
EMP3	3.7137E6-49	0.292767972	0.983	0.917	1.2573I4-44
ANP32E	4.9728E-25	0.291938129	0.684	0.521	1.6835B6-20
SIVA1	7.3715S6-37	0.290079865	0.867	0.709	2.4957I6-32
RAB3F	5.1075B6-35	0.290036319	0.819	0.658	1.7292E-30
LY6K	1.2650I1E-88	0.289641453	0.136	0.014	4.2628Z6-84
GAPDH	5.6839I6-76	0.289387694	1	0.999	1.9243SE-71
PFKP	2.2180T6-41	0.288084381	0.59	0.35	7.5095E-37
PLIN3	3.221E-30	0.287476401	0.67	0.487	1.0906E-25
MESP1	1.6257I6-33	0.287236113	0.32	0.315	5.5041E6-29
PSMB5	1.5586I3-61	0.286913892	0.985	0.949	5.2775T6-57
RANBP1	1.5893I3E-23	0.286521144	0.863	0.757	5.3808I3-19
XRCC5	1.9572I6-40	0.28564957	0.892	0.787	6.6263B6-36
EPAS1	5.9599E6-81	0.284604521	0.345	0.101	2.0178E-76
HMGA1	3.7723S6-38	0.283423416	0.83	0.625	1.2771IE-33
MPHOSPH6	2.3773E6-41	0.282838897	0.687	0.441	8.0488T6-37
DYNLL1	6.8902E-48	0.282103483	0.979	0.905	2.3327S6-43
CXCL3	3.9471S6-62	0.281718369	0.222	0.056	1.3363I6E-57
PTMA	4.8887E-45	0.281510702	0.994	0.99	1.6551I2E-40
CYQB1	1.2328T6-44	0.281069086	0.944	0.836	4.1740Z6-40
NDP52	2.1369A6-46	0.280555352	0.962	0.929	7.2416I5-42
SLC25A37	2.4145I6-38	0.279709855	0.764	0.55	8.1745SE-34
AHNAK2	2.3036S5-24	0.279626858	0.606	0.689	7.7992I6-20
FKBP4	2.1971I6E-55	0.279490359	0.492	0.228	7.4387T6-51
PTN1	4.7749S5-65	0.2791125	0.992	0.974	8.1616I5E-60
CPS1	5.0188Z6-36	0.278887272	0.874	0.673	1.6991T6-31
CCN2	2.7511I6-11	0.278332804	0.387	0.276	9.3480T6-07
CREM	1.1444I6E-40	0.277322911	0.589	0.345	3.8746E-36
ITGA2	4.2115Z6-14	0.27705465	0.386	0.264	1.4259BE-09
CYCI	1.3092I1-36	0.277029732	0.938	0.835	4.4324T6-32
MIR4435-2HG	9.8281I6-37	0.276612058	0.52	0.301	3.3274T6-32
RBM9A	2.9662I6-43	0.276073218	0.972	0.9	1.0042T6-38
VIM	1.0233S5-36	0.276058658	0.969	0.904	3.4646S2-32
SNRPD1	2.0313I6-35	0.27541378	0.9	0.746	6.8774I3-31
ANXA1	3.3593H5-27	0.273827785	0.937	0.844	1.1375AE-22
LDHB	1.7497I6-40	0.270335476	0.935	0.836	3.9239I6-36
PPIA	3.7255S5-55	0.269797191	0.987	0.976	1.2614I2E-50
CHCHD2	2.0225I6-51	0.269654349	0.989	0.938	6.8510I3E-47
IFITM2	1.1454T6-39	0.267445471	0.954	0.877	3.8781I1E-35
NDUFB3	1.8606I6-32	0.267383284	0.851	0.7	5.688E-28
SEC61G	1.1393S6-32	0.266807023	0.958	0.877	3.8224I3E-28
AURKA	4.7432I6-25	0.266722578	0.377	0.208	1.8058I6E-20
UBE2C	4.2925S1E-17	0.26243842	0.345	0.21	1.4228E-12
HMOX1	9.0115I-27	0.261538564	0.3	0.146	3.6509I3-22
PDIA1	5.5967I6-49	0.26097883	0.966	0.912	2.0396I6-45
EIF5A	3.6826T6-48	0.260312785	0.971	0.925	1.2279I6-35
NFE2L2	1.9466E-67	0.259737235	0.856	0.709	7.1021E-63
CXCL1	6.5496I6E-57	0.258947348	0.249	0.065	2.2174S6-52
S100A13	1.0134S5-36	0.258584184	0.936	0.815	3.6941I3-32
DBI	2.2249E-32	0.255445077	0.819	0.634	7.5325E-28
PPGRSC	7.5467I6-36	0.253257447	0.604	0.393	2.5360BE-31
SOX1	1.7460T6-63	0.253374447	0.236	0.048	5.9162T6-61
HSPE1	1.1393S6-32	0.253003523	0.752	0.615	3.8224S6-28
ADM	5.3862Z6-38	0.252132428	0.971	0.889	1.8242E6-33
UBE2S	2.7445T6-14	0.251850238	0.494	0.698	9.2392I6E-10
CD320	3.4154T6-16	0.251830394	0.885	0.789	1.1356E6-11
PSMA1	1.5963T6-49	0.251670143	0.743	0.535	2.6966I6-45
ADH1	3.5813E-27	0.251621247	0.802	0.633	9.6847I6-23
HMGB1	2.7877S6-37	0.251572967	0.992	0.949	1.0067I6-32
KRAS	6.5372B6-32	0.250012944	0.707	0.505	2.2120E-27
BLCAP	6.5381I2E-19	0.250093945	0.304	0.455	2.2135SE-14
PNISR	4.9738S6-19	0.250613314	0.697	0.756	1.6839AE-14
RHOB	1.3928Z6-08	0.251833438	0.633	0.674	0.000471552

Gene	p_val	avg_logFC	pct.1	pct.2	p_val_adj
HSPA9	1.6135E-13	-0.25286446	0.871	0.967	5.4626E-09
ZKSCAN1	1.3656E-15	-0.25361469	0.554	0.836	4.637E-11
RPS6KB2	8.2009E-19	-0.25369846	0.341	0.475	2.7765E-14
KANK2	1.5254E-15	-0.25393328	0.488	0.583	5.1643E-11
CPE	1.6394E-20	-0.25406319	0.213	0.37	5.5555E-16
TENT5A	1.41E-12	-0.25464747	0.438	0.537	4.7738E-08
AAMDC	4.3026E-17	-0.25472272	0.243	0.383	1.4568E-12
UBE2H	1.7675E-16	-0.25480868	0.505	0.598	5.9841E-12
FZD10	5.062E-21	-0.25655888	0.16	0.318	1.7138E-16
SOX4	2.8429E-24	-0.25752261	0.979	0.982	9.6246E-20
SQSTM1	9.6026E-23	-0.25799884	0.799	0.837	3.0479E-18
TNRC6B	2.4233E-18	-0.25937441	0.651	0.715	8.2045E-14
SERINC5	6.1351E-17	-0.25899431	0.203	0.342	2.0771E-12
RNF217	5.4443E-25	-0.25986438	0.151	0.329	1.8432E-20
GADD45A	7.2218E-24	-0.26133433	0.154	0.327	2.445E-19
ZFAS1	9.381E-27	-0.2619464	0.95	0.958	3.176E-22
DYNLL2	1.7782E-20	-0.26344386	0.23	0.386	6.0203E-16
PPP1R15A	2.3753E-18	-0.26380755	0.349	0.488	8.0533E-14
TAPBP	1.573E-16	-0.26488886	0.539	0.622	5.3322E-12
PCSK7	1.7627E-16	-0.2685146	0.439	0.539	6.0354E-12
LMAN2	6.9714E-25	-0.26584626	0.799	0.829	2.3602E-20
PABPC1	8.6447E-37	-0.26962215	0.958	0.971	2.9273E-32
PGLS	3.3599E-21	-0.2698266	0.578	0.683	1.1375E-16
EIF4B	5.8985E-22	-0.27026839	0.647	0.732	1.997E-17
UBXN1	6.5508E-21	-0.27182546	0.652	0.726	2.2178E-16
TNS3	2.6579E-23	-0.27184659	0.238	0.413	8.9985E-19
ALDH3A2	2.5469E-17	-0.27257035	0.509	0.601	8.6228E-13
PGT	8.1137E-20	-0.2729902	0.834	0.701	2.747E-15
FOS	1.6616E-29	-0.2746287	0.961	0.964	5.6256E-25
ANKAJ	1.1361E-53	-0.27520733	0.953	0.989	3.8531E-49
RHOBTB2	1.5209E-29	-0.2755603	0.097	0.287	5.1491E-25
TUBA1A	1.0616E-13	-0.27565857	0.29	0.405	3.5942E-09
CMTM4	6.6626E-21	-0.27655573	0.432	0.561	2.2557E-16
ITGB4	1.3923E-19	-0.2771524	0.452	0.579	4.7139E-15
PCNX4	6.21E-13	-0.27829619	0.487	0.569	2.1024E-08
TNC4	8.6161E-33	-0.28035556	0.627	0.21	2.915E-28
KLF2	5.5901E-09	-0.27905897	0.401	0.472	0.000189206
RPS4Y1	1.6944E-68	-0.27918593	1	0.998	5.7368E-64
LIMCH1	2.0082E-42	-0.27919913	0.02	0.244	6.7998E-38
SSBP4	1.7409E-21	-0.28003329	0.603	0.686	5.8938E-17
GUK1	2.6892E-34	-0.28180058	0.902	0.927	9.1046E-30
PPP2CA	6.7461E-19	-0.2837346	0.403	0.532	2.2822E-14
RNF19A	5.1621E-19	-0.28607639	0.505	0.612	1.7477E-14
SELENOM	5.8851E-21	-0.28749487	0.589	0.685	1.9925E-16
HNGNS	4.4045E-26	-0.28784422	0.575	0.705	1.4912E-21
TMTSF2	1.5669E-23	-0.2897359	0.216	0.393	5.3035E-19
KCNF1	4.8641E-11	-0.28988903	0.578	0.616	1.6468E-06
NCN	3.581E-25	-0.29019311	0.358	0.522	1.2124E-20
RP11-153B9.8	1.4774E-28	-0.29047771	0.163	0.359	5.0017E-24
ATOH8	6.6801E-34	-0.29075506	0.645	0.241	2.3632E-29
SNHG7	4.3399E-20	-0.29160891	0.419	0.549	1.469E-15
MAP1B	6.7856E-21	-0.29959353	0.243	0.396	2.2973E-16
CHMP2A	1.9692E-38	-0.30000052	0.84	0.883	6.667E-34
TPBG	8.4478E-23	-0.30053853	0.505	0.633	2.861E-18
ZFAND2A-DT	1.1739E-25	-0.30103474	0.286	0.46	3.9743E-21
CMBL	5.801E-31	-0.30116827	0.771	0.842	1.964E-26
FKBP5	3.3284E-41	-0.3024191	0.027	0.246	1.1269E-36
CPLANE1	3.1641E-26	-0.30128765	0.321	0.454	1.0714E-21
LENG8	1.6844E-21	-0.30133282	0.439	0.574	5.7036E-17
STK17A	1.1497E-24	-0.30141994	0.642	0.736	3.8931E-20
SESN3C	2.4473E-25	-0.31171876	0.624	0.724	8.2863E-21
PPP3CA	1.7554E-20	-0.31229315	0.215	0.407	5.9451E-16
RNF145	4.7658E-32	-0.31316191	0.736	0.797	1.613E-27
PBXIP1	8.4249E-24	-0.31419858	0.173	0.366	2.8531E-19
RPL23	6.2482E-43	-0.31387402	0.963	0.989	2.1147E-38
RPL7	1.4268E-44	-0.31397966	0.993	0.999	4.8309E-40
SHOC2	1.7993E-24	-0.31807963	0.673	0.774	6.0924E-20
TMSB10	2.1182E-45	-0.31928105	0.973	0.989	7.1703E-41
SNHG14	3.6947E-25	-0.3185558	0.381	0.543	1.2509E-20
RPL10A	2.1352E-57	-0.31918792	0.987	0.968	7.229E-53
CKB	2.3238E-26	-0.31966328	0.156	0.337	7.867E-22
AC052256.1	2.223E-35	-0.32128746	0.111	0.331	7.5282E-31
VMP1	2.3965E-29	-0.32199145	0.714	0.806	8.1141E-25
PRTG	2.9549E-26	-0.32339958	0.342	0.517	1.0004E-21
DANCR	1.5943E-28	-0.32340024	0.506	0.651	5.3987E-24
PDK4	2.5637E-25	-0.32429978	0.144	0.325	8.6798E-21
P3MIB8	2.9164E-31	-0.32564443	0.25	0.449	9.8187E-27
S100A14	4.1277E-31	-0.32663542	0.041	0.222	1.3975E-26
RP1-57A41.2	7.313E-33	-0.33029357	0.163	0.372	2.4756E-28
RBM3	5.763E-48	-0.33386076	0.871	0.908	1.9511E-43
EEF1A1	5.651E-94	-0.33206163	1	1	1.9132E-89
PER1	1.1619E-29	-0.33267403	0.251	0.451	3.9337E-25
POLR2I	2.0356E-42	-0.33373222	0.919	0.933	6.8919E-38
IER2	3.1956E-23	-0.33418508	0.739	0.798	1.0823E-18
MFGE8	1.3569E-31	-0.33453463	0.327	0.527	4.5935E-27
CENPX	7.3369E-36	-0.33567805	0.777	0.844	2.484E-31
DDX5	9.806E-40	-0.33653473	0.861	0.896	3.3196E-35
PDK1	2.5637E-25	-0.33429978	0.144	0.325	8.6798E-21
P3MIB8	2.9164E-31	-0.32564443	0.25	0.449	9.8187E-27
S100A14	4.1277E-31	-0.32663542	0.041	0.222	1.3975E-26
RP1-57A41.2	7.313E-33	-0.33029357	0.163	0.372	2.4756E-28
RBM3	5.763E-48	-0.33386076	0.871	0.908	1.9511E-43
EEF1A1	5.651E-94	-0.33206163	1	1	1.9132E-89
PER1	1.1619E-29	-0.33267403	0.251	0.451	3.9337E-25
POLR2I	2.0356E-42	-0.33373222	0.919	0.933	6.8919E-38
IER2	3.1956E-23	-0.33418508	0.739	0.798	1.0823E-18
MFGE8	1.3569E-31	-0.33453463	0.327	0.527	4.5935E-27
CENPX	7.3369E-36	-0.33567805	0.777	0.844	2.484E-31
DDX5	9.806E-40	-0.33653473	0.861	0.896	3.3196E-35
SYNM	2.0098E-32	-0.37191493	0.32	0.512	6.8014E-28
PAHB	4.1294E-60	-0.37446885	0.921	0.948	1.3981E-55
ID2	4.047E-24	-0.37552856	0.461	0.603	1.3702E-19
PQP1	3.3394E-36	-0.37919465	0.247	0.467	1.1306E-31
NRNA1	2.8311E-39	-0.37964145	0.687	0.809	9.5851E-35
CAV1	2.9782E-37	-0.3790867	0.224	0.446	1.008E-32
KRT8	4.5579E-36	-0.38249268	0.938	0.941	1.5431E-31
CYFIP2	1.4656E-39	-0.38600071	0.202	0.438	4.963E-35
CHMP1B	7.1699E-43	-0.38709495	0.893	0.939	2.4274E-38
C9orf16	6.2964E-45	-0.39454226	0.677	0.795	2.1317E-40
MAP2	2.6707E-27	-0.39663394	0.205	0.392	9.0418E-23
MIR22HG	1.745E-27	-0.39913934	0.428	0.581	5.908E-23
TMEM238	7.1193E-56	-0.39945507	0.762	0.855	2.4103E-51
TOMM7	5.3264E-43	-0.39951909	0.175	0.424	1.8033E-38
ZNF503	1.6112E-29	-0.40716998	0.338	0.51	3.4236E-25
GRN	1.8465E-43	-0.40853215	0.546	0.72	6.2536E-39
CD24	1.2073E-30	-0.41248387	0.243	0.442	4.0874E-26
PDE10A	1.21E-40	-0.41955563	0.466	0.651	4.0985E-36
PTPRR	1.9484E-63	-0.42431284	0.041	0.35	6.5964E-59
FBXO2	2.402E-56	-0.42655979	0.68	0.816	8.1222E-52
EEF2	6.6004E-89	-0.42947191	0.975	0.986	2.2023E-84
ID1	1.4517E-45	-0.43142391	0.926	0.92	4.9149E-41
CASC15	1.2541E-53	-0.43271413	0.77	0.842	4.2458E-49
PSAP	2.2598E-62	-0.43569971	0.79	0.87	7.6501E-58
CLU	9.0752E-64	-0.43656293	0.9	0.948	3.0725E-59
ZFYVE1	3.9566E-32	-0.44654155	0.58

of cells with respect to all others for each obtained cluster. Differentially expressed genes between the two groups of cells were identified using a non-parametric Wilcoxon Rank Sum test (Seurat default). Pct.1 corresponds to the fraction of cells in column "cluster" in the table, and pct.2 corresponds to the rest of cells in the other clusters/identities. The 'avg_logFC' column is giving the difference found in that gene in that cluster/identity compared to the rest. If the number is positive, it means that is upregulated, and if it is negative, it is downregulated. P_val_adj, adjusted p-value, based on Bonferroni correction using all features in the dataset.

Supplementary Table 10.

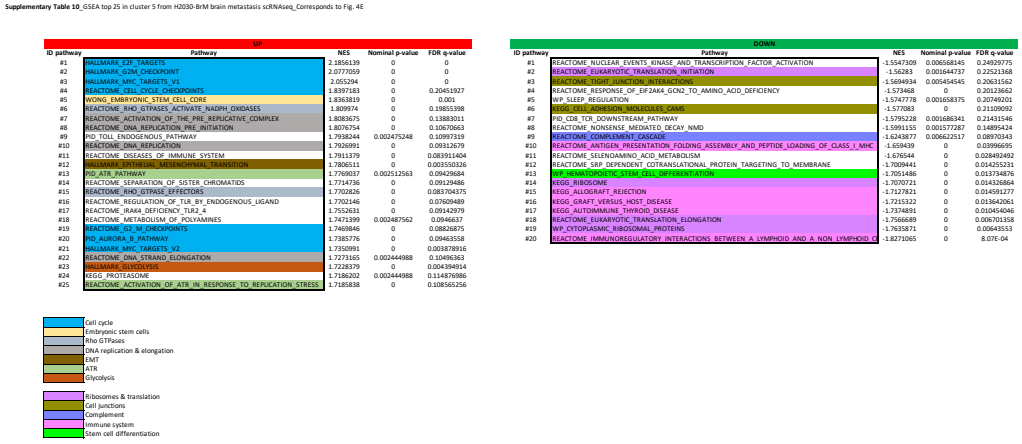

Supplementary Table 10_GSEA top 25 in cluster 5 from H2030-BrM brain metastasis scRNAseq_Corresponds to Fig. 4E

UP

ID pathway	Pathway	NES	Nominal p-value	FDR q-value
#1	HALLMARK_E2F_TARGETS	2.1856139	0	0
#2	HALLMARK_G2M_CHECKPOINT	2.0777059	0	0
#3	HALLMARK_MYC_TARGETS_V1	2.055294	0	0
#4	REACTOME_CELL_CYCLE_CHECKPOINTS	1.8397183	0	0.20451927
#5	WONG_EMBRYONIC_STEM_CELL_CORE	1.8363819	0	0.001
#6	REACTOME_RHO_GTPASES_ACTIVATE_NADPH_OXIDASES	1.809974	0	0.19855398
#7	REACTOME_ACTIVATION_OF_THE_PRE_REPLICATIVE_COMPLEX	1.8083675	0	0.13883011
#8	REACTOME_DNA_REPLICATION_PRE_INITIATION	1.8076754	0	0.10670663
#9	PID_TOLL_ENDOGENOUS_PATHWAY	1.7938244	0.002475248	0.10997319
#10	REACTOME_DNA_REPLICATION	1.7926991	0	0.09312679
#11	REACTOME_DISEASES_OF_IMMUNE_SYSTEM	1.7911379	0	0.083911404
#12	HALLMARK_EPITHELIAL_MESENCHYMAL_TRANSITION	1.7806511	0	0.003550326
#13	PID_ATR_PATHWAY	1.7769037	0.002512563	0.09429684
#14	REACTOME_SEPARATION_OF_SISTER_CHROMATIDS	1.7714736	0	0.09129486
#15	REACTOME_RHO_GTPASE_EFFECTORS	1.7702826	0	0.083704375
#16	REACTOME_REGULATION_OF_TLR_BY_ENDOGENOUS_LIGAND	1.7702146	0	0.07609489
#17	REACTOME_RAK4_DEFICIENCY_TLR2_4	1.7552631	0	0.09142979
#18	REACTOME_METABOLISM_OF_POLYAMINES	1.7471399	0.002487562	0.0946637
#19	REACTOME_G2_M_CHECKPOINTS	1.7469846	0	0.08826875
#20	PID_AURORA_B_PATHWAY	1.7385776	0	0.09463558
#21	HALLMARK_MYC_TARGETS_V2	1.7350991	0	0.003878916
#22	REACTOME_DNA_STRAND_ELONGATION	1.7271165	0.002444988	0.10496363
#23	HALLMARK_GLYCOLYSIS	1.7228379	0	0.004394914
#24	KEGG_PROTEASOME	1.7186202	0.002444988	0.114876986
#25	REACTOME_ACTIVATION_OF_ATR_IN_RESPONSE_TO_REPLICATION_STRESS	1.7185838	0	0.108565256

DOWN

ID pathway	Pathway	NES	Nominal p-value	FDR q-value
#1	REACTOME_NUCLEAR_EVENTS_KINASE_AND_TRANSCRIPTION_FACTOR_ACTIVATION	-1.5547309	0.006568145	0.249297775
#2	REACTOME_EUKARYOTIC_TRANSLATION_INITIATION	-1.56283	0.001644737	0.22521368
#3	REACTOME_TIGHT_JUNCTION_INTERACTIONS	-1.5694934	0.005454545	0.20631562
#4	REACTOME_RESPONSE_OF_EIF2AK4_GCN2_TO_AMINO_ACID_DEFICIENCY	-1.573468	0	0.20123662
#5	WP_SLEEP_REGULATION	-1.5747778	0.001658375	0.20749201
#6	KEGG_CELL_ADHESION_MOLECULES_CAMS	-1.577083	0	0.21109092
#7	PID_CD8_TCR_DOWNSTREAM_PATHWAY	-1.5795228	0.001686341	0.21431546
#8	REACTOME_NONSENSE_MEDIATED_DECAY_NMD	-1.5991155	0.001577287	0.14895424
#9	REACTOME_COMPLEMENT_CASCADE	-1.6243877	0.006622517	0.08970343
#10	REACTOME_ANTIGEN_PRESENTATION_FOLDING_ASSEMBLY_AND_PEPTIDE_LOADING_OF_CLASS_I_MHC	-1.659439	0	0.03996695
#11	REACTOME_SELENOAMINO_ACID_METABOLISM	-1.676544	0	0.028492492
#12	REACTOME_SRP_DEPENDENT_COTRANSLATIONAL_PROTEIN_TARGETING_TO_MEMBRANE	-1.7009441	0	0.014255231
#13	WP_HEMATOPOIETIC_STEM_CELL_DIFFERENTIATION	-1.7051486	0	0.013734876
#14	KEGG_RIBOSOME	-1.7070721	0	0.014326864
#15	KEGG_ALLOGRAFT_REJECTION	-1.7127821	0	0.014591277
#16	KEGG_GRAFT_VERSUS_HOST_DISEASE	-1.7215322	0	0.013642061
#17	KEGG_AUTOIMMUNE_THYROID_DISEASE	-1.7374891	0	0.010454046
#18	REACTOME_EUKARYOTIC_TRANSLATION_ELONGATION	-1.7566689	0	0.006701358
#19	WP_CYTOPLASMIC_RIBOSOMAL_PROTEINS	-1.7635871	0	0.00643553
#20	REACTOME_IMMUNOREGULATORY_INTERACTIONS_BETWEEN_A_LYMPHOID_AND_A_NON_LYMPHOID_CE	-1.8271065	0	8.07E-04

Cell cycle
Embryonic stem cells
Rho GTPases
DNA replication & elongation
EMT
ATR
Glycolysis

Ribosomes & translation
Cell junctions
Complement
Immune system
Stem cell differentiation

GSEA in Cluster 5 as defined by scRNAseq in H2030-BrM brain metastasis. The GSEAPreranked module was used to conduct gene set enrichment analysis on a pre-ranked gene list. GSEAPreranked calculates an enrichment score for each gene set. A gene set's enrichment score reflects how often members of that gene set occur at the top or bottom of the ranked data set. Top 15 signatures up or down according to NES (FDR q value <0.25 and nominal p-value <0.01) in cluster 5.

Supplementary Table 11.

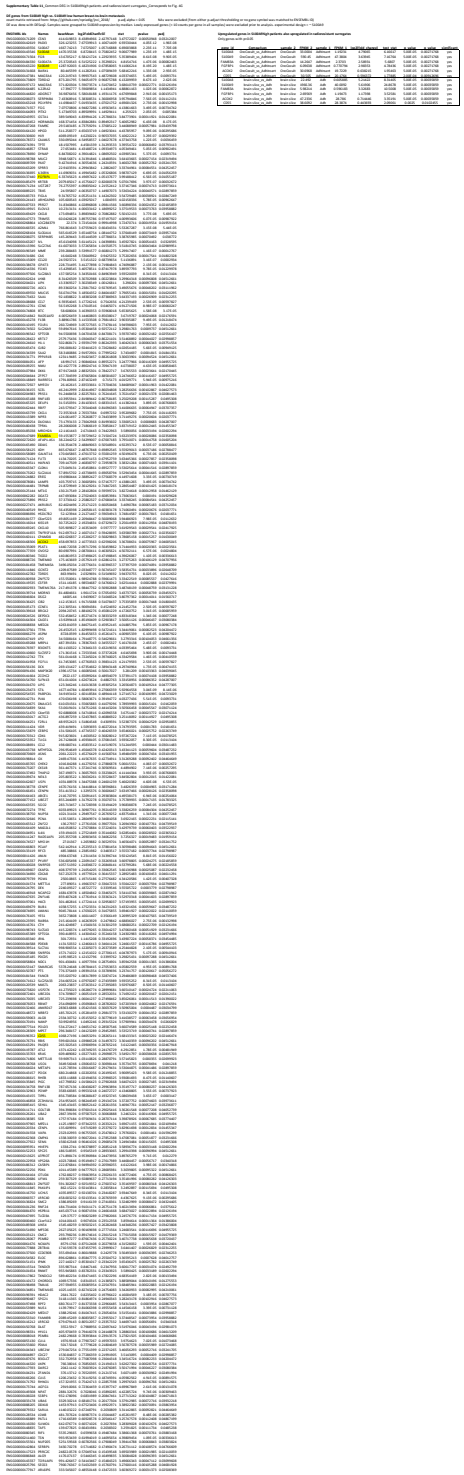

Common DEG in S100A9^{high} patients and radioresistant surrogates. Gene expression profile of human brain metastasis from breast cancer were classified in to high and low expression of

S100A9. DESeq2 was used to identify differentially expressed genes between two groups of samples based on a negative binomial distribution model. Values in the table represent normalized base mean expression level, Log2 fold change, shrinkage of effect size (lfcSE), Wald statistic, Wald test p-value and adjusted p-value below a given FDR cutoff, alpha = 0.05. Those upregulated were evaluated among in vitro and ex vivo surrogates of radio-resistance. In these preparations Cuffdiff (Cufflinks 2.2.1) was used to identify differentially expressed genes between two groups of samples based on the beta negative binomial distribution. The estimated significance level (P value) was corrected to account for multiple hypotheses testing using a Benjamin and Hochberg False Discovery Rate (FDR) adjustment.

Supplementary Table 12.

Supplementary Table 12_Identification of specific NF-kB targets in radioresistant conditions_Corresponds to Fig. 4R

Specific components of the signature hallmark_TNFA_signaling_via_NFKB identified among significantly (P-adjust < 0.05) upregulated genes in both in vitro and ex vivo radio-resistant conditions

GENE SYMBOL
CEBPB
DUSP5
FOS
HES1
JUNB
NR4A2
SAT1
SNN
TNC

Identification of specific NF-κB targets in radioresistant conditions. Individual genes of the NF-κB hallmark signature significantly upregulated in both *in vitro* and *ex vivo* radio-resistant conditions are shown.

Supplementary Table 13.

Supplementary Table 13_Cohort of 66 human brain metastases stained for S100A9, RAGE and JunB_Corresponds to Fig. 2J, Fig. S4J

										IHC score		
Samples	ID	H12O/HLP ID	Cohort	Primary tumor	Gender	Age at brain metastasis diagnosis	Date diagnosis brain metastasis	Date surgery brain metastasis	KPS	S100A9	RAGE	JunB
#1	hBrMM41	17-37637	Hospital 12 de Octubre	Lung	Man	68yo	01.12.2017	04.12.2017	60	0	1	2
#2	hBrMM44	18-08235	Hospital 12 de Octubre	Lung	Man	74yo	02.03.2018	09.03.2018	80	1	1	3
#3	hBrMM45	18-8430	Hospital 12 de Octubre	Lung	Man	67yo	03.03.2018	12.03.2018	80	2	1	3
#4	hBrMM52	19-03189	Hospital 12 de Octubre	Lung	Man	62yo	10.01.2019	31.02.2019	80	0	0	3
#5	hBrMM53	B19-10204	Hospital 12 de Octubre	Breast	Woman	60yo	04.03.2019	28.03.2019	80	3	2	3
#6	hBrMM54	B19-11122A	Hospital 12 de Octubre	Breast	Woman	38yo	12.11.2018	04.04.2019	70	1	1	1
#7	hBrMM55	19-14588	Hospital 12 de Octubre	Lung	Man	59yo	28.04.2019	XX.05.20219	70		1	1
#8	hBrMM56	B19-15287	Hospital 12 de Octubre	Lung	Man	42yo	1st diagn: XX.12.2018; Relapse: XX.05.2019	17.05.2019	70	2	2	3
#9	hBrMM57	B-1920190	Hospital 12 de Octubre	Breast	Woman	46yo	17.06.2019	26.06.2019	70	1	0	2
#10	hBrMM58	B1922871	Hospital 12 de Octubre	Breast	Woman	82yo	24.06.2019	19.07.2019	50	2	2	2
#11	hBrMM59	B19-24715	Hospital 12 de Octubre	Lung	Woman	56yo	05.08.2019	12.08.2019	90	0	0	3
#12	hBrMM60	B19-30578	Hospital 12 de Octubre	Colorectal	Woman	48yo	01.07.2019	14.10.2019	70		0	3
#13	hBrMM62	20-2342	Hospital 12 de Octubre	Lung	Man	58yo	01.05.2019	24.01.2020	60	2	2	1
#14	hBrMM63	B-20-4586	Hospital 12 de Octubre	Lung	Man	50yo	11.02.2020	12.02.2020	70	0	1	1
#15	hBrMM67	B20-15783	Hospital 12 de Octubre	Lung	Man	59yo	04.12.2018	24.07.2020	80	1	2	3
#16	hBrMM68	20-16380	Hospital 12 de Octubre	Lung	Man	67yo	25.06.2020	03.08.2020	90	0	2	2
#17	hBrMM69	20-16600	Hospital 12 de Octubre	Lung	Man	56yo	06.02.2020	05.08.2020	80	1	1	2
#18	hBrMM72	B-20-20390-8	Hospital 12 de Octubre	Uterine	Woman	31yo	18.09.2020	01.10.2020	70	0	1	
#19	hBrMM74	B20-223558	Hospital 12 de Octubre	Rectal	Man	79yo	01.08.2020	25.10.2020	60	2	2	2
#20	hBrMM75	B-20-23341	Hospital 12 de Octubre	Lung	Woman	47yo	01.11.2020	05.11.2020	70	0	2	3
#21	hBrMM76	B-20-25228	Hospital 12 de Octubre	Breast now	Woman	30yo	14.11.2020	26.11.2020	80	0		
#22	hBrMM77	CIPA;1406751186/ 375444	Hospital de La Princesa	Lung	Woman	67yo	18.11.2020	27.11.2020	80	0	2	3
#23	hBrMM78.1	20826116	Hospital 12 de Octubre	Lung	Woman	45yo	27.11.2020	04.12.2020	70	2	2	3
#24	hBrMM79	B-20-26624-D	Hospital 12 de Octubre	Breast	Woman	39yo	12.11.2018	16.12.2020	80	1	2	
#25	hBrMM80	1312622743	Hospital de La Princesa	Breast	Woman	46yo	10.12.2020	21.12.2020	60	3	2	3
#26	hBrMM87	1423781154	Hospital de La Princesa	Lung	Woman	58yo	06.02.2021	18.02.2021	80			1
#27	hBrMM89	B-21-5970	Hospital 12 de Octubre	Breast	Woman		XX.07.2019	11.03.2021				3
#28	hBrMM90	CIPA;1528263856	Hospital de La Princesa	Lung	Woman	58yo	02.08.2019	17.03.2021				3
#29	6		Toulouse	Lung	Woman	68yo		23/09/2011	60	2	2	2
#30	12		Toulouse	Lung	Man	81yo		01/09/2012	90	2	2	1
#31	13		Toulouse	Lung	Man	69yo		24/07/2018	90	0	0	1
#32	18		Toulouse	Lung	Man	46yo		14/09/2011	80	0	1	2
#33	20		Toulouse	Lung	Woman	45yo		25/05/2012	100	0	1	1
#34	23		Toulouse	Lung	Woman	67yo		17/04/2012	80	2	1	2
#35	28		Toulouse	Lung	Man	54yo		24/02/2015	80	3	2	2
#36	35		Toulouse	Lung	Man	63yo		07/06/2012	40	1	1	3
#37	36		Toulouse	Lung	Man	83yo		06/10/2016	90	0	2	2
#38	37		Toulouse	Lung	Man	47yo		20/09/2017	100	0	2	2
#39	39		Toulouse	Lung	Woman	59yo		31/03/2016	100	0	0	2
#40	41		Toulouse	Lung	Woman	57yo		15/10/2014	80	0	1	3
#41	42		Toulouse	Lung	Man	63yo		08/06/2011	80	0		1
#42	43		Toulouse	Lung	Man	60yo		10/09/2018	70	0	0	2
#43	57		Toulouse	Lung	Woman	50yo		24/10/2014	100	0	2	1
#44	58		Toulouse	Lung	Man	47yo		03/05/2012	90	0	2	3
#45	2017/I/2850		Turin	Breast	Woman	50yo	01/01/2017	13/04/2017	100	0	1	1
#46	912/2019/I		Turin	Breast	Woman	43yo	01/12/2018	14/01/2019	80	0	0	1
#47	16063/2018/I		Turin	Breast	Woman	59yo	01/07/2018	13/07/2018	100	0	0	1
#48	2014/I3/4630		Turin	Breast	Woman	68yo	01/01/2013	23/01/2013	90	0	0	3
#49	2016/I/12744		Turin	Breast	Woman	63yo	03/06/2016	03/06/2016	70	0	0	1
#50	201/T/I181		Turin	Breast	Woman	43yo	04/01/2017	04/01/2017	80	0	0	1
#51	2015/I/14860		Turin	Breast	Woman	40yo	08/07/2015	08/07/2015	100	0	2	1
#52	1161/2018/I		Turin	Breast	Woman	61yo	01/12/2017	16/01/2018	100	1	1	3
#53	11320/2018/SI		Turin	Breast	Woman	54yo	01/10/2018	23/10/2018	70	1	1	1
#54	103935/2012/RI		Turin	Breast	Woman	53yo	01/11/2010	12/04/2012	100	2	0	1
#55	9805/2019/I		Turin	Breast	Woman	64yo	01/03/2019	16/04/2019	90	2	2	1
#56	2016/I/23640		Turin	Breast	Woman	50yo	16/11/2015	19/10/2016	80	2	2	1
#57	2016/I/15698		Turin	Breast	Woman	41yo	24/05/2016	08/07/2016	100	3	2	3
#58	110735/2011/RI		Turin	Breast	Woman	74yo	07/05/2010	24/10/2011	100	3	1	1
#59	442/I/15		Turin	Breast	Woman	47yo	01/03/2007	09/01/2015	100	3	2	1
#60	11319/2018/SI		Turin	Breast	Woman	46yo	01/10/2018	23/10/2018	100	3	0	1
#61	2014/I3/853		Turin	Breast	Woman	57yo	27/01/2014	27/01/2014	100	3	2	1
#62	12455/2017/I		Turin	Breast	Woman	39yo	01/05/2017	30/05/2017	70	3	2	1
#63	2014/I3/4631		Turin	Breast	Woman	57yo	27/04/2017	27/04/2017	80	3		
#64	106240/2015/RI		Turin	Breast	Woman	45yo	01/05/2015	09/06/2015	90	3	0	1
#65	103047/2011/RI		Turin	Breast	Woman	58yo	01/02/2011	23/03/2011	80	3	2	1
#66	11869/2019/I		Turin	Breast	Woman	46yo	01/05/2019	24/05/2019	80	3	2	1

Cohort of 66 human brain metastases stained for S100A9, RAGE and JunB. 26 human brain metastases stained with indicated antibodies and their respective score.

Supplementary Table 14.

Supplementary Table 14_Cohort of 140 human brain metastases to determine the expression of S100A9 in different brain metastases of different primary origin_Corresponds to Fig.5B

Sample	ID	Cohort	Retrospective study	Primary tumor	Gender	S100A9 Score
#1	244	Manchester	S100A9 expression by primary origin	Breast	female	0
#2	490	Manchester	S100A9 expression by primary origin	Breast	female	0
#3	560	Manchester	S100A9 expression by primary origin	Breast	female	1
#4	707	Manchester	S100A9 expression by primary origin	Breast	female	0
#5	712	Manchester	S100A9 expression by primary origin	Breast	female	0
#6	722	Manchester	S100A9 expression by primary origin	Breast	female	0
#7	725	Manchester	S100A9 expression by primary origin	Breast	female	0
#8	788	Manchester	S100A9 expression by primary origin	Breast	female	0
#9	943	Manchester	S100A9 expression by primary origin	Breast	female	0
#10	972	Manchester	S100A9 expression by primary origin	Breast	female	0
#11	1040	Manchester	S100A9 expression by primary origin	Breast	female	2
#12	1148	Manchester	S100A9 expression by primary origin	Breast	female	0
#13	1158	Manchester	S100A9 expression by primary origin	Breast	female	0
#14	1170	Manchester	S100A9 expression by primary origin	Breast	female	3
#15	1709	Manchester	S100A9 expression by primary origin	Breast	female	0
#16	2302	Manchester	S100A9 expression by primary origin	Breast	female	2
#17	2401	Manchester	S100A9 expression by primary origin	Breast	female	0
#18	2586	Manchester	S100A9 expression by primary origin	Breast	female	0
#19	2597	Manchester	S100A9 expression by primary origin	Breast	female	0
#20	2925	Manchester	S100A9 expression by primary origin	Breast	female	2
#21	B19-10204	Hospital 12 de Octubre	S100A9 expression by primary origin	Breast	female	3
#22	B19-11122A	Hospital 12 de Octubre	S100A9 expression by primary origin	Breast	female	1
#23	B-1920190	Hospital 12 de Octubre	S100A9 expression by primary origin	Breast	female	1
#24	B1922871	Hospital 12 de Octubre	S100A9 expression by primary origin	Breast	female	2
#25	B-20-25228	Hospital 12 de Octubre	S100A9 expression by primary origin	Breast	female	0
#26	B-20-26624-D	Hospital 12 de Octubre	S100A9 expression by primary origin	Breast	female	1
#27	1312627743	Hospital de La Princesa	S100A9 expression by primary origin	Breast	female	3
#28	2017/I/2850	Turin	S100A9 expression by primary origin	Breast	female	0
#29	912/2019/I	Turin	S100A9 expression by primary origin	Breast	female	0
#30	16063/2018/I	Turin	S100A9 expression by primary origin	Breast	female	0
#31	2014/I3/4630	Turin	S100A9 expression by primary origin	Breast	female	0
#32	2016/I/12744	Turin	S100A9 expression by primary origin	Breast	female	0
#33	2017/I/181	Turin	S100A9 expression by primary origin	Breast	female	0
#34	2015/I/14860	Turin	S100A9 expression by primary origin	Breast	female	0
#35	1161/2018/I	Turin	S100A9 expression by primary origin	Breast	female	1
#36	11320/2018/SI	Turin	S100A9 expression by primary origin	Breast	female	1
#37	103935/2012/RI	Turin	S100A9 expression by primary origin	Breast	female	2
#38	9805/2019/I	Turin	S100A9 expression by primary origin	Breast	female	2
#39	2016/I/22640	Turin	S100A9 expression by primary origin	Breast	female	2
#40	2016/I/15698	Turin	S100A9 expression by primary origin	Breast	female	3
#41	110735/2011/RI	Turin	S100A9 expression by primary origin	Breast	female	3
#42	442/I/15	Turin	S100A9 expression by primary origin	Breast	female	3
#43	11319/2018/SI	Turin	S100A9 expression by primary origin	Breast	female	3
#44	2014/I3/853	Turin	S100A9 expression by primary origin	Breast	female	3
#45	12455/2017/I	Turin	S100A9 expression by primary origin	Breast	female	3
#46	2014/I3/4631	Turin	S100A9 expression by primary origin	Breast	female	3
#47	106240/2015/RI	Turin	S100A9 expression by primary origin	Breast	female	3
#48	103047/2011/RI	Turin	S100A9 expression by primary origin	Breast	female	3
#49	11869/2019/I	Turin	S100A9 expression by primary origin	Breast	female	3
#1	78	Manchester	S100A9 expression by primary origin	lung	female	3
#2	215	Manchester	S100A9 expression by primary origin	lung	male	0
#3	221	Manchester	S100A9 expression by primary origin	lung	male	0
#4	517	Manchester	S100A9 expression by primary origin	lung	female	3
#5	541	Manchester	S100A9 expression by primary origin	lung	male	0
#6	666	Manchester	S100A9 expression by primary origin	lung	female	0
#7	684	Manchester	S100A9 expression by primary origin	lung	female	0
#8	847	Manchester	S100A9 expression by primary origin	lung	female	0
#9	865	Manchester	S100A9 expression by primary origin	lung	female	0
#10	866	Manchester	S100A9 expression by primary origin	lung	male	0
#11	940	Manchester	S100A9 expression by primary origin	lung	male	3
#12	1011	Manchester	S100A9 expression by primary origin	lung	female	0
#13	1031	Manchester	S100A9 expression by primary origin	lung	male	3
#14	1060	Manchester	S100A9 expression by primary origin	lung	male	0
#15	1311	Manchester	S100A9 expression by primary origin	lung	female	3
#16	1348	Manchester	S100A9 expression by primary origin	lung	female	0
#17	1438	Manchester	S100A9 expression by primary origin	lung	female	0
#18	1601	Manchester	S100A9 expression by primary origin	lung	female	3
#19	1757	Manchester	S100A9 expression by primary origin	lung	male	0
#20	17-37637	Hospital 12 de Octubre	S100A9 expression by primary origin	lung	male	0
#21	18-08235	Hospital 12 de Octubre	S100A9 expression by primary origin	lung	male	1
#22	18-8430	Hospital 12 de Octubre	S100A9 expression by primary origin	lung	male	2
#23	19-03189	Hospital 12 de Octubre	S100A9 expression by primary origin	lung	male	0
#24	B19-15287	Hospital 12 de Octubre	S100A9 expression by primary origin	lung	male	2
#25	B19-24715	Hospital 12 de Octubre	S100A9 expression by primary origin	lung	female	0
#26	20-2342	Hospital 12 de Octubre	S100A9 expression by primary origin	lung	male	2
#27	B-20-4586	Hospital 12 de Octubre	S100A9 expression by primary origin	lung	male	0
#28	B20-15783	Hospital 12 de Octubre	S100A9 expression by primary origin	lung	male	1
#29	20-16380	Hospital 12 de Octubre	S100A9 expression by primary origin	lung	male	0
#30	20-16600	Hospital 12 de Octubre	S100A9 expression by primary origin	lung	male	1
#31	B-20-23341	Hospital 12 de Octubre	S100A9 expression by primary origin	lung	female	0
#32	CIPA:1406751186/375444	Hospital de La Princesa	S100A9 expression by primary origin	lung	female	0
#33	20826116	Hospital 12 de Octubre	S100A9 expression by primary origin	lung	female	2
#34	6	Toulouse	S100A9 expression by primary origin	lung	female	2
#35	12	Toulouse	S100A9 expression by primary origin	lung	male	2
#36	13	Toulouse	S100A9 expression by primary origin	lung	male	0
#37	18	Toulouse	S100A9 expression by primary origin	lung	male	0
#38	20	Toulouse	S100A9 expression by primary origin	lung	female	0
#39	23	Toulouse	S100A9 expression by primary origin	lung	female	2
#40	28	Toulouse	S100A9 expression by primary origin	lung	male	3
#41	35	Toulouse	S100A9 expression by primary origin	lung	male	1
#42	36	Toulouse	S100A9 expression by primary origin	lung	male	0
#43	37	Toulouse	S100A9 expression by primary origin	lung	male	0
#44	39	Toulouse	S100A9 expression by primary origin	lung	female	0
#45	41	Toulouse	S100A9 expression by primary origin	lung	female	0
#46	42	Toulouse	S100A9 expression by primary origin	lung	male	0
#47	43	Toulouse	S100A9 expression by primary origin	lung	male	0
#48	57	Toulouse	S100A9 expression by primary origin	lung	female	0
#49	58	Toulouse	S100A9 expression by primary origin	lung	male	0
#50	87	Toulouse	S100A9 expression by primary origin	lung	female	2
#51	88	Toulouse	S100A9 expression by primary origin	lung	female	0
#52	90	Toulouse	S100A9 expression by primary origin	lung	male	2
#53	91	Toulouse	S100A9 expression by primary origin	lung	male	2
#1	1431	Manchester	S100A9 expression by primary origin	Melanoma	male	0
#2	1465	Manchester	S100A9 expression by primary origin	Melanoma	male	0
#3	1700	Manchester	S100A9 expression by primary origin	Melanoma	male	1
#4	1708	Manchester	S100A9 expression by primary origin	Melanoma	male	0
#5	2216	Manchester	S100A9 expression by primary origin	Melanoma	Female	0
#6	2388	Manchester	S100A9 expression by primary origin	Melanoma	male	1
#7	2392	Manchester	S100A9 expression by primary origin	Melanoma	male	3
#8	2574	Manchester	S100A9 expression by primary origin	Melanoma	male	2
#9	2588	Manchester	S100A9 expression by primary origin	Melanoma	Female	0
#10	2635	Manchester	S100A9 expression by primary origin	Melanoma	male	0
#11	2768	Manchester	S100A9 expression by primary origin	Melanoma	Female	0
#12	2772	Manchester	S100A9 expression by primary origin	Melanoma	male	0
#13	3045	Manchester	S100A9 expression by primary origin	Melanoma	Female	3
#14	3142	Manchester	S100A9 expression by primary origin	Melanoma	male	0
#15	H001068T1PTa	Manchester	S100A9 expression by primary origin	Melanoma	Male	0
#16	H001604T1PTa	Manchester	S100A9 expression by primary origin	Melanoma	Female	0
#17	H001664T1PTa	Manchester	S100A9 expression by primary origin	Melanoma	Female	3
#18	H001669T1PTa 28/01/2015	Manchester	S100A9 expression by primary origin	Melanoma	Male	0
#19	H001682T1PTa	Manchester	S100A9 expression by primary origin	Melanoma	Male	0
#20	H001686T1PTa 11/02/2015	Manchester	S100A9 expression by primary origin	Melanoma	Male	0
#21	H001835T1PTa 14/01/2016	Manchester	S100A9 expression by primary origin	Melanoma	Female	0
#22	H001839T1PTa 22/01/2016	Manchester	S100A9 expression by primary origin	Melanoma	Male	0
#23	H001845T1PTa	Manchester	S100A9 expression by primary origin	Melanoma	Female	3
#24	H001936T1PTa 22/06/2016	Manchester	S100A9 expression by primary origin	Melanoma	Male	0
#25	H003034T1PTa	Manchester	S100A9 expression by primary origin	Melanoma	Male	0
#26	H003275T1PTa	Manchester	S100A9 expression by primary origin	Melanoma	Female	0
#27	H000576T1PTa	Manchester	S100A9 expression by primary origin	Melanoma	Male	2
#28	H001576T1PTa	Manchester	S100A9 expression by primary origin	Melanoma	Male	0
#29	H003084T1PTa	Manchester	S100A9 expression by primary origin	Melanoma	Male	2
#30	H003166T1PTa	Manchester	S100A9 expression by primary origin	Melanoma	Male	0
#31	H003220T1PTa	Manchester	S100A9 expression by primary origin	Melanoma	Male	0
#32	H003229T1PTa	Manchester	S100A9 expression by primary origin	Melanoma	Male	0
#33	H003274T1PTa	Manchester	S100A9 expression by primary origin	Melanoma	Male	0
#34	H003306T1PTa	Manchester	S100A9 expression by primary origin	Melanoma	Female	0
#35	H003309T1PTa	Manchester	S100A9 expression by primary origin	Melanoma	Male	0
#36	H003332T1PTa	Manchester	S100A9 expression by primary origin	Melanoma	Female	0
#37	H003407T1PTa	Manchester	S100A9 expression by primary origin	Melanoma	Male	1
#38	H003428T1PTa	Manchester	S100A9 expression by primary origin	Melanoma	Male	1

Cohort of 140 human brain metastases to determine the expression of S100A9 in different

brain metastases of different primary origin. The levels of S100A9 were analyzed respect to the primary tumor source of the brain metastasis.

Supplementary Table 15.

Supplementary Table 15_Cohort of 22 lung cancer human brain metastases to determine the prognostic value of S100A9 to radiotherapy_Corresponds to Fig.5D

ID	Sample	Cohort	Retrospective study	Primary tumor	Gender	Age at neurosurgery	KPS	S100A9 IHC	Date neurosurgery	Date of local relapse	Date of last follow-up	Time to local relapse from neurosurgery/WBRT (days)
6	#1	Toulouse	Relapse after adjuvant radiotherapy	Lung	female	68	60	high	23/09/2011	29/11/2011		67
12	#2	Toulouse	Relapse after adjuvant radiotherapy	Lung	male	81	90	high	01/09/2012	14/02/2013		166
13	#3	Toulouse	Relapse after adjuvant radiotherapy	Lung	male	69	90	low	24/07/2018	no relapse	26/08/2020	764
18	#4	Toulouse	Relapse after adjuvant radiotherapy	Lung	male	46	80	low	14/09/2011	no relapse	22/07/2012	312
20	#5	Toulouse	Relapse after adjuvant radiotherapy	Lung	female	45	100	low	25/05/2012	24/01/2013		244
23	#6	Toulouse	Relapse after adjuvant radiotherapy	Lung	female	67	80	high	17/04/2012	no relapse	09/11/2012	206
28	#7	Toulouse	Relapse after adjuvant radiotherapy	Lung	male	54	80	high	24/02/2015	16/07/2015		142
33	#8	Toulouse	Relapse after adjuvant radiotherapy	Lung	male	63	100	low	07/06/2012	27/12/2013		568
35	#9	Toulouse	Relapse after adjuvant radiotherapy	Lung	male	83	40	high	06/10/2016	no relapse	08/01/2018	459
36	#10	Toulouse	Relapse after adjuvant radiotherapy	Lung	male	47	90	high	20/09/2017	04/01/2019		471
37	#11	Toulouse	Relapse after adjuvant radiotherapy	Lung	female	59	100	low	31/03/2016	13/06/2017		439
39	#12	Toulouse	Relapse after adjuvant radiotherapy	Lung	female	57	100	low	15/10/2014	25/05/2016		588
41	#13	Toulouse	Relapse after adjuvant radiotherapy	Lung	male	63	80	low	08/06/2011	no relapse	04/11/2013	880
42	#14	Toulouse	Relapse after adjuvant radiotherapy	Lung	male	53	80	low	29/10/2012	no relapse	16/08/2021	3213
43	#15	Toulouse	Relapse after adjuvant radiotherapy	Lung	male	60	70	low	10/09/2018	no relapse	11/06/2019	274
57	#16	Toulouse	Relapse after adjuvant radiotherapy	Lung	female	50	100	low	24/10/2014	no relapse	08/04/2016	532
58	#17	Toulouse	Relapse after adjuvant radiotherapy	Lung	male	47	90	low	03/05/2012	13/02/2013		286
66	#18	Toulouse	Relapse after adjuvant radiotherapy	Lung	male	53	100	low	02/03/2016	no relapse	13/07/2021	1959
87	#19	Toulouse	Relapse after adjuvant radiotherapy	Lung	female	50	60	low	27/08/2019	no relapse	06/07/2021	679
88	#20	Toulouse	Relapse after adjuvant radiotherapy	Lung	female	52	80	high	30/04/2021	no relapse	17/08/2021	109
90	#21	Toulouse	Relapse after adjuvant radiotherapy	Lung	male	69	60	high	01/02/2020	no relapse	07/06/2020	127
91	#22	Toulouse	Relapse after adjuvant radiotherapy	Lung	male	70	70	high	03/12/2019	no relapse	12/06/2020	192

Cohort of 22 lung cancer human brain metastases to determine the prognostic value of S100A9 to radiotherapy. The levels of S100A9 immunohistochemistry (low <5% positive cancer cells) were evaluated with the time to local relapse to determine their correlation to the response to WBRT.

Supplementary Table 16.

Supplementary Table 16_Cohort of 42 breast cancer human brain metastases to determine the prognostic value of S100A9 to radiotherapy_Corresponds to Fig.5E and Fig. S5B-C

Sample	ID	Cohort	Retrospective study	Primary tumor	Gender	Age at brain met diagnosis	S100A9 mRNA (log2 (TMM-CPM+1)) in brain metastasis	S100A8 mRNA (log2 (TMM-CPM+1)) in brain metastasis	Cut--Off group (S100A9)	OS from brain met diagnosis (months)
#1	17_PIH	Vanesija, Priedigkeit *et al*., JNCI 2019	Relapse after adjuvant radiotherapy II	Breast	female	37	0.08	0.04	low	30
#2	MAYO_3	GSE173661	Relapse after adjuvant radiotherapy II	Breast	female	26	0.18	0.49	low	29
#3	6_RCS	Vanesija, Priedigkeit *et al*., JNCI 2019	Relapse after adjuvant radiotherapy II	Breast	female	49	0.19	0.00	low	21
#4	MAYO_2	GSE173661	Relapse after adjuvant radiotherapy II	Breast	female	40	0.24	0.63	low	33
#5	MAYO_20	GSE173661	Relapse after adjuvant radiotherapy II	Breast	female	58	0.28	0.78	low	20
#6	47_PIH	Vanesija, Priedigkeit *et al*., JNCI 2019	Relapse after adjuvant radiotherapy II	Breast	female	66	0.32	0.27	low	74
#7	MAYO_1	GSE173661	Relapse after adjuvant radiotherapy II	Breast	female	62	0.45	1.35	low	7
#8	MAYO_23	GSE173661	Relapse after adjuvant radiotherapy II	Breast	female	62	0.66	0.10	low	9
#9	4_RCS	Vanesija, Priedigkeit *et al*., JNCI 2019	Relapse after adjuvant radiotherapy II	Breast	female	59	0.66	0.00	low	24
#10	MAYO_13	GSE173661	Relapse after adjuvant radiotherapy II	Breast	female	29	0.68	0.80	low	10
#11	2_RCS	Vanesija, Priedigkeit *et al*., JNCI 2019	Relapse after adjuvant radiotherapy II	Breast	female	64	0.72	0.25	low	48
#12	3_RCS	Vanesija, Priedigkeit *et al*., JNCI 2019	Relapse after adjuvant radiotherapy II	Breast	female	64	0.80	0.72	low	67
#13	MAYO_5	GSE173661	Relapse after adjuvant radiotherapy II	Breast	female	46	0.80	0.68	low	13
#14	68_PIH	Vanesija, Priedigkeit *et al*., JNCI 2019	Relapse after adjuvant radiotherapy II	Breast	female	53	1.05	0.43	low	114
#15	72_PIH	Vanesija, Priedigkeit *et al*., JNCI 2019	Relapse after adjuvant radiotherapy II	Breast	female	38	1.17	0.39	low	5
#16	MAYO_10	GSE173661	Relapse after adjuvant radiotherapy II	Breast	female	44	1.22	0.74	low	4
#17	51_PIH	Vanesija, Priedigkeit *et al*., JNCI 2019	Relapse after adjuvant radiotherapy II	Breast	female	65	1.37	0.62	low	9
#18	MAYO_6	GSE173661	Relapse after adjuvant radiotherapy II	Breast	female	47	1.61	0.88	low	21
#19	71_PIH	Vanesija, Priedigkeit *et al*., JNCI 2019	Relapse after adjuvant radiotherapy II	Breast	female	28	1.66	1.68	low	147
#20	MAYO_15	GSE173661	Relapse after adjuvant radiotherapy II	Breast	female	53	1.95	2.40	low	5
#21	MAYO_22	GSE173661	Relapse after adjuvant radiotherapy II	Breast	female	37	2.07	2.61	low	59
#22	1_RCS	Vanesija, Priedigkeit *et al*., JNCI 2019	Relapse after adjuvant radiotherapy II	Breast	female	51	2.72	1.75	low	11
#23	7_PIH	Vanesija, Priedigkeit *et al*., JNCI 2019	Relapse after adjuvant radiotherapy II	Breast	female	40	2.93	3.08	low	13
#24	MAYO_19	GSE173661	Relapse after adjuvant radiotherapy II	Breast	female	50	3.18	3.87	low	65
#25	64_PIH	Vanesija, Priedigkeit *et al*., JNCI 2019	Relapse after adjuvant radiotherapy II	Breast	female	46	3.46	2.72	high	5
#26	5_RCS	Vanesija, Priedigkeit *et al*., JNCI 2019	Relapse after adjuvant radiotherapy II	Breast	female	40	3.77	2.88	high	17
#27	MAYO_14	GSE173661	Relapse after adjuvant radiotherapy II	Breast	female	40	4.12	2.90	high	35
#28	MAYO_18	GSE173661	Relapse after adjuvant radiotherapy II	Breast	female	53	4.13	2.29	high	4
#29	MAYO_16	GSE173661	Relapse after adjuvant radiotherapy II	Breast	female	44	4.13	0.54	high	49
#30	MAYO_21	GSE173661	Relapse after adjuvant radiotherapy II	Breast	female	51	4.73	3.94	high	18
#31	MAYO_7	GSE173661	Relapse after adjuvant radiotherapy II	Breast	female	40	4.76	3.94	high	7
#32	MAYO_24	GSE173661	Relapse after adjuvant radiotherapy II	Breast	female	35	5.18	5.58	high	3
#33	12_PIH	Vanesija, Priedigkeit *et al*., JNCI 2019	Relapse after adjuvant radiotherapy II	Breast	female	41	5.27	5.26	high	14
#34	52_PIH	Vanesija, Priedigkeit *et al*., JNCI 2019	Relapse after adjuvant radiotherapy II	Breast	female	67	5.30	4.30	high	7
#35	MAYO_11	GSE173661	Relapse after adjuvant radiotherapy II	Breast	female	67	5.54	5.43	high	26
#36	MAYO_9	GSE173661	Relapse after adjuvant radiotherapy II	Breast	female	45	5.73	5.33	high	13
#37	6_PIH	Vanesija, Priedigkeit *et al*., JNCI 2019	Relapse after adjuvant radiotherapy II	Breast	female	68	5.95	6.38	high	12
#38	MAYO_17	GSE173661	Relapse after adjuvant radiotherapy II	Breast	female	40	6.13	4.57	high	18
#39	MAYO_4	GSE173661	Relapse after adjuvant radiotherapy II	Breast	female	55	6.80	7.53	high	16
#40	MAYO_8	GSE173661	Relapse after adjuvant radiotherapy II	Breast	female	57	7.35	8.16	high	32
#41	62_PIH	Vanesija, Priedigkeit *et al*., JNCI 2019	Relapse after adjuvant radiotherapy II	Breast	female	67	7.77	8.30	high	6
#42	192_PIH	Vanesija, Priedigkeit *et al*., JNCI 2019	Relapse after adjuvant radiotherapy II	Breast	female	58	7.78	7.27	high	16

Cohort of 42 breast cancer human brain metastases to determine the prognostic value of S100A9 to radiotherapy. *S100A9* expression in brain metastasis was collected from a published cohort and evaluated with overall survival (OS) from the diagnosis of the brain metastasis.

Supplementary Table 17.

Supplementary Table 17_Cohort of 34 human brain metastases to determine the prognostic value of S100A9 to radiotherapy_Corresponds to Fig.5F

Sample	ID	Cohort	Retrospective study	Primary tumor	Gender	Age at time of neurosurgery	KPS	S100A9 IHC	OS from brain met diagnosis (days)	OS from brain met diagnosis (months)
#1	2574	Manchester/Preston	Relapse after adjuvant radiotherapy III	melanoma	male	60s		high	500	17
#2	3045	Manchester/Preston	Relapse after adjuvant radiotherapy III	melanoma	female	40s		high	178	6
#3	1170	Manchester/Preston	Relapse after adjuvant radiotherapy III	breast	female	60s		high	196	7
#4	2302	Manchester/Preston	Relapse after adjuvant radiotherapy III	breast	female	70s		high	77	3
#5	1700	Manchester/Preston	Relapse after adjuvant radiotherapy III	melanoma	male	50s		high	115	4
#6	2014/I3/4630	Turin	Relapse after adjuvant radiotherapy III	breast	female	68	90	high	793	26
#7	2016/I/12744	Turin	Relapse after adjuvant radiotherapy III	breast	female	63	70	high	248	8
#8	2017/I/181	Turin	Relapse after adjuvant radiotherapy III	breast	female	43	80	high	294	10
#9	2014/I3/853	Turin	Relapse after adjuvant radiotherapy III	breast	female	57	100	high	383	13
#10	11320/2018/SI	Turin	Relapse after adjuvant radiotherapy III	breast	female	54	70	high	191	6
#11	103935/2012/RI	Turin	Relapse after adjuvant radiotherapy III	breast	female	53	100	high	873	29
#12	9805/2019/I	Turin	Relapse after adjuvant radiotherapy III	breast	female	64	90	high	315	11
#13	12455/2017/I	Turin	Relapse after adjuvant radiotherapy III	breast	female	39	70	high	161	5
#14	2014/I3/4631	Turin	Relapse after adjuvant radiotherapy III	breast	female	57	80	high	94	3
#15	2216	Manchester/Preston	Relapse after adjuvant radiotherapy III	melanoma	female	60s		low	153	5
#16	2401	Manchester/Preston	Relapse after adjuvant radiotherapy III	breast	female	50s		low	1372	46
#17	2586	Manchester/Preston	Relapse after adjuvant radiotherapy III	breast	female	50s		low	993	33
#18	3142	Manchester/Preston	Relapse after adjuvant radiotherapy III	melanoma	male	70s		low	194	6
#19	707	Manchester/Preston	Relapse after adjuvant radiotherapy III	breast	female	60s		low	544	18
#20	943	Manchester/Preston	Relapse after adjuvant radiotherapy III	breast	female	60s		low	759	25
#21	1158	Manchester/Preston	Relapse after adjuvant radiotherapy III	breast	female	50s		low	479	16
#22	H001068	Manchester/Preston	Relapse after adjuvant radiotherapy III	melanoma	male	49	80	low	638	21
#23	H001604	Manchester/Preston	Relapse after adjuvant radiotherapy III	melanoma	female	40		low	623	21
#24	H001682	Manchester/Preston	Relapse after adjuvant radiotherapy III	melanoma	male	80	100	low	291	10
#25	H001835	Manchester/Preston	Relapse after adjuvant radiotherapy III	melanoma	female	45	100	low	358	12
#26	H001839	Manchester/Preston	Relapse after adjuvant radiotherapy III	melanoma	male	64	60	low	566	19
#27	H003275	Manchester/Preston	Relapse after adjuvant radiotherapy III	melanoma	female	37		low	560	19
#28	H003229	Manchester/Preston	Relapse after adjuvant radiotherapy III	melanoma	male	44	100	low	737	25
#29	H003274	Manchester/Preston	Relapse after adjuvant radiotherapy III	melanoma	male	87	100	low	665	22
#30	H003306	Manchester/Preston	Relapse after adjuvant radiotherapy III	melanoma	female	46		low	567	19
#31	2014/I3/4630	Turin	Relapse after adjuvant radiotherapy III	breast	female	68	90	low	793	26
#32	2016/I/12744	Turin	Relapse after adjuvant radiotherapy III	breast	female	63	70	low	248	8
#33	2017/I/181	Turin	Relapse after adjuvant radiotherapy III	breast	female	43	80	low	294	10
#34	2015/I/14860	Turin	Relapse after adjuvant radiotherapy III	breast	female	40	100	low	2297	77

Cohort of 34 human brain metastases from breast cancer and melanoma to determine the prognostic value of S100A9 to radiotherapy. The levels of S100A9 immunohistochemistry (low <5% positive cancer cells) were evaluated with the time to local relapse to determine their correlation to the response to WBRT.

Supplementary Table 18.

Supplementary Table 18_Cohort of 36 lung cancer human brain metastases to determine the prognostic value of S100A9 to SRS_Corresponds to Fig.S5B

ID	Sample	Cohort	Retrospective study	Primary tumor	S100A9 IHC	Date neurosurgery	Date of local relapse	Date of last follow-up	Time to local relapse from neurosurgery/SRS
2	#1	Toulouse	Relapse after adjuvant SRS	Lung	high	21/07/2017		13/11/2019	845
8	#2	Toulouse	Relapse after adjuvant SRS	Lung	high	16/02/2018		05/04/2019	413
10	#3	Toulouse	Relapse after adjuvant SRS	Lung	high	08/09/2014		22/10/2019	1870
11	#4	Toulouse	Relapse after adjuvant SRS	Lung	high	12/07/2018		16/10/2019	461
14	#5	Toulouse	Relapse after adjuvant SRS	Lung	high	21/04/2017		27/12/2017	250
16	#6	Toulouse	Relapse after adjuvant SRS	Lung	high	12/11/2018		20/11/2019	373
22	#7	Toulouse	Relapse after adjuvant SRS	Lung	low	05/07/2016		18/07/2017	378
26	#8	Toulouse	Relapse after adjuvant SRS	Lung	low	09/04/2018		27/11/2019	597
27	#9	Toulouse	Relapse after adjuvant SRS	Lung	low	11/05/2018	04/01/2019		238
29	#10	Toulouse	Relapse after adjuvant SRS	Lung	low	15/11/2018		01/10/2019	320
30	#11	Toulouse	Relapse after adjuvant SRS	Lung	low	10/01/2018		26/11/2019	685
31	#12	Toulouse	Relapse after adjuvant SRS	Lung	low	19/06/2014		14/10/2016	848
34	#13	Toulouse	Relapse after adjuvant SRS	Lung	low	26/08/2015		04/06/2017	648
40	#14	Toulouse	Relapse after adjuvant SRS	Lung	low	15/04/2015		24/02/2017	681
46	#15	Toulouse	Relapse after adjuvant SRS	Lung	low	13/12/2016	24/12/2018		741
47	#16	Toulouse	Relapse after adjuvant SRS	Lung	low	27/06/2014		11/02/2018	1325
48	#17	Toulouse	Relapse after adjuvant SRS	Lung	low	05/09/2018		20/10/2019	410
50	#18	Toulouse	Relapse after adjuvant SRS	Lung	low	01/12/2015		08/03/2018	828
51	#19	Toulouse	Relapse after adjuvant SRS	Lung	low	02/03/2015		24/08/2019	1636
54	#20	Toulouse	Relapse after adjuvant SRS	Lung	low	29/05/2017		05/06/2019	737
55	#21	Toulouse	Relapse after adjuvant SRS	Lung	low	10/08/2015		30/12/2016	508
56	#22	Toulouse	Relapse after adjuvant SRS	Lung	low	06/11/2018		03/12/2019	392
60	#23	Toulouse	Relapse after adjuvant SRS	Lung	low	09/02/2016		15/10/2017	614
61	#24	Toulouse	Relapse after adjuvant SRS	Lung	low	10/08/2017		17/05/2018	280
67	#25	Toulouse	Relapse after adjuvant SRS	Lung	low	01/10/2018		15/11/2019	410
68	#26	Toulouse	Relapse after adjuvant SRS	Lung	low	03/08/2018		18/02/2019	199
70	#27	Toulouse	Relapse after adjuvant SRS	Lung	low	29/09/2011		01/07/2019	2832
71	#28	Toulouse	Relapse after adjuvant SRS	Lung	low	07/06/2018		03/12/2019	544
72	#29	Toulouse	Relapse after adjuvant SRS	Lung	low	28/01/2018		30/08/2019	579
73	#30	Toulouse	Relapse after adjuvant SRS	Lung	low	27/02/2017		29/11/2019	1005
74	#31	Toulouse	Relapse after adjuvant SRS	Lung	low	17/11/2017		20/11/2018	368
75	#32	Toulouse	Relapse after adjuvant SRS	Lung	low	07/12/2015		28/11/2019	1452
76	#33	Toulouse	Relapse after adjuvant SRS	Lung	low	30/11/2016		20/11/2019	1085
77	#34	Toulouse	Relapse after adjuvant SRS	Lung	low	06/11/2018		27/11/2019	386
78	#35	Toulouse	Relapse after adjuvant SRS	Lung	low	11/02/2019		23/05/2019	101
79	#36	Toulouse	Relapse after adjuvant SRS	Lung	low	22/02/2019		30/11/2019	281

Cohort of 36 lung cancer human brain metastases to determine the prognostic value of S100A9 to SRS. The levels of S100A9 immunohistochemistry (low <5% positive cancer cells) were evaluated with the time to local relapse to determine their correlation to the response to SRS.

Supplementary Table 19.

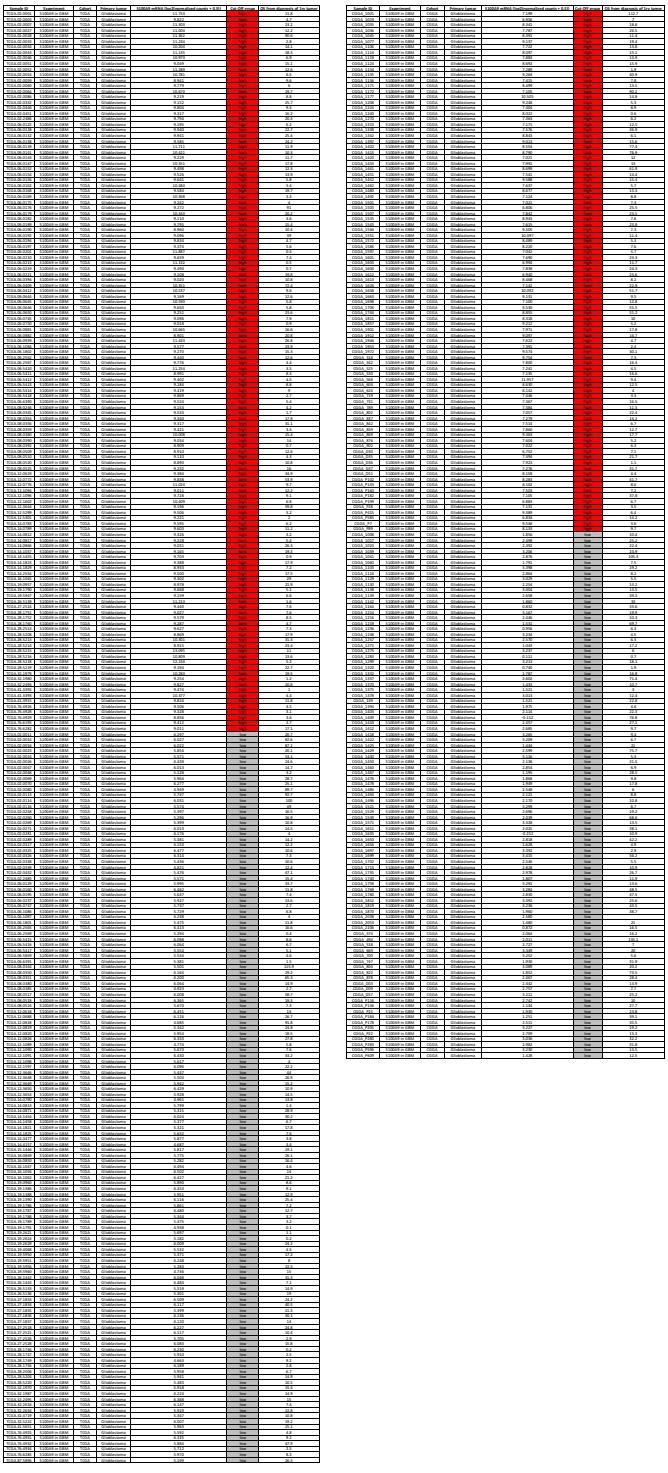

Cohort of human glioblastomas to estimate the prognostic value of S100A9 to radiotherapy. Both TCGA and CGGA cohorts were used to evaluate the correlation between *S100A9* gene expression and overall survival (OS) from glioblastoma diagnosis.

Supplementary Table 20.

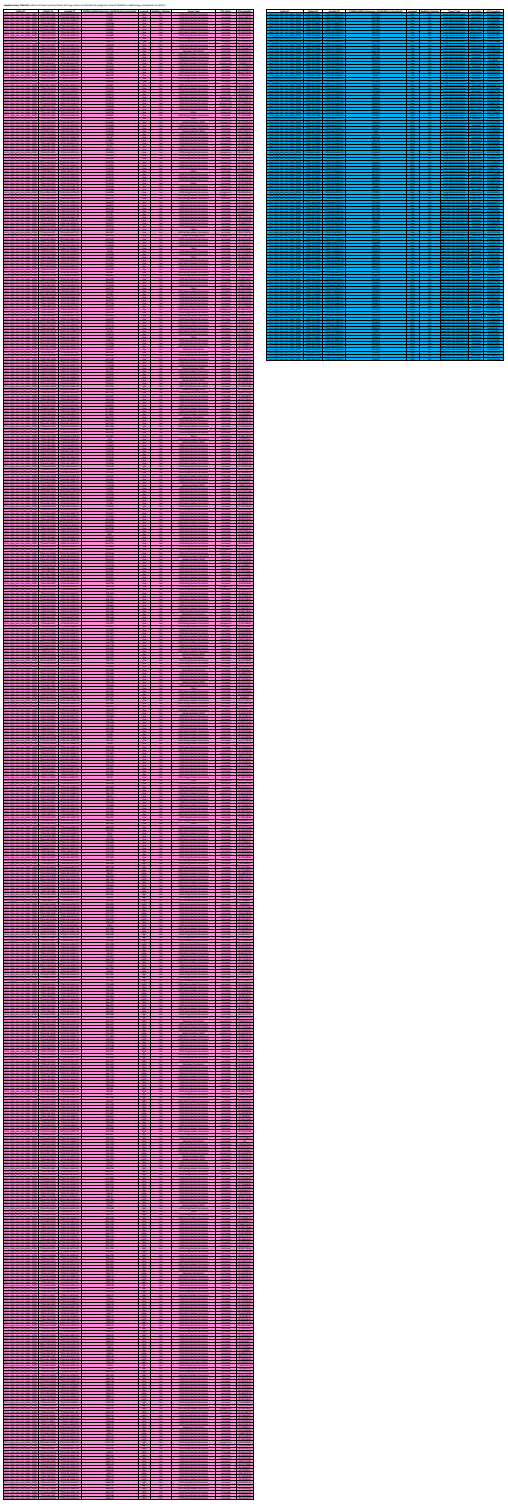

Cohorts of human primary breast and lung cancers to estimate the prognostic value of

S100A9 to radiotherapy. TCGA data on primary breast and lung cancer was filtered by the presence of WBRT and levels of S100A9 evaluated for any clinical correlation.

Supplementary Table 21.

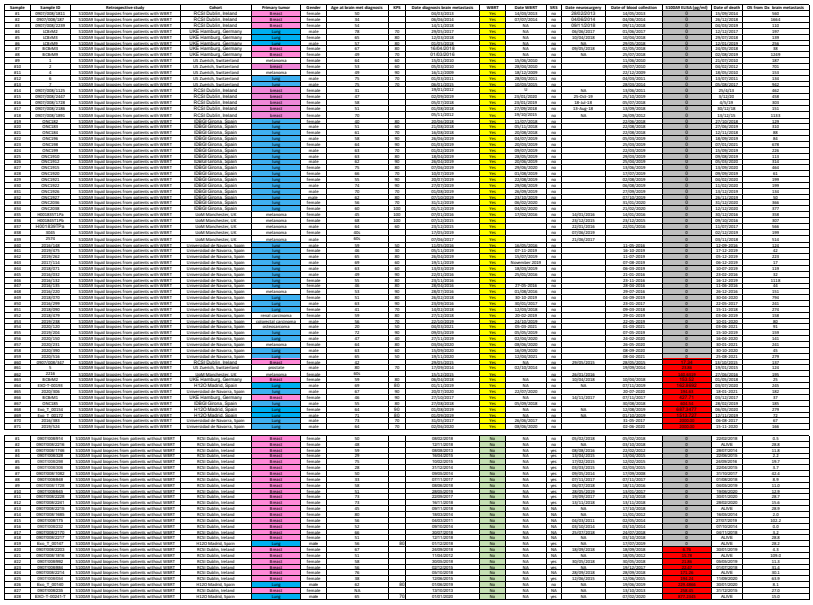

Cohort of 71 human brain metastases with available blood liquid biopsy. Blood liquid biopsies from three independent institutions were collected and evaluated for S100A9 circulating levels using ELISA. Samples were obtained from patients with brain metastasis that received or not WBRT. The correlation of S100A9 levels with overall survival (OS) from brain metastasis diagnosis was later evaluated. N/A: data not available.

Supplementary Table 22.

Supplementary Table 22_Human brain metastases processed as patient-derived organotypic cultures (PDOC)_Corresponds to Fig.6I-K and Fig.S6J-O

Sample	ID	hBrM	H120 ID	Gender	Birthdate	KPS 2nd surgery	Experiment	Primary tumor	S100A9 IF score	Date of 1st brain met surgery	Date of 1st brain met radiation	Date of relapsed brain met surgery
#1	Patient #1	hBrM#41	17-37637	Man	68yo	60	PDOC	Lung	Negative (0)	04/12/2017	Unknown	No relapse
#2	Patient #2	hBrM#62	20-2342	Man	58yo	60	PDOC	Lung	Positive (2)	XX/07/2019	30/07/2019	24/01/2020
#3	Patient #3	hBrM#67	B20-15783	Man	59yo	80	PDOC	Lung	Positive (1)	None	04/12/2020	24/07/2020
#4	Patient #4	hBrM#69	20-16600	Man	56yo	80	PDOC	Lung	Positive (1)	Unknown	Unknown	05/08/2020
#5	Patient #5	hBrM#79	B-20-26624-D	Woman	39yo	80	PDOC	Breast	Positive (1)	04/04/2019	25/02/2019	16/12/2020
#6	Patient #6	hBrM#45	18-8430	Man	67yo	80	PDOC	Lung	Positive (2)	Unknown	Unknown	12/03/2018
#8	Patient #7	hBrM#89	B-21-5970	Woman			PDOC	Breast	Positive (1)			11.03.2021
#9	Patient #8	hBrM#98	B-21-12482	Woman			PDOC	Breast	Positive (1)			19.05.2021

Human brain metastases processed as patient-derived organotypic cultures (PDOC). 8 PDOC established from brain metastasis were evaluated for S100A9 levels by

immunofluorescence and for their response to radiotherapy and FPS-ZM1. Samples from patients #2 to #8 correspond to relapsed metastases that received previous radiotherapy.

Supplementary Table 23.

Supplementary Table 23_Assesment of general health status in tumor free mice one month after completing the treatment with irradiation alone or with FPS-ZM1

	Irradiated + vehicle					Irradiated + FPS-ZM1					Note
Mice tag	#1	#2	#3	#4	#5	#6	#7	#8	#9	#10	
Skin	0	0	0	0	0	0	0	0	0	0	
Fur	0	0	0	0	0	0	0	0	0	0	Presence of white hair in the head (not present pre-treatment) of all mice
Whiskers	0	0	0	0	0	0	0	0	0	0	
Eyes	0	0	0	0	0	0	0	0	0	0	
Movement_regular	0	0	0	0	0	0	0	0	0	0	
Movement_circles	0	0	0	0	0	0	0	0	0	0	
Movement_Unstable	0	0	0	0	0	0	0	0	0	0	
Movement_Other alterations	0	0	0	0	0	0	0	0	0	0	
Agressive response post-manipulation	0	0	0	0	0	0	0	0	0	0	
Any other aspect	0	0	0	0	0	More active	More active	More active	More active	More active	

0: no alteration/ 1: alteration

Assessment of general health status in tumor free mice one month after completing the treatment with irradiation alone or with FPS-ZM1. Results from health status evaluation of two cohorts of mice, one irradiated and treated with a vehicle and the other also irradiated but receiving FPS-ZM1.

Supplementary Table 24.

Supplementary Table 24_Significant P values of behavioral tests

Contextual Fear Conditioning (Extended Data Figure 6g)	Mixed ANOVA	Significant effect of Trial (F(2,70)=125.659; p = 6.89E-24)					
	Pairwise Comparisons (Sidak)	Acquisition/Short Term Memory	Control (p=8.86E-16)				
			Irradiation(p=1.16E-07)				
			Irradiation+FPS-ZM1(p=1.15E-13)				
		Short Term Memory/Context Change	Control (p=0.00022)				
			Irradiation(p=0.022)				
			Irradiation+FPS-ZM1 (p=0.001)				
Elevated Plus Maze (Extended Data Fig. 6f)	Intragroup (t test)	Control (p=1E-08), Irradiation (p=4.15E-07), Irradiation+FPS-ZM1 (p=0.000028)					
Morris Water Maze (Fig.6h)	Learning trials	Mixed ANOVA	Significant effect of trial (F(3,108)=90.482; p = 2.4E-29)				
		Pairwise Comparisons (Sidak)	Intragroup	Control	1/2 (p=0.0008)		
					1/3 (p=1.73E-08)		
					1/4 (p=4.92E-14)		
					2/4 (p=0.00014)		
				Irradiation	1/2 (p=0.013)		
					1/3 (p=0.000303)		
					1/4 (p=1.41E-12)		
					2/4 (p=0.00018)		
				Irradiation+FPS-ZM1	1/2 (p=0.00021)		
					1/3 (p=2.33E-12)		
					1/4 (p=0)		
					2/3 (p=0.00022)		
					2/4 (p=8.82E-08)		
	Probe	One sample T test (probe quadrant vs rest of quadrants)	Intergroup	Day 4 Control/Irradiation (p=0.042)			
			Irradiation+FPS-ZM1 (t(19)=2.778; p=0.012) (more time on probe quadrant)				
Pattern Separation (Supplementary Fig.6r)	Mixed ANOVA	Significant effect of trial (F(1,35)=32.953; p=1.69E-06)					
	Pairwise Comparisons (Sidak)	Control (p=0.005)					
		Irradiation (p=0.012)					
		Irradiation+FPS-ZM1 (p=0.00081)					
Novel Object Recognition (Supplementary Fig.6q)	Discrimination Index	Mixed ANOVA	F(2,68)=57.42; p<0.0001				
		Pairwise comparisons (Sidak)	Intragroup	Control	ACQ/STM	0.000234	
					ACQ/LTM	0.00019	
				Irradiation	ACQ/STM	5.00E-08	
					ACQ/LTM	0.00012	
				Irradiation+FPS-ZM1	ACQ/STM	1.8E-09	
					ACQ/LTM	1.2E-06	
	Time Exploring	Mixed ANOVA	F(2,68)=101.955; p<0.0001				
		Pairwise comparisons (Sidak)	Intragroup	Control	ACQ/STM	2.00E-04	
					STM/LTM	6.00E-03	
				Irradiation	ACQ/STM	5.50E-08	
					ACQ/LTM	8.30E-11	
					STM/LTM	3.00E-08	
				Irradiation+FPS-ZM1	ACQ/STM	1.80E-08	
					ACQ/LTM	8.10E-12	
					STM/LTM	6.00E-07	

Significant *P* values of behavioral tests. This table reflects statistical tests applied to Fig. 6h, Extended Data Figure 6f-g, Supplementary Figure 6q-r and their results. Only those reaching statistical significance are shown.

RENACER:

Cecilia Sobrino[39], Nuria Ajenjo[39], Maria-Jesus Artiga[39], Eva Ortega-Paino[39], Patricia Baena[2], Juan Manuel Sepúlveda[3], Ángel Pérez-Núñez[4,5], Jose Fernández-Alén[6], Manuel Valiente[2].

[39]Biobank; CNIO; Madrid, 28029; Spain.

[2]Brain Metastasis Group, CNIO; Madrid, 28029, Spain.

[3]Neuro-Oncology Unit, Hospital Universitario 12 de Octubre; Madrid, 28041, Spain.

[4]Neurosurgery Unit, Hospital Universitario 12 de Octubre; Madrid, 28041, Spain.

[5]Department of Surgery, Universidad Complutense de Madrid, Madrid, 28040; Spain.

[6]Department of Neurosurgery, Hospital Universitario de La Princesa; Madrid, 28006, Spain.